DYNAMIC FLUID-STRUCTURE INTERACTION
ANALYSIS OF FLOATING PLATFORMS

POTTI V. THANGAM-BABU

CANADIAN THESES ON MICROFICHE

I.S.B.N.

THESES CANADIENNES SUR MICROFICHE

NOTICE

The quality of this microfiche is heavily dependent upon the quality of the original thesis submitted for microfilming. Every effort has been made to ensure the highest quality of reproduction possible.

If pages are missing, contact the university which granted the degree.

Some pages may have indistinct print especially if the original pages were typed with a poor typewriter ribbon or if the university sent us a poor photocopy.

AVIS

La qualité de cette microfiche dépend grandement de la qualité de la thèse soumise au microfilmage. Nous avons tout fait pour assurer une qualité supérieure de reproduction.

S'il manque des pages, veuillez communiquer avec l'université qui a conféré le grade.

La qualité d'impression de certaines pages peut laisser à désirer, surtout si les pages originales ont été dactylographiées à l'aide d'un ruban usé ou si l'université nous a fait parvenir une photocopie de mauvaise qualité.

**THIS DISSERTATION
HAS BEEN MICROFILMED
EXACTLY AS RECEIVED**

**LA THÈSE A ÉTÉ
MICROFILMÉE TELLE QUE
NOUS L'AVONS REÇUE**

Canadä

DYNAMIC FLUID-STRUCTURE INTERACTION ANALYSIS OF

FLOATING PLATFORMS

by

© P.V. Thangam Babu, B.Sc., B.Tech., M.Tech., M.S.

A Thesis submitted in partial fulfillment of the

requirements for the degree of

Doctor of Philosophy

Faculty of Engineering and Applied Science

Memorial University of Newfoundland

July 1981

St. John's   Newfoundland

Dedicated to my Parents

Potti Venkatachalapathy N. and Potti Thulasi V.

SYNOPSIS

The thesis presents finite element analyses of dynamic fluid-structure interaction effects on the response of floating structures subjected to earthquake forces.

The transmission of seismic accelerations from the sea bottom to the surface through the water medium is studied using a system of lumped masses, springs and dashpots. Horizontal accelerations are not transmitted to the surface since the water is a shear-free medium. Depending on the water depth, vertical accelerations transmitted to the bottom of the floating structure are found to be amplified to about 30 to 40 times compared to those at the sea-bottom. Cavitation, a non-linear effect of the water medium wherein the fluid detaches from the structure, is a possibility for greater depths and higher accelerations.

The coupled fluid-structure interaction is studied with finite element modelling. The resulting unsymmetric coupled equations of motion incorporate surface wave effects, radiation damping effects, fluid-structure interface hydrodynamic interaction, and the structural flexibility.

A new numerical integration scheme, based on the Wilson-θ method, to solve the coupled unsymmetric equations of motion is discussed in detail. The procedure is illustrated for a floating nuclear plant (FNP) and a liquid petroleum gas (LPG) storage facility subjected to amplified earthquake accelerations. The results are compared with those obtained by using approximate techniques.

As an alternative approach, since the principle of superposition is valid for linear analysis, the structure and the fluid are isolated and analyzed separately. The analysis discussed in the previous paragraph yields the hydrodynamic pressures acting at the interface of the floating structure. Thus, the floating platform itself is modelled as a thick plate resting on an elastic foundation; the platform is discretised with a newly developed high precision triangular thick plate bending element resting on an elastic foundation. The hydrodynamic pressures are simulated as external forces acting on the fluid-structure interface, in addition to the earthquake forces, and the response is evaluated using the standard Wilson-θ method in the time domain; the frequency domain analysis is also carried out. Two illustrative numerical examples (the floating nuclear plant and the liquid petroleum gas storage facility) are provided.

A computer program, FLOSIN, has been developed to perform all the above analyses described. Its organization is similar to NONSAP, and is very flexible to adapt for other types of offshore structures.

ACKNOWLEDGEMENT

TABLE OF CONTENTS

LIST OF RELATED PUBLICATIONS BY THE AUTHOR

Thangam Babu, P.V. and D.V. Reddy, 1978. Existing Methodologies in the Design and Analysis of Offshore Floating Nuclear Power Plants, Proc. Fourth Int. Conf. Struct. Mech. in Reactor Tech., San Francisco.

Thangam Babu, P.V. and D.V. Reddy, 1978. Existing Methodologies in the Design and Analysis of Offshore Nuclear Power Plants (extended version), Nuc. Eng. and Design, 48.

Thangam Babu, P.V. and D.V. Reddy, 1977. Frequency Analysis of FNP Platforms Using a High-Precision Thick Plate Bending Element, Proc. Fourth Int. Conf. Struct. Mech. in Reactor Tech., San Francisco.

Reddy, D.V., M. Arockiasamy, A.K. Haldar, and P.V. Thangam Babu, 1978. Response of an Offshore Nuclear Plant to Seismic Forces, Proc. Conf. B.N.E.S. Vibration in Nuclear Plant, Session 9, Keswick, U.K.

Arockiasamy, M., D.V. Reddy, P.V. Thangam Babu, and A.K. Haldar, 1978. Stochastic Response of Floating Nuclear Plants to Seismic Forces, Proc. Fifth National Meeting Univ. Council Earthquake Eng. Res. (UCEER), Cambridge, Mass.

Thangam Babu, P.V., M. Arockiasamy, and D.V. Reddy, 1979. Probabilistic Seismic Fluid-Structure Interaction of Floating Nuclear Plants, Proc. Fifth Int. Conf. Struct. Mech. in Reactor Tech., Berlin.

Thangam Babu, P.V., D.V. Reddy, and D.S. Sodhi, 1979. Frequency Analysis of Thick Plates on Elastic Foundation Using a High Precision Triangular Thick Plate Bending Element, Int. J. for Numerical Methods in Eng., Vol. 14, No. 4.

Thangam Babu, P.V. and D.V. Reddy, 1980. Dynamic Fluid-Structure Interaction Analysis of Floating Nuclear Plants Including the Effects of Mooring, J. of Ocean Engineering, Vol. 7, No. 6.

Thangam Babu, P.V. and D.V. Reddy, 1981. A Numerical Integration Technique to Solve the Coupled Equation of Fluid-Structure Interaction System, accepted for presentation at the Conf. on Numerical Methods for Coupled Problems, Swansea, England.

Thangam Babu, P.V., M. Arockiasamy and D.V. Reddy, 1981. Dynamic Fluid-Structure Interaction Analysis of Floating Platforms, Eighth Canadian Congress of Applied Mechanics, Moncton, N.B., Canada.

LIST OF OTHER PUBLICATIONS BY THE AUTHOR

Thangam Babu, P.V., and D.V. Reddy, 1971. Frequency Analysis of Skew Orthotropic Plates by the Finite Strip Method, J. of Sound and Vibration, Vol. 18, No. 4.

Thangam Babu, P.V., and D.V. Reddy, 1973. Frequency Analysis of Orthotropic Circular Cylindrical Panels by the Finite Srip Method, J. of Building Science, Vol. 8.

Thangam Babu, P.V., and D.V. Reddy, 1976. Finite-Strip-Difference Calculus Technique for Skew Orthotropic Plate Vibration, Proc. of the Int. Conf. on Finite Element Methods in Eng., Adelaide, Australia.

Thangam Babu, P.V., and D.V. Reddy, 1977. Finite-Strip-Difference Calculus Technique for Skew Orthotropic Plate Buckling, Proc. of the Fourth Canadian Congress on Applied Mechanics, Vancouver, B.C., Canada.

Mc Daniel, T.J., F.J. Testa, and P.V. Thangam Babu, 1977. Solution Bounds to Certain Non-linear Transient Vibration Problems, J. of Applied Mechanics, Vol. 44, No. 1.

Thangam Babu, P.V., and D.V. Reddy, 1978. Buckling of Skew Orthotropic Plates by the Finite Strip Method, Int. J. of Computers and Structures, Vol. 8.

Riggs, N.P., P.V. Thangam Babu, M. Sullivan, and W.E. Russell, 1980. Iceberg Drift Observations in Lancaster Sound, J. of Cold Regions Science and Technology, Vol. 1

LIST OF TABLES

LIST OF FIGURES

CHAPTER 1

INTRODUCTION

1.1 Offshore Environment

Escalating world oil prices, dwindling non-renewable onshore resources, and ever-growing world energy needs have accelerated the need for exploitation and exploration of mineral resources in the offshore areas of oceans. This new development poses many unforeseen technical difficulties which demands a considerable extension and transposition of available technology for land based structures. The challenge of recent offshore explorations, particularly in the cold regions, has resulted in a rapid increase in many innovative techniques in structural design and analysis procedures. An offshoot of this development is the new generation of structures such as self-elevating steel platforms, concrete gravity-type structure, self-propelled semi-submersible platforms and floating barge-type structures. Of these, the last two types have become the most popular due to their adaptability, mobility, economy and ease in construction and installation procedures.

A floating structure located in an offshore environment is subjected to a wide variety of continuously varying loads due to wind, wave, current, drifting sea-ice, earthquake and associated tsunami and sea-bed slide, etc. Wind loads, which constitute only 5% of the total, are important especially with respect to the overall stability of the

structure. Current loads are significant only in certain
locations but it is usually the wave loading which
significantly influences the design. If the structure is
located in an earthquake belt, then the dynamic
earthquake-induced response of the structure, which is
strongly affected by the inertia, damping,
amplification/attenuation characteristics of the surrounding
fluid, becomes very important. There are evidences of
damages to ships (van Huena, 1972) and underwater cables
(Gupta, 1974) due to earthquakes and associated tsunami and
submarine land slides.

The dynamic response of a floating structure in an ocean
environment is a complex one due to its interaction with the
ocean current, gravity wave, shock and blast waves, etc.
The hydrodynamic interaction leads to coupled
fluid-structure problems. In such systems the relative
motion of the flexible structure and the surrounding fluid
produce inertial and viscous forces on the structure. These
hydrodynamic forces have been expressed by hydrodynamicists
in terms of frequency dependent hydrodynamic added mass
coefficients and hydrodynamic damping coefficients
associated with the floating structure. Evaluation of these
coefficients is a complex problem. However, assuming that
the floating structure is a 'rigid' one, analytical
solutions have been developed to determine these
coefficients for structures of well defined geometry.

1.2 Purpose of This Research

The problem of a coupled fluid-structure interaction system in its entirety and complexity is shown in Fig. 1.1. It shows a flexible floating structure oscillating in a compressible fluid of finite depth and of infinite extent. It includes the gravity surface waves generated by the oscillations of the flexible structure, the energy loss due to the radiation damping of these gravity waves at infinity (far enough that there is no reflection of waves), termed the radiation damping boundary, and the sea-bed and the fluid-structure interface whereat there exists hydrodynamic forces due to the relative displacement of the structure and the fluid. The solution of this problem is a complex, three dimensional, non-linear one and extremely difficult to determine by classical analytical techniques. However, recent advances in numerical methods, such as the finite element method, have paved the way to analyse this kind of problem rationally and economically.

Most of the early finite element applications to hydrodynamic interaction problems were based on the rigid body assumption. Both two and three dimensional finite element analyses of rigid floating structures oscillating with a free surface have been presented by Bai (1977a, 1978), Newton (1975), Visser and van der Vilt (1975), and others. One of the earliest finite element formulation of the coupled problem was presented by Zienkiewicz and Newton (1969) and applied only for free vibration analysis of

FREE SURFACE WAVE

FLOATING STRUCTURE

FREE SURFACE WAVE

FLUID - STRUCTURE INTERFACE

RADIATION DAMPING BOUNDARY

COMPRESSIBLE FLUID REGIONS

RADIATION DAMPING BOUNDARY

SEA-BED
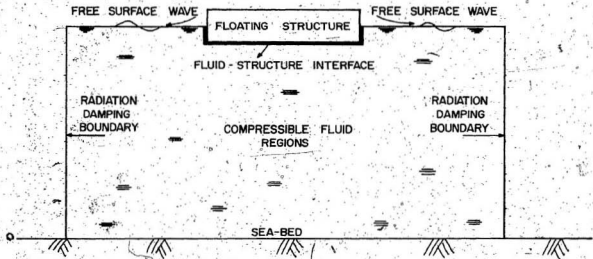
FIGURE I.1: Schematic of the Coupled Fluid-Structure Interaction Problem

bottom fixed dam-reservoir systems. Due to the unsymmetric nature of the resulting coupled equations of equilibrium this formulation has not found an extensive application. In recent years, several methods have been developed involving approximations to convert the unsymmetric matrix into a symmetric one so as to use the well-known solution techniques. Most of these analyses were restricted to bottom fixed structures, assuming undamped systems. Recently, Sharan (1978) applied this formulation to evaluate the response of a complex dam-reservoir foundation system subjected to earthquake. He developed a new numerical integration scheme to solve the unsymmetric coupled equations of equilibrium. But, the numerical examples lack the inclusion of the surface wave and radiation damping in the coupled equation. In a recent paper, Zienkiewicz and Bettess (1978) described the applicability of the methodology to a wide range of problems ranging from oscillation of rigid ships or wave power devices in a free sea-way. Kaul (1977) developed a three-step procedure to determine the dynamic response of floating bodies, but here the problem is not solved in its entirety. Also, the only literature on the water transmitted earthquake is by Williamson, Kennedy, Backman and Chow (1975) used to determine the dynamic response of a submarine ship.

A review of this past work reveals that no detailed complex fluid-structure interaction analysis has been

carried out to determine the dynamic response of floating structures subjected to water-transmitted earthquake. The safety of the proposed facilities, such as offshore floating nuclear plants, LNG and LPG storage and transportation facilities rely heavily on such a complicated and thorough analysis.

1.3 Objective and Scope of This Research

As mentioned in the previous section there is a dire need to develop a generalized finite element method to study the complex dynamic fluid-structure interaction effects on the response of floating structures subjected to water transmitted earthquakes. In order to achieve this goal, a hierarchy of physical problems is to be selected and the development of the program is to be carried out one step at a time.

The first step is to study the existing state-of-the-art of solving coupled fluid-structure interaction problems, its limitations, approximations and versatilities. In Chapter 2, an extensive account of the application of floating platforms, explanation of fluid-structure interaction problems and existing methodologies in solving this kind of problem are detailed.

In the next chapter the phenomenon of the water transmitted earthquake is studied in detail with the assumption that most floating facilities are permanently

installed at shallower depths permanently. The linear and non-linear effects of the fluid medium are discussed, and the resulting amplification factors for the earthquake acceleration transmitted from the seabed to the bottom of the structure are evaluated using a system of lumped masses, springs, and dashpots modelling the fluid and the structure.

The two-dimensional finite element formulation of the complex dynamic fluid-structure interaction problem is detailed in Chapter 4. A new numerical integration scheme, based on Wilson-θ method, has been proposed to solve the resulting unsymmetric coupled equations of motion. Several approximate techniques used in the fluid-structure interaction problem are outlined. The dynamic response of floating platforms subjected to amplified earthquakes, obtained in Chapter 3, are evaluated and compared with those obtained with approximate techniques.

Chapter 5 describes a new technique of modelling the floating platform as a thick plate resting on an elastic foundation. The structure is isolated from the fluid and the hydrodynamic pressures evaluated in the previous chapter are incorporated as external loads acting at the fluid-structure interface nodes in addition to the amplified earthquake accelerations, and the response of floating platforms are evaluated.

A user's manual for a computer program developed to perform the above analyses is presented in Chapter 6. It details the program organization, its capabilities, options, and flag conditions to perform different analyses. A card-by-card explanation of the list of inputs needed to perform different analyses (depending on the condition codes) is also provided. The output from the program is explained in sequence. The adaptability of the program for other related analyses and possible extension to include other finite element libraries are briefly discussed.

The contributions of the present research to the field of coupled fluid-structure interaction analysis, assumptions, limitations and general conclusions are presented in Chapter 7. Also a few recommendations for future research are outlined.

The numerical examples illustrated in this research use FPS units. The conversion factors from FPS units to SI units are provided below.

$$1 \text{ ft} = 0.3048 \text{ m}$$
$$1 \text{ lb} = 0.4536 \text{ kg}$$
$$1 \text{ lb} / \text{ft}^2 = 4.8824 \text{ kg/m}^2$$
$$1 \text{ lb} / \text{in}^2 = 0.0703 \text{ kg/m}^2$$

CHAPTER 2

STATE-OF-THE-ART

2.1 Introduction

The floating-type structure is of particular interest due to its mobility, adaptability and operational advantages.

The various fields of application for floating platforms (existing and envisioned) are listed below:

i) Floating power plants: nuclear plant (Fig. 2.1) and ocean thermal energy conversion plant (Fig. 2.2),

ii) Liquid petroleum gas storage platform (Fig. 2.3),

iii) Paper pulp and power plant system (Fig. 2.4),

iv) LNG liquefaction plant (Fig. 2.5),

v) Single and multiple barge loading terminal (Figs. 2.6, 2.7),

vi) Offshore processing facility (Fig. 2.8),

vii) Desalination plant barge (Fig. 2.9),

viii) Crude oil storage barge (Fig. 2.10), and

ix) Pipe loading barges (Fig. 2.11).

The advantages of floating platforms are the following:

a) the mobility of the platforms enables easy transporta-
tion, and service, maintenance, repair, and modification
of the unit can be carried out in sheltered waters;

b) the fluid medium isolates the floating platform from
seismic activities to a considerable degree, and the
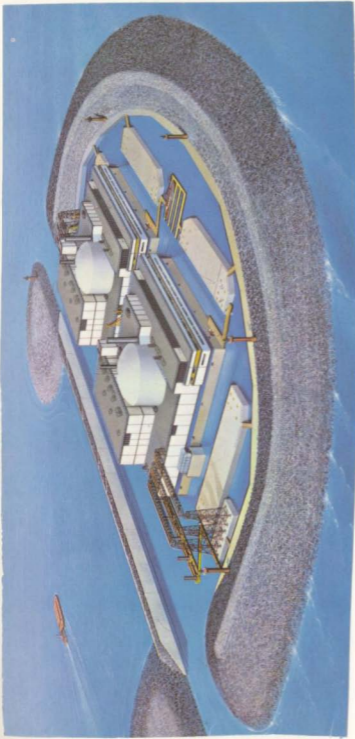
FIGURE 2.1. Layout of a Floating Nulcear Plant
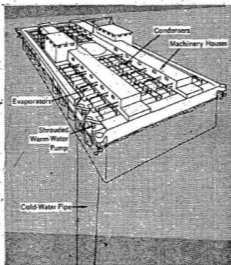
FIGURE 2.2. Floating Ocean Thermal Energy Conversion Plant (ref. Dugger et al., 1975)
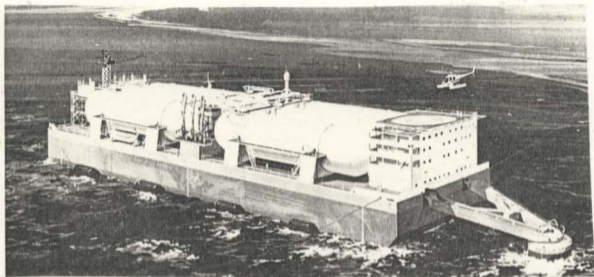
FIGURE 2.3.   Floating LPG Storage for Java Sea
             (ref. Anderson, 1975)

Pulp Plant Platform

Power Plant Platform
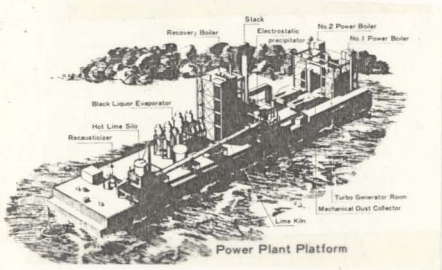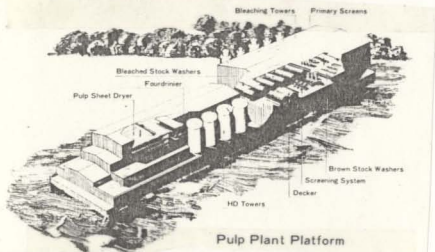
FIGURE 2.4.   Floating Pulp and Power Plants
             (ref. Ishibashi, 1977)
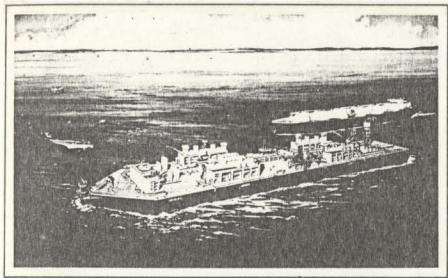
FIGURE 2.5. Floating LNG Liquefaction Facility
(ref. Person, 1977)
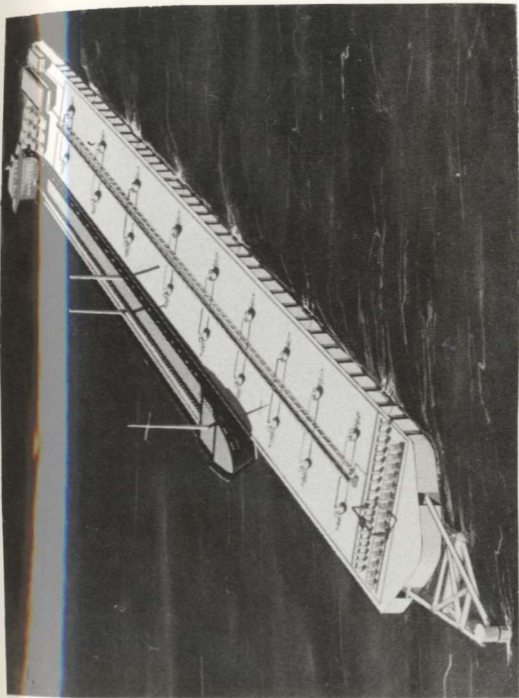
FIGURE 2.6. Single Leg Moored Floating Barge Type Loading Terminal
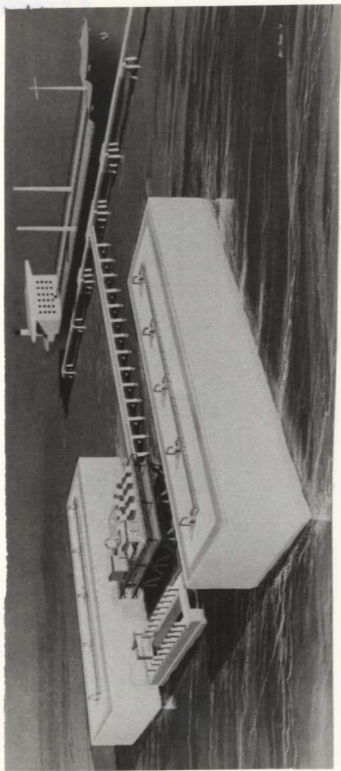
FIGURE 2.7. Multiple Barge Loading Terminal
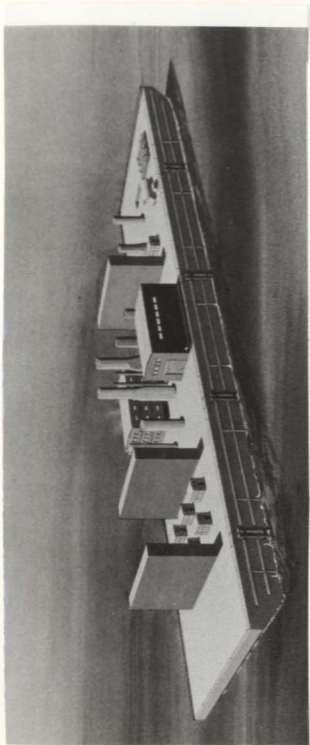
FIGURE 2.8: Floating Offshore Processing Facility
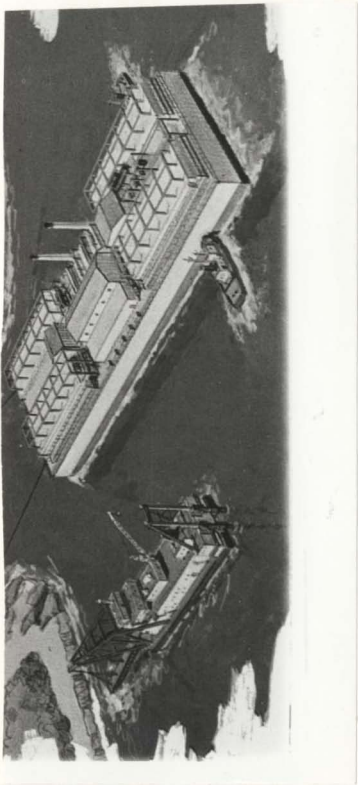
FIGURE 2.9. Floating Desalination Plant Barge
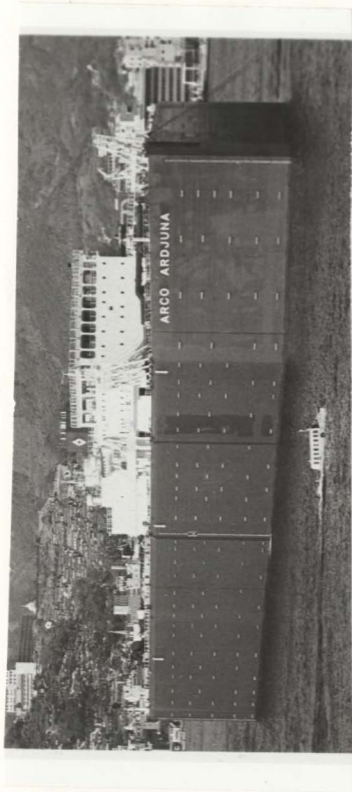
FIGURE 2.10. Floating Crude Oil Storage Barge

FIGURE 2.11. Pipe Laying Barge

wave period of tsunami is so large that the floating
facility will be immune to such a phenomenon;

c) the costs of production of such facilities, fully
equipped and ready for operation, are much cheaper
compared to onshore facilities since:

    i) the construction time is substantially shorter as
most of the fabrication can be carried out in
shipyards with specialized engineering capability
and skilled workers thus allowing plant operation
to meet advance schedules by reducing the offshore
construction to a minimum, and

    ii) the site preparation and construction work is
drastically reduced.

2.2 Dynamic Response of Offshore Structures

The dynamic analysis of offshore structures is a
complex, three-dimensional, non-linear one involving
multi-degree of freedom systems. These structures are
subjected to environmental loadings, such as wind, wave,
current, and earthquake which are random in nature, both in
space and time. The representation of boundary conditions,
such as free surface wave, radiation boundary,
structure-medium interface, are more complex than spring and
dashpot modelling. Fluid damping plays a vital role in the
response calculations. Thus approximate lumped parameter
analyses using single-degree-of-freedom systems are rarely
adequate. Therefore, a comprehensive dynamic analysis with
multi-degree of freedom is necessary. The finite element

method provides an unified approach which can be applied to completely arbitrary and highly complex structures, and modern computing facilities make it possible to solve equations of motions involving thousands of degrees of freedom evaluated at hundreds of time points selected for the dynamic analysis.

The finite element discretisation introduces approximations into the analysis, both of the geometric form of the structure and its displacements. The required degree of refinement and complexity of the discretisation depends on the complex behaviour of the system. There are a wide range of finite elements, two and three dimensional (Zienkiewicz, 1979), to choose from for any given structure-medium configuration. Evaluation of structural properties is a standard well-known operation. With reference to the mass matrix, the selection of lumped or consistent mass matrix needs a little discussion. It has been proved by Clough (1971) that the consistent mass matrix provides a better approximation of the inertia forces acting on the structure. Though the diagonalized lumped mass matrix is advantageous in the solution of eigenvalue problems and also in the direct integration procedures, for cases where higher order elements such as isoparametric elements are used a satisfactory lumping procedure is not available. Moreover, the consistent mass matrix formulation over-estimates the natural frequencies when compatible elements are used.

Damping forces in an offshore environment consist of structural (Rayleigh type) damping, fluid (hydrodynamic) damping, and foundation or soil damping. Hydrodynamic damping stems from two sources, one from the generation of surface waves radiating to infinity and second due to the fluid drag force. The first is similar to viscous damping for a structural system and is proportional to the structure velocity and is frequency dependent. The second one, is associated with the square of the velocity of the fluid with a constant drag coefficient depending on the shape of the structure. Similarly, foundation damping consists of radiation and viscous damping, both proportional to local structural velocity. Normally damping is incorporated in the mathematical model as a linearized viscous damping expressed in terms of damping coefficient, of the order of 2% to 5% of the critical damping. Techniques have been developed to incorporate radiation damping of fluid (Zienkiewicz and Newton, 1969) and foundation (Dunger, 1978) in the equilibrium equation.

The general aspects of the dynamic analysis of offshore structures subjected to environmental loads can be briefly classified as:

 i) time and frequency domain analyses,

 ii) modal superposition and direct integration methods of solving the equations of motion, and

iii) deterministic and probabilistic approaches.

2.2.1   Time and Frequency Domain Analyses

In time domain analysis, the time history of the forcing function is available, the initial conditions are specified, the response is obtained by analytical techniques using response functions to unit impulses and Duhamel's integral, or by direct step-by-step numerical integration of the differential equation. Both linear and non-linear formulations can be handled. Frequency domain analysis presupposes that the existing force can be decomposed into steady-state harmonic components; the solution of the basic differential equation is evaluated for various frequencies. The general solution is obtained by superimposing results of different frequencies through Fourier series or Fourier Integral methods. No non-linear effects can be studied in this method. Vugts and Hayes (1979) compare these two techniques as given in Table 2.1.

Response of offshore structures subjected to random wave loading can easily be treated in the frequency domain. Also, the frequency dependent hydrodynamic coefficients can easily be handled in this method. But the restriction of both the excitation and response to being simple harmonics limits its application. Time domain analysis is more universal and adaptable to many varied loading conditions.

The time and frequency domain analyses can easily be linked by using the Fourier transform technique (Clough and

TABLE 2.1

Comparison of Frequency and Time Domain Analyses

Frequency Domain Analysis	Time Domain Analysis
Constant and frequency dependent coefficients can simply and equally be handled. In both cases the equations are essentially algebraic.	For constant coefficients, the equations are differential equations, but the frequency dependent coefficients lead to integro-differential equations.
Only steady state solution is obtained for different frequencies.	Transient and steady state solutions are possible. Initial conditions need to be specified.
Nonlinearities can be handled only by linearization.	Nonlinearities can be included provided adequate mathematical formulation and solution procedure is provided.
For N degrees of freedom, a system of 2 N linear algebraic equations are solved for each frequency. Spectral analysis can be used to obtain the response to random excitation	For N degrees of freedom, a set of N second order differential equations are replaced by N simultaneous equations for every time step integration. The accuracy and stability of the procedure can demand small integration steps resulting in a tedious and time consuming process. Response to random excitation is obtained directly through numerical integration.

Penzien, 1975). The time domain series, $F(t)$, can be transformed into the frequency domain, $F(\omega)$, by using forward Fourier transform.

$$F(\omega) = \int_{-\infty}^{\infty} F(t)e^{-i\omega t}dt \qquad (2.2.1)$$

and from the frequency domain to the time domain using the inverse Fourier transform:

$$F(t) = 1/(2\pi) \int_{-\infty}^{\infty} F(\omega)e^{i\omega t}d\omega . \qquad (2.2.2)$$

The random response analysis can be deterministic or probabilistic. There are two methods of solving the equations of motion in time domain using the deterministic approach, namely, modal superposition and direct step-by-step numerical integration procedure. In the probabilistic approach the power spectral density (PSD) function and probabilistic extreme values are evaluated in the frequency domain. A review of the applications of deterministic and probabilistic approaches for the random response analysis of structural systems has been presented by Hitchings and Dance (1974).

2.2.2   Deterministic Approach

2.2.2.1   Mode Superposition Method

In this method the coupled N-degrees of freedom equations are uncoupled by substituting the original

variables (displacements) by a new set of variables (eigenvectors). Each equation then can be solved as a single-degree-of-freedom problem and transformed back to express the results in terms of the original variables (displacements). But the uncoupling is possible only if the damping of the structure is of a Rayleigh type, which is the most popular one used. This method needs the evaluation of eigenvalues and eigenvectors of the structural system which is a considerably expensive analysis for large complex systems. Though the decoupling process is time consuming and expensive it needs to be done only once; the repetitive calculations of the response for different random loads is just a matter of solving individual equations with the new loads, thus saving considerable time. The uncertainty in this method is the number of modes to be considered for superposition in order to attain a desirable accuracy. Also, this method cannot handle system non-linearities. Due to these disadvantages the usage of this technique is limited only to linear systems with relatively few degrees of freedom.

2.2.2.2 Direct Step-by-Step Numerical Integration Method

The most efficient method of solving coupled dynamic equations of equilibrium is the step-by-step integration procedure in which the unknowns (displacement, velocity, acceleration) at time (t+Δt) are computed from their values at time (t), while satisfying the dynamic equilibrium conditions. The term 'direct' means that the procedure is

applied directly for the equations of equilibrium without transforming them into any other form. There are many different procedures available which can be classified into two kinds, namely 'explicit' and 'implicit' methods. In the explicit method the unknown variables at $(t+\Delta t)$ are obtained by using the equilibrium conditions at time t, whereas in the implicit approach they are obtained by satisfying the equilibrium conditions at $t+\Delta t$.

The various methods differ in their assumed variation of unknown variables during the interval between discrete points, and the accuracy and stability of the formulations depend on this variation. The most extensively used and popular procedures are the Newmark, Hubolt and Wilson-θ methods (Bathe and Wilson, 1976). All these methods are accurate when $\Delta t/T$ is smaller than 0.01 where T is the fundamental period.

2.2.3 Probabilistic Approach

When the average values in any random process are constant with time, it is called stationary and is similar to the steady state response in the deterministic case. Non-stationary random processes are similar to the transient deterministic case. For deterministic input it is possible to assess the stresses and deformations in the structure. However, for a random input it is not possible to give definite values.

A stationary random variable having a zero mean can be decomposed into its frequency components using Fourier analysis. The ouput power spectral density of a function $f(t)$ over the interval $-T/2 < t < T/2$ is obtained by using the relation:

$$S_h(\omega) = \underset{T \to \infty}{Lt} \frac{\left| \int_{-T/2}^{T/2} f(t) e^{-i\omega t} dt \right|^2}{2\pi T} \qquad (2.2.3)$$

The mean square response value, as the variance of the output process, is obtained as:

$$(E[h^2]) = (\sigma_h^2) = \int_{o}^{\omega_{max}} S_h(\omega) d\omega \qquad (2.2.4)$$

where

ω_{max} denotes the upper bound to the frequency range of interest and E is the expectation.

The moments of the output spectral density function are:

$$m_i = \int_{o}^{\omega_{max}} \omega^i S_h(\omega) d\omega \qquad (2.2.5)$$

where

m_i is the ith moment of the output spectral density function.

2.3 Fluid-Structure Interaction

Dynamic fluid-structure interaction problems can be categorized into interior and exterior types. Interior fluid-structure interaction comprises fluid sloshing in

water tanks, nuclear fuel bundles immersed in the coolant contained in a nuclear reactor vessel, LNG and LPG storage tanks, etc. Examples of exterior interaction problems include offshore structures surrounded by water of infinite extent, dam-reservoir interaction explosion effects on submerged structures, ship-wave interaction, etc. This thesis is restricted to exterior fluid-structure inter-actions of floating barge-type structures subjected to random environmental forces as well as the hydrodynamic forces resulting due to the oscillations of the floating body.

The static analysis of structures surrounded by water is an uncoupled one since both the fluid and the structure can be treated in isolation whereas in dynamic analysis the interaction between the fluid medium and the structure makes the problem a coupled one. However, there are different degrees of interaction:

i) Compressibility effect of the fluid is non-existent in problems with large relative motions such as flutter of aircraft wings, wind-induced oscillations of suspension bridges, etc.

ii) For short duration problems such as explosion or impact effects on submerged structures in which the displacements of both the fluid and the structure are limited, the nonlinear effect is pronounced and the compressibility of the fluid is of considerable importance.

iii) Transient response analysis of an offshore structure subjected to wave or earthquake loading is a long duration problem for which the non-linear effects are either absent or limited. In this case, frequency domain analyses are more economical and practical. Due to the low frequency nature of the phenomenon, the effect of compressibility of the fluid is small.

Subsequent discussions will focus on the third category mentioned above, in particular, floating structures in the ocean environment subjected to earthquake forces.

2.3.1   Hydrodynamic Analysis

The basic difference between the dynamic behaviour of structures surrounded by water and those on land is the effect of inertia of the water on the structures (hydrodynamic added mass), and damping (hydrodynamic damping) characteristics, which in turn are related to the hydrodynamic pressures from the surrounding water acting on the vibrating structure. These hydrodynamic characteristics are frequency dependent, and the component in phase with the periodic acceleration of the vibrating body, contributes the hydrodynamic added mass to the structure and the out-of-phase component contributes the hydrodynamic added damping to the structure. The buoyancy of the fluid medium supporting the medium contributes an added stiffness to the structure. Hence, the simplest form of equations of motion

of the structure vibrating in a fluid medium is:

$$(M+\overline{M})\{\ddot{\delta}\} + (C+\overline{C})\{\dot{\delta}\} + (K+\overline{K})\{\delta\} = \{F\} \qquad (2.3.1)$$

where

M is the mass of the structure,

$\overline{M}$ is the hydrodynamic added mass,

C is the damping of the structure,

$\overline{C}$ is the hydrodynamic added damping,

K is the stiffness of the structure,

$\overline{K}$ is the added stiffness due to the buoyancy of the fluid medium,

F is the external force acting on the structure,

and

$\delta, \dot{\delta}, \ddot{\delta}$ are the displacement, velocity and acceleration of the vibrating structure, respectively.

In its most complex form, the coupled fluid-structure problem is a three-dimensional, non-linear one including the flexibility of the structure, the compressibility of the fluid, generation of surface waves, and wave radiation damping. However, this coupling can be taken into account with different degrees of simplifications and assumptions, such as:

  i) small oscillations, and linearized governing equations and boundary conditions,

  ii) rigid floating structure and incompressible fluid,

iii) flexible structure vibrating in an incompressible fluid,

iv) rigid structure vibrating in a compressible fluid,

v) flexible structure vibrating in a compressible fluid,

vi) including surface wave and radiation damping effects,

and

vii) incorporating wave diffraction and refraction effects.

2.3.2 Uncoupled Fluid-Structure Interaction

The basic assumption that the vibrating structure is a rigid one simplifies the coupled problem into an uncoupled one enabling the analysis of the fluid and structure separately. Most of the published literature is based on this assumption and the results are the frequency-dependent hydrodynamic added mass and damping coefficients of rigid floating bodies of different configurations. Existing knowledge on the hydrodynamic analysis of rigid structures with particular relevance to floating structures is detailed below.

The surface oscillations of an inviscid, incompressible fluid in the vicinity of a floating structure can be described by a boundary value problem governed by Laplace's equation with a mixed boundary condition at the free surface, a homogeneous Neumann condition at the bottom of the fluid boundary, an appropriate radiation boundary condition at infinity, and the fluid-structure interface condition (matching of the normal velocity of the body and

the fluid). Mathematical analysis of this problem for analytical solutions uses potential flow theory and is limited to only well-defined structural geometries of high slenderness ratios. Wehausen (1971) has listed extensive literature on this topic.

The finite element method has been employed by various authors for the hydrodynamic analysis of rigid floating structures. Røren (1969) studied the oscillation of a system of parallel girders positioned in a water basin as well as vertical harmonic excitations of a rigid ship. Holand (1969) evaluated the hydrodynamic added mass for a rigid cylinder moving in an infinite fluid and for a rectangular basin with a moving vertical side wall. Matsumoto (1972) considered rigid as well as flexible bodies vibrating in an incompressible fluid taking into account the infinite boundaries. Application to a rigid ship hull, excluding surface waves, has been presented by Matsuura and Kawakami (1970). Newton (1975) studied the oscillations of rigid hulls taking into account the free surface wave and a radiation damping boundary condition. Transient response of rigid rectangular bodies to an initial excitation, including bodies tied to mooring caissons by mooring struts treated as springs, has been studied by Visser and Van der Wilt (1975). Two and three-dimensional hydrodynamic analyses of rigid circular cylindrical, rectangular and axi-symmetric rigid floating bodies, using a localized finite element technique have been reported by Bai (1975, 1977a, 1977b). In this

analysis, the fluid domain is reduced to a small local domain by making use of known solutions, in terms of an eigen-function or Green's function. A similar approach has been used by Chen and Mei (1975) and Mei and Chen (1976) to solve two-dimensional problems.

2.3.3   Coupled Fluid-Structure Interaction

The relative motion of the compressible fluid and the flexible structure causes viscous and inertial forces on the structure that are difficult to evaluate using classical closed form techniques. The finite element method, has been proved to be versatile in analyzing the coupled problem economically.

The first step in applying the finite element method to any differential equation is to transform the differential equation into an integro-functional form such that minimization of this functional in some sense implies the satisfaction of the differential equations. A variety of approaches are available to establish this integro-functional. Virtual work and variational principles are the most common. In general, for a coupled problem, Galerkin's weighted residual process is the most suitable and the best alternative when a variational or virtual work method is not available (Hutton, 1974). In the finite element discretisation process, the displacements are taken as the nodal unknowns for the structural part of the system. The fluid medium, unlike the solid, does not show elastic restoring

force when the fluid particles are displaced relative to one
another. (For example, consider a bowl of water initially
at rest under its own weight, then stirred, then allowed to
come to rest again. Clearly, the final stress state is
spatially the same as the initial stress state, however, the
particle locations in the final state are unrelated to the
initial state, Katona and Migliore, 1977.)

Thus, for the fluid part, the concern is with particle
velocities and accelerations which generate viscous and
inertial stresses respectively. Hence, in the fluid
discretisation the selections of velocity field as the nodal
unknown rather than the displacements seems to be more
logical. Two basic formulations, namely the Lagrangian and
Euler-Lagrangian approaches, have been used in solving
problems of this category. In the Lagrangian method the
fluid displacements are used in the same manner as for the
structure, and the fluid is treated as an elastic medium
with a small but finite shear modulus. Shantaram et al.
(1976), Wilson (1977) and Bathe and Hahn (1979) have used
this approach to evaluate the transient response of fluid-
structure systems. In this formulation, a finite value of
bulk modulus has to be assigned to the fluid and hence
incompressibility can be approximated only by increasing the
value of the bulk modulus. The advantage is that the final
matrix is a symmetric one, but the pitfall is that the
negligible shear values incorporated into the matrix could
lead to unstable matrices yielding spurious results.

The Euler-Lagrangian formulation uses pressure, which in turn is related to the velocity potential, as the nodal unknown for the fluid elements and the displacements as the unknown variable for the structure. One of the earliest applications of this technique to coupled problems with free surface wave and radiation boundary condition is that of Zienkiewicz, Irons and Nath (1966), and Zienkiewicz and Newton (1969). The advantage of this approach lies in the small number of equations in the fluid domain since only one unknown, pressure or velocity potential, is associated with each node. But the resultant coupled matrix is an unsymmetric one with large bandwidth which needs special numerical integration techniques. Further discussion of the coupled problem is presented in Section 4.2.

2.4 Discussion

The review of the literature presented herein reveals the fact that the complexity and the unsymmetric nature of the resulting equations of motion of the coupled problem has limited the applied usage of the formulation. In the

subsequent chapters, the development of a new numerical integration technique to overcome the difficulties of the solution procedure is presented and its effectiveness is demonstrated with numerical examples.

CHAPTER 3

THE SEAQUAKE PHENOMENON

3.1 Introduction

The shock waves generated in the sea by the seismic motion consist solely of acoustic (compressional) waves, since water cannot transmit shear waves. These compressional waves are refracted at the sea floor and travel in paths close to vertical to the sea floor. The term 'seaquake' relates to this phenomenon of shock waves travelling through the water due to earthquakes with epicentres either on-shore or off-shore. However, this definition excludes the effect of tsunamis associated with seaquake. Water-transmitted seismic vibrations from the seabed to a floating structure cause high frequency response and the motion primarily consists of vertical pulses only. The horizontal travelling wave effects on the sides of the floating structure have very little influence and hence are neglected.

The effect of seaquake on ships has been reported as early as 1887 by Rudolph and after seveal years by Richter (1958). Since the 1964 Alaskan earthquake several reports on seaquake effects have been presented (Von Huena, 1972). Vertical accelerations have been said to have caused a foot high water spout rising from the live bait tank of a fishing

boat. The ship responses have been described as a violent shaking, mostly vertical, as if running aground or striking a submerged object or being lifted out of water. This suggests that the response is largely in the high frequency range. The seaquake pressures in the water have been found to be much less compared to those in underwater explosions. However, they can be as severe as an underwater explosion that can cause serious damage to the floating structure.

3.2 Approximate Linear/Nonlinear Lumped Parameter Fluid Model

In this analytical approach, the floating body is assumed to be rigid, except for a small bottom portion of the structure which can either be rigid or flexible. The items of importance in defining the behaviour of the dynamic model are:

i) the elastic vibrational properties of the water column,

ii) the related cavitation in the water medium,

iii) the estimated free-field water pressure, and

iv) the estimated stress transmitted to the bottom of the ship.

Consider the water column extending from the seabed to the surface as an equivalent elastic bar with a free end at the top. Then the period of oscillation can be found as (Den Hartog, 1956):

$$T_m = 4H/(2m-1)C \qquad (3.2.1)$$

where

H is the height of the water column,

m is the mode,

and

$$C = \sqrt{AE/\mu} \qquad (3.2.2)$$

in which

A is the area of cross section of the column,

E is the modulus of elasticity, and

μ is the mass per unit length of the column.

3.2.1   Cavitation in the Water Medium

The vertical motion of the sea bed induces a series of compression-tension waves in the water medium. If the tensile stress at any depth exceeds the compressive stress due to the atmospheric pressure plus the weight of the water above, then cavitation results. Figure 3.1 shows the maximum allowable vertical acceleration on the water columns of various depth for the 'no-cavitation' condition. The allowable vertical acceleration decreases rapidly with increasing depth and approaches 1 g at larger depths. The inference from this figure is that the occurrence of cavitation at shallow depths is less likely than at moderate depths. The dynamic analysis performed by Williamson et al. (1975) with lumped masses and linear springs confirmed this inference. On the contrary, results using nonlinear elastic springs showed the likelihood of occurrence of cavitation throughout the entire depth of the water column.
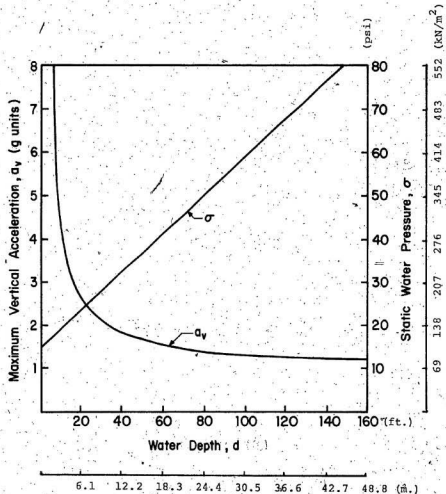
FIGURE 3.1. Allowable Limits of Acceleration vs Water Depth (ref. Williamson, 1975)

3.2.2 Dynamic Models

The vertical column of water is modelled as a system of lumped masses, springs and dashpots. The lumped mass of the system is calculated as:

$$m = \rho AS \qquad (3.2.3)$$

where

ρ is the density of the water,

A is the cross-sectional area,

and

S is the spacing of the masses.

The axial stiffness of the interconnecting springs are calculated by the relation:

$$k_b = AE/S \qquad (3.2.4)$$

where

E is the modulus of elasticity of the water column.

The water column is considered to have damping properties represented by equivalent viscous damping of 0.5% of critical.

Two types of models have been suggested by Williamson et al. (1975):

   i) Free Field Model, and

   ii) Trapped Water Model.

i) Free Field Model: The free field model assumes that there is no interaction between water and the floating body that would affect the pressure acting on the

structure; those pressures are equal to the free field
pressures.

ii) Trapped Water Model: In the trapped water model, shown
in Fig. 3.2, the water column is assumed to act as an
elastic bar with its vertical sides restrained against
horizontal displacement by an imaginary membrane
surrounding the structure and the water column. In this
study, only this model will be detailed and
corresponding numerical examples with linear springs
will be discussed.

In Fig. 3.2 the flexibility of the structure is
represented by modelling the structure into two sub-
structures of weights W_s and W_p ($W_p \ll W_s$) connected by a
spring K_p and dashpot C_p. The water column is modelled as a
series of lumped masses and springs, with the top mass being
lumped with mass associated with W_s. The connecting elastic
spring stiffnesses, K, of the water column depend on the
compressibility of the water column.

3.2.3   Nonlinear Analysis

As mentioned earlier, cavitation at any depth occurs
when the tensile stress in the water exceeds the cut-off
stress represented by the water pressure at that depth plus
the atmospheric pressure. For nonlinear analysis, this
phenomenon can be accounted for through the use of elastic
bilinear springs as shown in Fig. 3.3 with provisions for
tension cut-off.
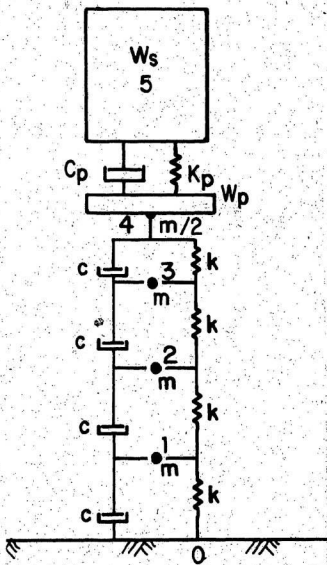
FIGURE 3.2. Trapped Water Model
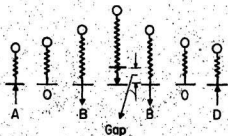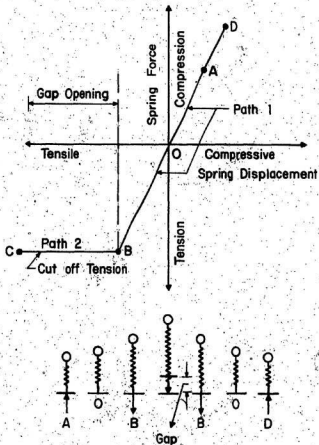
FIGURE 3.3. Non-linear Spring Behaviour
(ref. Williamson et al., 1975)

When the tensile stress in the water reaches the cut-off limit, further increases are simulated by a gap opening at constant tensile stress. Upon unloading, this gap closes and the cycle is repeated. The closure of the gap is treated as an elastic impact (in contrast to plastic impact) problem for the sake of a conservative analysis (no energy loss).. The cut-off tension for each spring can be determined from Fig. 3.1 using the mid-height depth of the simulated spring. For example, for a spring whose mid-height depth is 60 feet the cut-off value of the allowable acceleration is 1.5 g above which cavitation will result. This implies that for very shallow depths cavitation is very unlikely to occur.

Since a major portion of the force-displacement diagram (Fig. 3.3) is linear elastic, the nonlinear analysis can be performed in two steps: (i) a linear analysis based upon the initial stiffnesses, and then (ii) adding nonlinear correction forces to the nodes as externally applied dynamic forces. Thus the nonlinear analysis is converted to an equivalent linear analysis.

3.2.3.1 Nonlinear Corrective Force

Let the bilinear spring shown in Fig. 3.4 have a linear elastic stiffness of K_i and the cut-off tension $T_{(c)i}$. If the displacements of the nodes j and k are X_j and X_k then the force on the spring, F_i, is given as:

$$F_i = F_{(1)i} - F_{(c)i} \qquad (3.2.5)$$
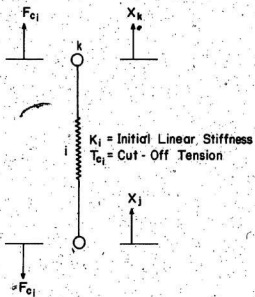
FIGURE 3.4. Determination of Non-linear Corrective
Forces (ref. Williamson et al., 1975)

where

$F_{(1)i}$ is the linear elastic force in the spring,

and

$F_{(c)i}$ is the correction force required to ensure that F_i
does not exceed $T_{(c)i}$

Also

$$F_{(1)i} = K_i (X_k - X_j) \qquad (3.2.6)$$

If $F_{(1)i}$ is less than $T_{(c)i}$, then $F_{(c)i}$ is equal to zero.
If not, the corrective force is

$$F_{(c)i} = F_{(1)i} - T_{(c)i} \quad \text{(for } F_{(1)i} \text{ greater than } T_{(c)i}) \qquad (3.2.7)$$

3.2.4   Linear Analysis

In linear analysis, the cavitation effect is ignored and
the water is presumed to be able to transmit any level of
tension. The accuracy of the results of linear analysis can
be guaranteed to within 2% of those of nonlinear analysis
by taking sufficient number of spring-mass idealizations to
incorporate sufficient modes in the discretised model and by
choosing small enough time. Furthermore, the errors in the
maximum positive and negative response values of the
structure in linear analysis cannot be more than 5% (Nigam
and Jennings, 1968).

3.2.4.1   Equations of Motion

The dynamic equations of motion of a lumped mass-
nonlinear spring system can be written as:

$$[M]\{\ddot{X}\} + [C]\{\dot{X}\} + [K]\{X\} = -\{m_x\}a_x + \{F_c\} \qquad (3.2.8)$$

where

[M] is the diagonal mass matrix,

[C] is the viscous damping matrix,

[K] is the equivalent linear spring stiffness matrix,

$\{X\}$ is the column vector of the vertical displacement of the masses relative to the ground vertical motion,

$\{\dot{X}\}$ is the column vector of the relative velocities,

$\{\ddot{X}\}$ is the column vector of the relative accelerations,

$\{m_x\}$ is the column vector with inertial terms corresponding to the vertical degrees of freedom,

a_x is the vertical ground acceleration, and

$\{F_c\}$ is the column vector of correction forces due to the nonlinearity of the spring.

For a system with linear springs, the term $\{F_c\}$ vanishes in the above equation.

This is a standard problem of dynamic structural response to random load excitation. The obvious choice of solution technique is the popular direct step-by-step time integration method, the solution procedure has been presented in detail by Kennedy (1969).

3.3 Numerical Examples

This section presents the water-transmitted earthquake accelerations acting at the bottom of:

i) a liquid petroleum gas storage plant, and

ii) a floating nuclear plant.

The trapped water model is used and the linear analysis is presented.

3.3.1. Amplified Acceleration at the Bottom of the LPG
Storage Platform

The LPG storage plant chosen for one of the example problems, is a floating platform similar to the ARCO-LPG (Atlantic Richfield Company, Liquid Petroleum Gas) facility installed at the Ardjuna field off Java Sea; the schematic is shown in Fig. 3.5. For a plane strain analysis, the longitudinal section of the prestressed concrete hull is idealized as an equivalent sandwich plate by 'smearing' (distributing the rigidities) of the web members across the platform width. The mass, stiffness, and damping values of the 'trapped water model' shown in Fig. 3.6 are calculated as follows.

The length, width and depth of the platform are 461' (140.605m), 136'(47.48m), and 56'(17.08m) respectively and the draft is 36'(10.98m). The platform is divided into a major part with weight W_p and a minor part with W_s, connected by a spring K_p and a dashpot C_p. The total weight of the platform is 152,320 kips (6.78 x 10^5 kN). The three bottom skirts of the platform, isolated as the minor portion, W_p, weigh 7,801 kips (34,714 kN). Hence, the weight of the major portion, W_s, is 144,519 kips (6.43 x 10^5 kN). W_p per unit area was calculated to be 0.8613 psi (5.943 kN/m^2).
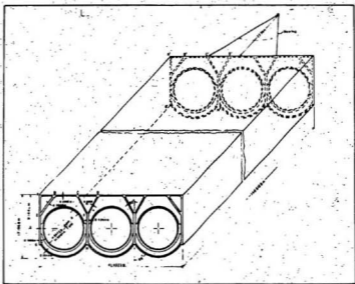
FIGURE 3.5. Schematic View of LPG Storage Platform
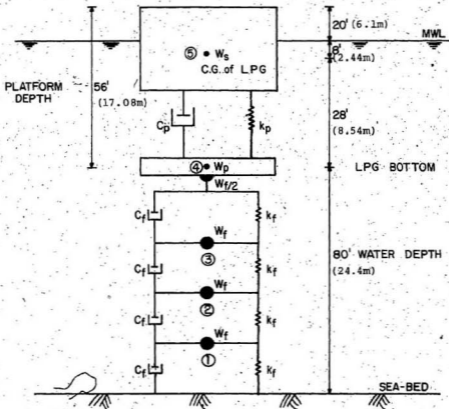
FIGURE 3.6. Trapped Water Model for LPG System

W_s per unit area was calculated to be 15.95 psi (110.01 kN/m^2).

The spring constant, K_p, force per unit deflection, was calculated from the design displacement as follows:

The design sagging moment of the platform supported by a wave trough $(Pl/4) = 700,000$ lb-ft. (950 kN-m). Therefore

$$P = 6073.75 \text{ lb. } (27.028 kN).$$

For the cantilever supported platform the maximum deflection

$$\delta = Pl^3/48EI.$$

Therefore $\delta = 0.0578'$ (0.0176m).

(The design deflection due to the hogging moment was less than the above.)

$K_p = 24.25$ psi per unit width (6,587.6 kN/m^2/unit width).

The damping coefficient is assumed to be 0.5% of the critical damping.

The water depth below the bottom of the structure is 80' (24.4m) divided into a series of 4 lumped mass, spring and damping systems with spacing of 20' (6.1m) each.

The weight of each mass $W_f = \gamma AS = 8.889$ psi (61.334 kN/m^2).

The spring constant $K_f = AE/S$. Assuming $E = 305$ kips/in^2 (2.105 x $10^6 kN/m^2$) and unit area, $K_f = 1270.8$ psi per unit width (345,217 kN/m^2 per unit width).

The damping C_E is assumed to be 0.5% of critical damping.

The above values are incorporated in the spring-mass system defined in Fig. 3.5, comprised of five degrees of freedom with modes 0, 1, 2, 3, 4 and 5, and analysed using the computer program TDYNE developed by Kennedy (1969). The results of the free vibration analysis are shown in Fig. 3.7. The mode shapes have an horizontal offset at the LPG bottom due to the deformations of the spring K_p connecting the rigid top portion of the LPG. The dynamic response of the system subjected to Taft earthquake loading, shown in Fig. 3.8, yielded the amplified accelerations transmitted to the bottom of the LPG (node 4), shown in Fig. 3.9. Table 3.1 shows that the peak accelerations are magnified 30 times which is a significant effect.

TABLE 3.1

Trapped Water Model - Peak Acceleration at the LPG Bottom
and the Amplification Factor

Damping	First Mode Period (sec.)	Second Mode Period (sec.)	Third Mode Period (sec.)	Peak Accn. Bottom Accn. of LPG (g's)	Peak Accn. Seabed (g's)	Amplification Factor
0.5%	0.27	0.069	0.025	-6.14	-0.1765	30.8

3.3.2 Amplified Acceleration at the Bottom of the FNP Platform

The second example chosen is a floating nuclear plant platform (proposed off the New Jersey coast) the cross-section of which is shown in Figure 3.10. The 'Trapped Water Model' of the platform installed in a water depth of 72' (21.96m) is as shown in Fig. 3.11.

MODE	1	2	3
FREQUENCY (rad/sec)	3.709	14.716	40.721
PERIOD (sec)	0.27	0.069	0.025

108' (32.94m)
80' (24.4m)
60' (18.3m)
40' (12.2m)
20' (6.1m)
SEA-BED
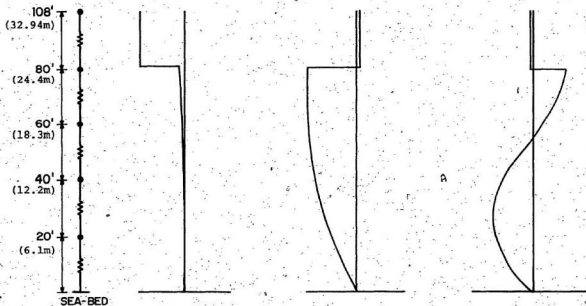
FIGURE 3.7: Frequencies and Mode Shapes of the Fluid-Structure Column of LPG System
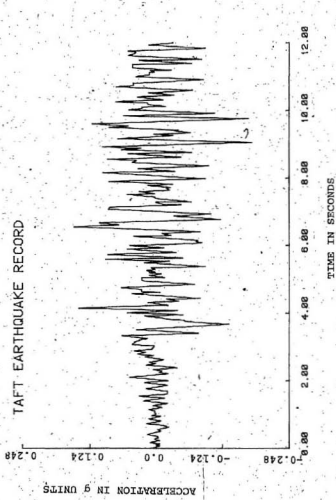
FIGURE 3.8. Time History of the Taft Earthquake — Vertical Acceleration Component
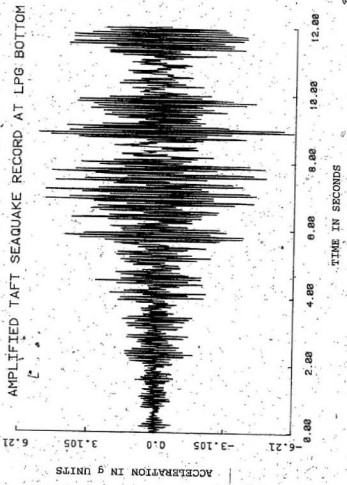
FIGURE 3.9. Time History of Amplified Vertical Acceleration Acting at the Bottom of LPG Platform

Closure Breakwater Caisson
Condenser Water Discharge
Crown Elevation, Closure Breakwater Roundhead = +32'
Submarine Discharge Conduit
Cooling Water Intake
Condenser Water Discharge
Platform
400.25'
375.75'
Platform
Mooring Caisson
Mooring Strut (8 per Platform)
Main Breakwater Caisson
Main Breakwater
Main Breakwater Crown, Elevation = +66'
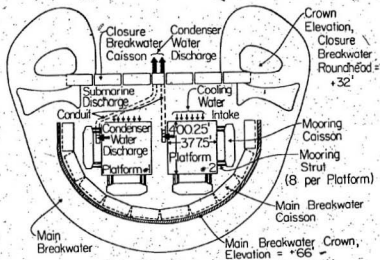
(a) Plan View of the Facility

FIGURE 3.10. Schematics of FNP Platform
(ref. Dotson and Orr, 1973)
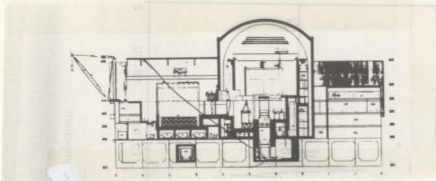
(b) Sectional View
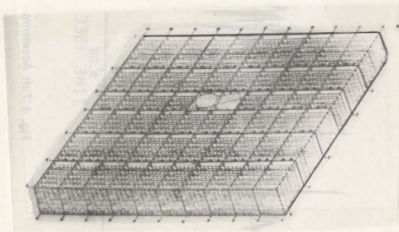
(c) Isometric View of the Platform

FIGURE 3.10. Schematic of FNP Platform (contd.)
(ref. Dotson and Orr, 1973)
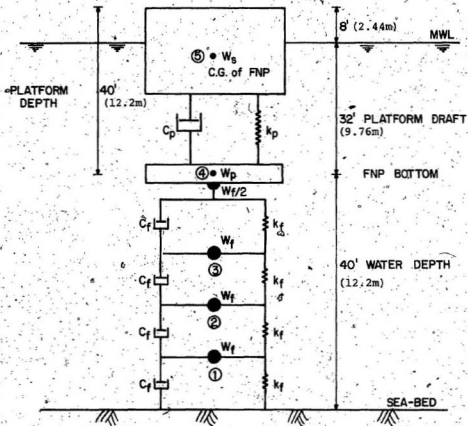
FIGURE 3.11: Trapped Water Model for FNP System

The steel platform has a plan area of 400' x 378',(122m x 115.29m), a depth of 40'(12.2m) and a draft of 32'(9.76m). The mass, stiffness, and damping values of the trapped water model of FNP are calculated as shown below:

Gross displacement of the platform is 300,000 kips(1.335 x 10^6kN). A major portion of the weight proportional to the draft/depth ratio, was assumed as W_s =194,920 kips(867,400 kN). Hence W_s per unit area = 8.952 psi(61.77 kN/m^2). The weight of the minor portion, W_p = 105,080 kips(467,600 kN). Hence W_p per unit area = 4.825 psi(33.29 kN/m^2). The spring stiffness, K_p, is calculated based on the design sagging moment as shown in the previous section to be equal to 14.684 psi/unit width (3988.9 kN/m^2/unit width). The damping, C_p, is assumed to be 0.5% of the critical damping.

The 40'(12.2m) water column below the platform is divided into four linear springs, masses, and dashpots system with spacing of 10' (3.05m).

Spring stiffness, K_f = AE/S = 2541.67 psi/unit width (6.9 x 10^5 kN/m^2/unit width).

Fluid weight, W_f = γAS = 4.44 psi (30.636 kN/m^2).

The fluid damping was assumed to be 0.5% of the critical damping.

Again, TDYNE was used for the free and forced vibration (subjected to Taft earthquake) analyses of this system. The results are shown in Figs. 3.12 and 3.13.

MODE	1	2	3
FREQUENCY (rad/sec)	5388	20.239	6.5321
PERIOD (sec)	0.18	0.049	0.015

72' (21.96m)   C.G. OF FNP

40' (12.20m)

30' (9.15m)

20' (6.1m)

10' (3.05m)

0   SEA-BED
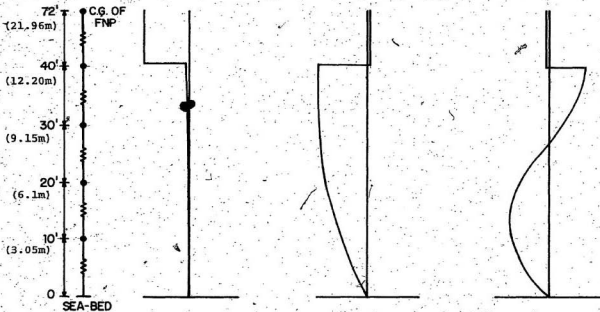
FIGURE 3.12: Frequencies and Mode Shapes of the Fluid-Structure Column of FNP Platform

AMPLIFIED TAFT SEAQUAKE RECORD AT FNP BOTTOM
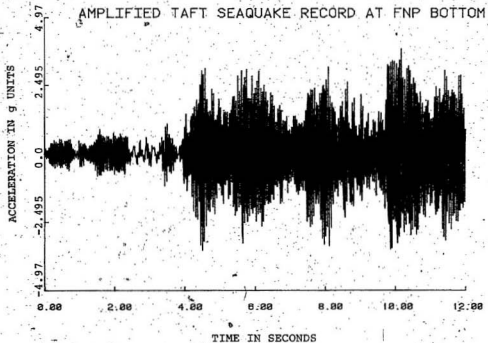
FIGURE 3.13. Time History of Amplified Vertical Acceleration Acting at the Bottom of FNP Platform

Table 3.2 shows that the amplification of the peak accelera-
tion from the seabed to FNP bottom is about 22, again a
significant value.

TABLE 3.2

Trapped Water Model of FNP - Peak Acceleration at the FNP Bottom
and the Amplification Factor

Damping	First Mode Period (sec.)	Second Mode Period (sec.)	Third Mode Period (sec.)	Peak Accn. FNP Bottom (g's)	Peak Accn. Seabed (g's)	Amplification Factor
0.51	0.8	0.049	0.015	-3.81	-0.1765	21.9

3.4 Discussion

From the above analysis, it is very clear that the seaquake
phenomenon is a more severe one compared to the earthquake. The
amplification factors of water transmitted earthquake
accelerations have been computed to be of the order 20 to 30.
But it is necessary to keep in mind that these calculations were
performed using a linear spring model and idealizing the water
medium into four discrete mass-spring equivalents. The results
can further be improved by using nonlinear springs as well as
subdividing the water medium into a greater number of lumped
masses and springs.

The cavitation effect has to be studied for its effect on the
amplification factor.

CHAPTER 4

FINITE ELEMENT DYNAMIC ANALYSIS OF FLOATING PLATFORMS

4.1 Introduction

Small oscillations of floating platforms in a fluid medium cause the fluid in contact with the platform also to move with it. This, inturn, induces an additional mass or inertia to the body which is termed as "hydrodynamic added mass". Again, the oscillations of the platform generate outgoing waves which are radiated outwards to infinity. A portion of the energy of the oscillating platform is utilized in creating these waves; within the framework of linear analysis and small amplitudes, this energy loss is directly proportional to the radiation damping force of the body. This is a harmonic conjugate to the added mass of the body in harmonic oscillations and is known as "hydrodynamic added damping". The cushioning effect of the supporting fluid medium offers an additional restoring stiffness to the platform which is directly proportional to the bulk modulus of water and is termed "hydrodynamic added stiffness". The evaluation of these hydromechanical properties and their effects on the dynamic response of floating platforms are discussed below.

4.2 Literature Overview

Complex coupled fluid-structure interaction problems have been treated by various researchers with different degrees of simplifications and complexities. Earlier

investigations of the coupled problems avoided the flexibility of the structure extra effort required to determine the complex frequency dependent added mass and damping coefficients and the forces associated with the wave diffraction effect. In principle, this problem is a three dimensional non-linear one but the non-linearities in the governing fluid equations of motion (Navier-Stokes Equation) and the Bernoulli's pressure conditions can be neglected if the derivative of the squares of the velocities are assumed to be small in comparison to the accelerations of the water particles. The non-linearities in the surface wave condition can also be disregarded when the ratio between the maximum wave height and the main dimension of the floating body is very small compared to unity. In linearized form the vibration of a floating body, in an incompressible and inviscid fluid of finite depth with a free surface, can be described by a boundary value problem governed by Laplace's equation with specified boundary conditions at the free surface, at the sea bottom, radiation damping at infinity, and at the fluid-structure interface. In order to alleviate the difficulties involved in solving the three dimensional problem, which is prohibitively expensive, most of the researchers have solved coupled problems using the simplified two-dimensional linear problem which describes adequately the motion of large floating structures.

Finite element applications to coupled fluid-structure interaction studies of bottom fixed and floating structures, incorporating surface waves and radiation damping boundary conditions, have been reported by Zienkiewicz, Irons and Nath (1966), and Zienkiewicz and Newton (1969). Transient response analysis of a fluid-structure system using the Lagrangian approach has been illustrated by Shantaram, Owen and Zienkiewicz (1976), and Wilson (1977). Dubois and de Rouvray (1978) formulated the free surface waves by the Lagrangian approach eliminating the fluid Eulerian equations, thus leading to a symmetric matrix equation for the dynamic fluid-structure-surface wave equilibrium. Dynamic analysis of a floating nuclear plant modelled with three dimensional beam elements supported on elastic springs has been reported by Johnson et al. (1975).

Studies on fluid-structure interaction using Euler-Lagrangian formulations include those of Wang, Cheng and Fistedis (1977), Wertheimer and Marcal (1977), and Donea Fasoli-Stella and Guiliani (1977). Studies of the effects of site-structure interaction on the seismic response of floating nuclear plant have been carried out using two dimensional plane strain finite elements by Smith, Vaish and Porter (1977). Infinite elements have been used by Zienkiewicz and Bettess (1975) to model the fluid medium in the fluid-structure interaction study. In order to reduce the complexity and the size of the fluid-structure problem,

Kaul (1977) proposed a procedure wherein the interactive effective forces of the fluid, obtained by isolating the fluid from the structure, are used to determine the structural response. A "Doubly Asymptotic Approximation Technique" together with the finite element method has been used by Geers (1975) and Geers and Felippa (1977) to solve the unsymmetric coupled equations describing the fluid-structure interaction. The use of NASTRAN for the coupled vibration analysis of submerged plates has been illustrated by Marcus (1978). A procedure to extend the finite element method to handle the unbounded fluid domain was described by Zaida (1976) and Hunt et al. (1974) by matching the finite element solutions computed at the finite fluid boundaries with known analytical solutions for the infinite fluid. Other hydrodynamic related studies using the finite element method include those of Chakrabarti and Chopra (1973), Sharan and Gladwell (1977), Wilson (1975), Saini, Zienkiewicz and Bettess (1976a, 1976b) analysing the dam-reservoir-foundation systems, Liaw and Chopra (1973) on offshore in-take towers, and Penzien and Tseng (1977) on fixed offshore platforms. The incorporation of wave forces in dynamic fluid-structure interaction studies has been described by Zienkiewicz and Bettess (1978a, 1978b).

4.3 Coupled Fluid-Structure Formulation

As mentioned earlier, a two dimensional plane strain finite element formulation of the coupled fluid-structure interaction which takes into account the fluid

compressibility, structural flexibility, surface wave effects, radiation damping condition, and scattered wave effects is presented below.

4.3.1 Structure Idealization

An eight-noded isoparametric rectangular plane strain element shown in Fig. 4.1 is used for discretizing the floating structure.

4.3.1.1 Two Dimensional Isoparametric Structural Element
(Lagrangian Displacement Approach)

The first step in isoparametric finite element formulation is to achieve a relationship between the element displacements at any point and the element nodal point displacements with the use of "Shape Functions". Isoparametric elements are those in which the same shape functions relate the global coordinate system (x, y) to the natural coordinates (ς, η) (refer Fig. 4.1). The basic procedure is to express the element coordinates and displacements in the form of shape functions using the natural coordinate of the system (ς, η). The shape functions are defined in such a way that the natural coordinates vary as $-1 \leq \varsigma \leq 1$, $-1 \leq \eta \leq -1$.

For the two dimensional isoparametric element shown in Fig. 4.1 the coordinate relationships are:
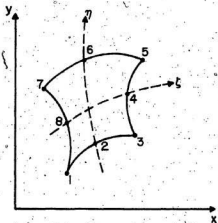
(a) Global Coordinate System
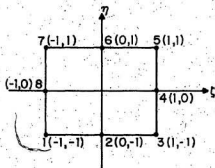
(b) Natural Coordinate System

FIGURE 4.1. Mapping of Two-dimensional Isoparametric
Element

$$x^e = \sum_{i=1}^{8} N_i x_i^e \qquad (4.3.1)$$

$$y^e = \sum_{i=1}^{8} N_i y_i^e$$

where N_i are shape functions, x and y are coordinates at any point of the element, and x_i, y_i, $i=1, 2...8$ are the nodal coordinates. The displacement relationships are:

$$\{\delta\}^e = \begin{Bmatrix} u^e \\ v^e \end{Bmatrix} = \begin{Bmatrix} \sum_{i=1}^{8} N_i^e u_i^e \\ \sum_{i=1}^{8} N_i^e v_i^e \end{Bmatrix} \qquad (4.3.2)$$

where u and v are the horizontal and vertical displacements at any point in the element and u_i, v_i, $i=1, 2...8$ are the nodal displacements.

The chosen interpolation functions (shape functions) satisfying the requirements of unit values at node i and zeros at all other nodes in the natural coordinate system, are given below:

$$N_i = 1/4 \ (1+\zeta\zeta_i)(1+\eta\eta_i)(\zeta\zeta_i+\eta\eta_i-1) \quad \text{for } i=1,3,5,7$$
$$N_i = 1/2 \ (1-\zeta^2)(1+\eta\eta_i) \qquad\qquad \text{for } i=2,6 \quad (4.3.3)$$
$$N_i = 1/2 \ (1+\zeta\zeta_i)(1-\eta^2) \qquad\qquad \text{for } i=4,8$$

4.3.1.2 Stiffness Matrix

The element strains are given by:

$$
\begin{Bmatrix} \epsilon_x \\ \epsilon_y \\ \gamma_{xy} \end{Bmatrix} = \begin{Bmatrix} \partial u/\partial x \\ \partial v/\partial y \\ \partial u/\partial y + \partial v/\partial x \end{Bmatrix} \tag{4.3.4}
$$

The relationship between the displacement derivatives in natural and global coordinates is:

$$
\begin{Bmatrix} \partial/\partial \zeta \\ \partial/\partial \eta \end{Bmatrix} = \begin{bmatrix} \partial x/\partial \zeta & \partial y/\partial \zeta \\ \partial x/\partial \eta & \partial y/\partial \eta \end{bmatrix} \begin{Bmatrix} \partial/\partial x \\ \partial/\partial y \end{Bmatrix} \tag{4.3.5}
$$

i.e.,
$$
\begin{Bmatrix} \partial/\partial \zeta \\ \partial/\partial \eta \end{Bmatrix} = J \begin{Bmatrix} \partial/\partial x \\ \partial/\partial y \end{Bmatrix} \tag{4.3.6}
$$

where J is the Jacobian Matrix. Using Eqn. 4.3.3

$$
[J] = \begin{bmatrix} \sum_{i=1}^{8} x_i\, \partial N_i/\partial \zeta & \sum_{i=1}^{8} y_i\, \partial N_i/\partial \zeta \\ \sum_{i=1}^{8} x_i\, \partial N_i/\partial \eta & \sum_{i=1}^{8} y_i\, \partial N_i/\partial \eta \end{bmatrix} = \begin{bmatrix} \bar{A}_{11} & \bar{A}_{12} \\ \bar{A}_{21} & \bar{A}_{22} \end{bmatrix} \tag{4.3.7}
$$

the determinant of the Jacobian matrix is given below:

$$
\det = (\bar{A}_{11}\,\bar{A}_{22} - \bar{A}_{21}\,\bar{A}_{12}) \tag{4.3.8}
$$

Therefore,

$$
[J]^{-1} = \begin{bmatrix} \bar{A}_{22}/\det & -\bar{A}_{12}/\det \\ -\bar{A}_{21}/\det & \bar{A}_{11}/\det \end{bmatrix} = \begin{bmatrix} A_{11} & A_{12} \\ A_{21} & A_{22} \end{bmatrix} \tag{4.3.9}
$$

As seen from Eqn. 4.3.7, the Jacobian matrix is a function of (ζ, η)

From Eqn. 4.3.6

$$\begin{Bmatrix} \partial/\partial x \\ \partial/\partial y \end{Bmatrix} = [J]^{-1} \begin{Bmatrix} \partial/\partial \zeta \\ \partial/\partial \eta \end{Bmatrix} \qquad (4.3.10)$$

Similarly, the transformation of derivatives of the coordinates with respect to which integrations are performed is given as:

$$dA = dx\,dy = \det d \zeta d \eta \qquad (4.3.11)$$

The strain displacement equation, 4.3.4, can be rewritten as:

$$\begin{Bmatrix} \varepsilon_x \\ \varepsilon_y \\ \gamma_{xy} \end{Bmatrix} = \begin{bmatrix} \partial/\partial x & 0 \\ 0 & \partial/\partial y \\ \partial/\partial y & \partial/\partial x \end{bmatrix} \begin{Bmatrix} u \\ v \end{Bmatrix} \qquad (4.3.12)$$

Using Eqn. 4.3.2 in Eqn. 4.3.12 will yield a relation

$$\{\varepsilon\} = [B]\{\delta\}, \qquad (4.3.13)$$

where

$$[B] = \begin{bmatrix} \partial N_i/\partial x & 0 \\ 0 & \partial N_i/\partial y \\ \partial N_i/\partial y & \partial N_i/\partial x \end{bmatrix} \qquad (4.3.14)$$

For a plane strain orthotropic case, the stress and strain can be related as:

$$\{\sigma\} = [D]\{\varepsilon\} \qquad (4.3.15)$$

where

$$D = \frac{E_y}{[(1+v_x)(1-v_x-2nv_y^2)]} \begin{bmatrix} c_{11} & c_{12} & c_{13} \\ c_{21} & c_{22} & c_{23} \\ c_{31} & c_{32} & c_{33} \end{bmatrix}$$

in which

E_x and E_y are the Young's moduli, v_x and v_y are the Poisson's ratios in the x and y directions, G is the shear modulus of the orthotropic material, $E_x/E_y = n$, $G/E_y = m$,

$c_{11} = n(1-nv_y^2)$,

$c_{12} = nv_y(1+v_x)$,

$c_{13} = 0$,

$c_{21} = nv_y(1+v_x)$,

$c_{22} = (1-v_x^2)$,

$c_{23} = 0$,

$c_{31} = 0$,

$c_{32} = 0$,

and

$c_{33} = m(1+v_x)(1-v_x-2nv_y^2)$.

From the principle of virtual work, the strain energy per unit area (for a two-dimensional plane strain) is equal to the workdone by the external forces, i.e.,

$$\int_A (\epsilon)^T (\sigma) dA = (\delta)^T (F) \qquad (4.3.17)$$

where F is the column of external forces, and A is the area of integration.

Substituting Eqs. 4.3.13 and 4.3.15 in Eqn. 4.3.17 and imposing unit virtual displacements at all nodes leads to the equilibrium equation

$$[K]^e \{6\}^e = \{F\}^e \qquad (4.3.18)$$

where

$$[K]^e = \int_A B^T DB dA \qquad (4.3.19)$$

is called the stiffness matrix of the element, and $[F]^e$ is the sum of all the external forces including body forces.

In order to calculate the stiffness matrix in the natural coordinates, the matrix B must be transformed into natural coordinates. This can be achieved by using Eqn. 4.3.10 in conjunction with Eqn. 4.3.14 and including the relation 4.3.11.

Hence, the stiffness matrix in natural coordinates can be written as:

$$[K]^e = \int_{-1}^{1} \int_{-1}^{1} B^T DB \det d\xi d\eta \qquad (4.3.20)$$

Exact integration of the above expression could be troublesome for complicated, curved and distorted elements. In such cases, numerical integration is the preferred alternative. Of the various numerical integration procedures available (Kopal, 1961; Irons, 1971; Hellen, 1972), the Gaussian quadrature formula, which requires the least number of points of evaluation is ideally suited for

such types of integrations (Zienkiewicz, 1977).

For the plane strain element assuming that $B^T DB$ det is constant through the (unit) thickness, the element stiffness matrix can be evaluated using a fourth order Gaussian quadrature formula as:

$$[K]^e_{ij} = \sum_{i=1}^{4} \sum_{j=1}^{4} H_i H_j B^T_{ij} DB_{ij} \text{ det} \qquad (4.3.21)$$

The weighting coefficients for the required order of the formula can be chosen from Table 4.1.

4.3.1.3 Mass Matrix

The mass matrix due to the inertia force of the vibrating structure (proportional to its acceleration) can be evaluated using the relation:

$$[M]^e = \int_A N^T \rho_s N dA \qquad (4.3.22)$$

where ρ_s is the mass per unit area of the structure.

Again, using the fourth order Gaussian quadrature formula the elements of the mass matrix can be evaluated from the relation:

$$[M]^e_{ij} = \sum_{i=1}^{4} \sum_{j=1}^{4} \rho_s H_i H_j N^T_{ij} N_{ij} \text{ det } [J] \qquad (4.3.23)$$

The mass matrix $[M]^e$ is the distributed element mass matrix known as the 'consistent mass matrix'.

TABLE 4.1

Abscissae and Weight Coefficients of the

Gaussian Quadrature Formula

(Ref. Zienkiewicz, 1977)

$$\int_{-1}^{1} f(x)\, dx = \sum_{j=1}^{n} H_j f(a_j)$$

±a		H
0	n = 1	
		2.00000 00000 00000
0.57735 02691 89626	n = 2	
		1.00000 00000 00000
0.77459 66692 41483	n = 3	0.55555 55555 55556
0.00000 00000 00000		0.88888 88888 88889
0.86113 63115 94053	n = 4	0.34785 48451 37454
0.33998 10435 84856		0.65214 51548 62546
0.90617 98459 38664	n = 5	0.23692 68850 56189
0.53846 93101 05683		0.47862 86704 99366
0.00000 00000 00000		0.56888 88888 88889
0.93246 95142 03152	n = 6	0.17132 44923 79170
0.66120 93864 66265		0.36076 15730 48139
0.23861 91860 83197		0.46791 39345 72691
0.94910 79123 42759	n = 7	0.12948 49661 68870
0.74123 11855 99394		0.27970 53914 80277
0.40584 51513 77397		0.38183 00505 05119
0.00000 00000 00000		0.41795 91836 73469
0.96028 98564 97536	n = 8	0.10122 85362 90376
0.79666 64774 13627		0.22238 10344 53374
0.52553 24099 16329		0.31370 66458 77887
0.18343 46424 95650		0.36268 37833 78362

4.3.1.4 Damping Matrix

The structural damping matrix is related non-linearly to the velocity of the structure. For simplicity, only linear

viscous damping is considered. In theory, the structural damping matrix can be evaluated using the relation:

$$[C]^e = \int_A N^T \nu_s N \, dA \qquad (4.3.24)$$

where ν_s is a constant evaluated based on the damping characteristics of the structure and A is the area of integration. In practice, it is rather difficult to define this parameter since the damping properties are frequency dependent (Ref. Bathe and Wilson, 1976). For this reason [C] is, in general, not evaluated using the above relation but is constructed using the stiffness and mass matrices of the structural system together with the experimental results of the damping. The most commonly used procedure is the 'Rayleigh damping' technique in which it is assumed that

$$[C]^e = \alpha [M]^e + \beta [K]^e \qquad (4.3.25)$$

where α and β are damping constants determined from two known damping ratios (experimentally determined) corresponding to two unequal frequencies of vibration. Bathe and Wilson (1976) illustrate the method of determining these constants for multidegree of freedom systems.

Since the damping matrix [C] is constructed using the consistent mass matrix, this also can be termed the consistent damping matrix.

4.3.1.5 Force Matrix

If {q} is the total load vector due to body forces, surface traction and other external loads, then the

consistent load matrix can be evaluated from the relation:

$$(F)^e = \int_A N^T q dA \qquad (4.3.26)$$

i.e.,

$$(F_i)^e = \sum_{i=1}^{4} \sum_{j=1}^{4} \bar{H}_i H_j N_{ij} q_i \det \qquad (4.3.27)$$

Once the element matrices are developed the assembly of matrices can be achieved by summing all the element matrices. The summation concerns only those portions of the matrices which contribute to a node. Thus,

$$[K] = \sum_{e=1}^{m} [K]^e \qquad (4.3.28)$$

etc., where m is the number of elements.

The resulting dynamic equations of motion of the floating structure is of the form:

$$[M] \{\ddot{\delta}\} + [C] \{\dot{\delta}\} + [K] \{\delta\} = \{F\} \qquad (4.3.29)$$

where

[M], [C], and [K] are the mass, damping, and stiffness

matrices of the structure, respectively;

$\{\ddot{\delta}\}$, $\{\dot{\delta}\}$, and $\{\delta\}$ are the displacement, velocity and acceleration

vector of the overall structure, respectively;

and

$\{F\}$ is the total external force acting on the structure.

For the coupled problem, the force vector can be divided into two parts as:

$$\{P\} = \{R\} + \{\bar{P}\} \qquad (4.3.30)$$

where

$\{R\}$ is a vector of external static or dynamic loads, e.g., earthquake load,

and

$\{\bar{P}\}$ is a force vector due to the interface fluid pressure.

4.3.1.6 Fluid-Structure Interface Coupling Matrix

The displacement of the structure causes hydrodynamic pressure, in excess to the hydrostatic pressure, normal to the fluid-structure interface and acting towards the structure.

Using Eqn. 4.3.2 the displacement at any point in the structure can be expressed as:

$$\{\delta\} = \sum_{e=1}^{m} [N]^e \{\delta\}^e = [N]\{\delta\} \qquad (4.3.31)$$

where

$\{\delta\}$ is the overall structural displacement vector,

and

m is the number of elements

The force due to hydrodynamic pressure at the structure-fluid interface determines the coupling between

the structure and fluid. This force can be written as:

$$(P) = [S](p) \qquad (4.3.32)$$

where [S] is the interface coupling matrix, the elements of which can be evaluated using the expression:

$$[S]_{ij} = \int_{\Gamma_i} N_i \, n \, N_j \, d\Gamma \qquad (4.3.33)$$

and (p) is the generalized pressure coordinates of the fluid elements. In the above relation, n is the unit normal vector at the interface and the integration is carried over the interface region Γ_i. It is to be noted that the matrix [S] will have non-zero elements corresponding to the interface nodes only.

4.3.2 Fluid Idealization

4.3.2.1 Governing Equation

If p is the pressure in excess of the hydrostatic pressure, then the Navier-Stokes equations of the compressible and viscous fluid motion in the two dimensional cartesian coordinates (x, y) are given as:

$$- \partial u_f / \partial t = 1/\rho_f \; \partial p / \partial x + [u_f \; \partial u_f / \partial x + v_f \; \partial u_f / \partial y]$$
$$- \mu_f / \rho_f \; \nabla_x^2 \; u_f - \mu_f / 3\rho_f \; \partial / \partial x \; [\partial u_f / \partial x + \partial v_f / \partial y]$$
$$(4.3.34a)$$

and

$$- \partial v_f / \partial t = 1/\rho_f \; \partial p / \partial y + [u_f \; \partial v_f / \partial x + v_f \; \partial v_f / \partial y]$$
$$- \mu_f / \rho_f \; \nabla^2 \; v_f - \mu_f / 3\rho_f \; \partial / \partial y \; [\partial u_f / \partial x + \partial v_f / \partial y]$$
$$(4.3.34b)$$

where u_f and v_f are the fluid velocity components in the x and y directions respectively, ρ_f is the fluid mass density, and ν_f is the fluid viscosity.

For a fluid phase with the basic assumption that:

i) the viscous forces are negligible, and

ii) the accelerations and velocities are so small that the convective acceleration terms can be neglected,

the above equation simplifies to:

$$\partial u_f/\partial t = - 1/\rho_f \; \partial p/\partial x \qquad (4.3.35a)$$

$$\partial v_f/\partial t = - 1/\rho_f \; \partial p/\partial y \qquad (4.3.35b)$$

The continuity relation is:

$$\partial u_f/\partial x + \partial v_f/\partial y + 1/K \; \partial p/\partial t = 0 \qquad (4.3.36)$$

where K is the bulk modulus of the fluid.

Eliminating the velocities from the above two equations yields:

$$- 1/\rho_f \; (\partial^2 p/\partial x^2 + \partial^2 p/\partial y^2) + 1/k \; \partial^2 p/\partial t^2 = 0 \qquad (4.3.37)$$

i.e.,

$$\nabla^2 p - \rho_f/K \; \partial^2 p/\partial t^2 = 0 \qquad (4.3.38)$$

Introducing the pressure wave velocity for deep waters

$$a^2 = K/\rho_f \qquad (4.3.39)$$

in the above equation yields the governing equation

$$\nabla^2 p - 1/a^2 \; p = 0 \qquad (4.3.40)$$

where ∇^2 is the Laplacian operator.

An alternative representation of the fluid motion is obtained by introducing a velocity potential related to the pressure by the relation:

$$p = -\rho_f \, \partial\phi/\partial t \qquad (4.3.41)$$

and the velocity components by

$$u = \partial\phi/\partial x, \text{ and } v = \partial\phi/\partial y. \qquad (4.3.42)$$

Either p or ϕ can be used in the fluid formulation.

4.3.2.2 Boundary Conditions

i) The normal velocity at the fluid-structure interface can be expressed in terms of the pressure gradient as:

$$1/\rho_f \, \partial p/\partial n = -\partial v_n/\partial t \qquad (4.3.43)$$

where v_n is the velocity in the normal direction to the interface.

ii) The free surface wave pressure at the surface, y = 0, is:

$$p = \rho_f g \zeta \qquad (4.3.44)$$

where ζ is the surface elevation of the wave above the mean sea water level.

Defining

$$\partial\zeta/\partial t = v_f \qquad (4.3.45)$$

i.e.,

$$\partial^2\zeta/\partial t^2 = \partial v_f/\partial t, \qquad (4.3.46)$$

differentiating Eqn. 4.3.44 twice with respect to t, and using relations 4.3.46 and 4.3.35b yields

$$\partial^2 p / \partial t^2 = \rho_f g (\partial^2 \xi / \partial t^2) = \rho_f g (-1/\rho_f \ \partial p / \partial y) \qquad (4.3.47)$$

i.e.,

$$\partial p / \partial y = - (1/g) \ \partial^2 p / \partial t^2 \qquad (4.3.48)$$

is the boundary condition due to the surface gravity waves.
In the absence of gravity waves the pressure at the surface
is zero.

iii) The boundary condition at the sea bottom, the Neumann
condition is

$$\partial p / \partial y = 0 \qquad (4.3.49)$$

iv) The infinite boundary of the fluid medium can be
truncated to a finite region by imposing the radiation
boundary condition (Newton, 1975, Zienkiewicz and
Newton, 1969). The general solution of the wave
equation is

$$p = f_1 (x+ct) + f_2 (x-ct) \qquad (4.3.50)$$

At large distances of x, the waves are only plane and
outgoing. Hence:

$$p = f_2 (x-ct) \ as \ x \to \infty \qquad (4.3.51)$$

In the above equations

$$c = \sqrt{(g\lambda / 2\Pi) \tanh kh} \qquad (4.3.52)$$

where k is the wave number, $2\Pi / \lambda$.

For deep water $h \to \infty$, i.e., $c = \sqrt{g\lambda / 2\Pi}$

For shallow water $\tanh kh \to kh$, i.e., $c = \sqrt{gh}$

Differentiation of Eqn. 4.3.51 yields

$$\partial p/\partial t = -cf_2 \qquad (4.3.53)$$

and

$$\partial p/\partial x = f_2' \qquad (4.3.54)$$

Eliminating f_2' from the above equations gives the radiation boundary condition as

$$\partial p/\partial x + 1/c \; \partial p/\partial t = 0 \qquad (4.3.55)$$

The above equation is called as the Sommerfeld radiation condition applicable at a finite distance from the structure.

Eqs. 4.3.40 to 4.3.55 define the fluid problem completely.

4.3.2.3 Fluid Matrices (Eulerian Pressure Formulations)

The fluid domain also is discretised using a similar isoparametric element to what is shown in Fig. 4.1. Thus, similar to the structural displacement vector (Eqn. 4.3.31), the pressure at any point of the fluid region $\{p\}$ can be expressed in terms of the vector of its nodal pressures $\{p\}$ as

$$\{\bar{p}\} = [N] \; \{p\} \qquad (4.3.56)$$

The shape functions, N, are defined in Eqn. 4.3.3. In the following sections the fluid matrices are developed in global coordinates. In actuality, the transformations (Section 4.3.2) from the local to the global coordinate system hold good for this section, and no specific reference or distinction between them are indicated.

Applying Galerkin's weighted residual procedure to the governing Eqn. 4.3.40 of the fluid, the ith weighted residual equation can be written as:

$$\int_A N_i [\nabla^2 p - 1/c^2 \ddot{p}] \, dA = 0 \qquad (4.3.57)$$

Using Green's theorem the above equation can be transformed to

$$\int_A (\partial N_i/\partial x \; \partial p/\partial x + \partial N_i/\partial y \; \partial p/\partial y) \, dA - 1/c^2 \int_A N_i \, \ddot{p} \, dA$$

$$+ \int_{\Gamma_b} N_i \; \partial p/\partial n \; d\Gamma = 0 \qquad (4.3.58)$$

where Γ_b is the boundary of the region A, and n is the outgoing normal at the fluid-structure interface.

Introducing Eqn. 4.3.56 in the above yields:

$$\int_A (\partial N_i/\partial x \; \partial N_j/\partial x + \partial N_i/\partial y \; \partial N_j/\partial y) \, p \, dx \, dy$$

$$- 1/c^2 \int_A N_i \, N_j \, \ddot{p} \, dx \, dy = - \int_{\Gamma_b} N_i \; \partial p/\partial n \; d\Gamma \qquad (4.3.59)$$

and Defining

$$G_{ij}^e = \int_A (\partial N_i/\partial x \; \partial N_j/\partial x + \partial N_i/\partial y \; \partial N_j/\partial y) \, dx \, dy, \qquad (4.3.60)$$

$$H_{ij} = 1/c^2 \int_A N_i N_j \, dx \, dy, \qquad (4.3.61)$$

and

$$E_i^e = \int_{\Gamma_b} N_i \, \partial p / \partial n \, d\Gamma, \qquad (4.3.62)$$

Eqn. 4.3.59 can be rewritten, after assembling all the element matrices as:

$$[H] \{\ddot{p}\} + [G] \{p\} = [E] \qquad (4.3.63)$$

where [G] is analogous to the 'fluid stiffness' matrix, [H] is the 'fluid inertia' matrix, and [E] takes care of the incorporation of pressure gradient conditions at different fluid boundaries, such as the free surface wave, radiation damping and the coupling of fluid-structure interface boundaries. The sea bottom condition does not contribute to this matrix since the normal derivative of the pressure is zero.

Prescribing the surface wave condition 4.3.49 in Eqn. 4.3.62 yields:

$$E_{wi} = \int_{\Gamma_s} N_i \, (-1/g) \, \ddot{p} \, d\Gamma \qquad (4.3.64)$$

where Γ_s is the free surface boundary region.

Substituting Eqn. 4.3.56 in Eqn. 4.3.64, Eqn. 4.3.61 changes to:

$$H^e_{ij} = 1/c^2 \int_A N_i \, N_j \, dx \, dy + 1/g \int_{r_s} N_i \, N_j \, dr \qquad (4.3.65)$$

Therefore Eqn. 4.3.63 becomes

$$[H] \, \{\ddot{p}\} + [G] \, \{p\} = \{E_R\} + \{E_I\} \qquad (4.3.66)$$

where $[E_R]$ and $[E_I]$ are due to the contributions of radiation damping and fluid-structure interface.

Introducing the radiation boundary condition 4.3.63 in Eqn. 4.3.62 gives:

$$E_{R_i} = \int_{r_d} N_i \, (-1/c \; \partial p/\partial t) dr \qquad (4.3.67)$$

where r_d is the radiation boundary.

Again, introducing Eqn. 4.3.56 in the above and transferring to the other side of the equation changes Eqn. 4.3.66 to:

$$[H] \, \{\ddot{p}\} + [T] \, \{\dot{p}\} + [G] \, \{p\} = [F_I] \qquad (4.3.68)$$

where

$$[T]^e_{ij} = 1/c \int_{r_d} N_i \, N_j \, dr \qquad (4.3.69)$$

Combining the structure-fluid interface boundary condition 4.3.44 with Eqn. 4.3.32 gives

$$\partial p/\partial n = -\rho_f \, N_i \, n^T \, \ddot{\delta}_n \qquad (4.3.70)$$

Substituting Eqn. 4.3.70 in Eqn. 4.3.62 results in

$$E_I = \int_{\Gamma_i} N_i \ (-\rho_f N_j \ n^T \ddot{\delta}) \ d\Gamma \qquad (4.3.71)$$

where Γ_i is the structure-fluid interface boundary region.

From Eqn. 4.3.33, it can be noted that Eqn. 4.3.71 can be written as:

$$E_I = -\rho_f [S]^T \{\ddot{\delta}\} \qquad (4.3.72)$$

Assembling this term on the left hand side of Eqn. 4.3.68 yields

$$[H] \{\ddot{p}\} + [T] \{\dot{p}\} + [G] \{p\} + \rho_f [S]^T \{\ddot{\delta}\} = 0 \qquad (4.3.73)$$

4.3.3 Coupled Equation

Substituting Eqs. 4.3.32 and 4.3.30 in Eqn. 4.3.29 and combining with Eqn. 4.3.73 yields the coupled equation of fluid-structure interaction as

$$\begin{bmatrix} M & 0 \\ \rho_f S^T & H \end{bmatrix} \begin{Bmatrix} \ddot{\delta} \\ \ddot{p} \end{Bmatrix} + \begin{bmatrix} C & 0 \\ 0 & T \end{bmatrix} \begin{Bmatrix} \dot{\delta} \\ \dot{p} \end{Bmatrix} + \begin{bmatrix} K & S \\ 0 & G \end{bmatrix} \begin{Bmatrix} \delta \\ p \end{Bmatrix} = \begin{Bmatrix} R \\ 0 \end{Bmatrix}$$

$$(4.3.74)$$

If the external force acting on the structure is an earthquake acceleration transmitted through the water medium to the structure, then the above equation can be rewritten as:

$$
\begin{bmatrix} M & O \\ \rho_{\varepsilon}S^T & H \end{bmatrix} \begin{Bmatrix} \ddot{\delta} \\ \ddot{p} \end{Bmatrix} + \begin{bmatrix} C & O \\ O & T \end{bmatrix} \begin{Bmatrix} \dot{\delta} \\ \dot{p} \end{Bmatrix} + \begin{bmatrix} K & S \\ O & G \end{bmatrix} \begin{Bmatrix} \delta \\ p \end{Bmatrix} = \begin{Bmatrix} -[M]\{a\} \\ 0 \end{Bmatrix}
$$

$$(4.3.75)$$

where a is the acceleration vector due to the earthquake.

Though the individual matrices in the above equation are symmetric, the coupled equation is unsymmetric and unbanded. Hence, the popular numerical integration techniques are not applicable. A special procedure for the solution of the above equation is presented in the following section.

4.4. Numerical Solution of the Coupled Equations

As mentioned earlier, well-known numerical methods are not applicable for the coupled problem. A fourth order Runge-Kutta method has been used by Visser and van der Wilt (1975) to determine the non-stationary response of ship, assumed as a rigid body, floating in an infinite fluid. The stability of using a Newmark-type time step solution to an interior fluid-structure interaction problem has been studied by Schumann (1979), with reference to various aspects such as well-posedness (positive-definite) of the coupled equation, and sensitivity of the numerical procedure to round-off errors and numerical damping.

The transient response analysis of flexible structure

submerged in an infinite fluid medium has been performed by
Geers (1978) using a 'doubly asymptotic approximation' which
converts the fluid equation to a first order one in time.
The convergence, stability and accuracy of the resulting
'staggered solution procedure' has been proved by Park,
Felippa and Runtz (1977).

Sharan (1978) has adopted the popular Newmark-β method
to solve the coupled equation and has successfully applied
it to study the dam-reservoir-foundation interaction. The
procedure is proved to be stable for the cases with no
surface wave and radiation damping. A new numerical
integration technique, based on the Wilson-θ interpolation
scheme, is developed in the next section to solve the
coupled equations.

4.4.1 Proposed Numerical Integration Scheme

The governing structural and fluid matrix equations of
the coupled equations (4.3.74) can be rewritten as:

$$[K]\{\delta\} + [C]\{\dot{\delta}\} + [M]\{\ddot{\delta}\} + [S]\{p\} = \{R\} \qquad (4.4.1)$$

and

$$[G]\{p\} + [T]\{\dot{p}\} + [H]\{\ddot{p}\} + \rho_f [S]^T\{\ddot{\delta}\} = \{0\} \qquad (4.4.2)$$

The Wilson-θ method assumes a linear variation in
acceleration (Bathe and Wilson, 1976) over a time increment
$\tau = \theta \Delta t$, wherein for unconditional stability θ must be
greater than or equal to 1.37. The above equations at time

$(t+\tau)$ can be written as

$$[K]\{\delta\}_{t+\tau} + [C]\{\dot{\delta}\}_{t+\tau} + [M]\{\ddot{\delta}\}_{t+\tau} + [S]\{p\}_{t+\tau} = \{R\}_{t+\tau}$$

and
$$(4.4.3)$$

$$[G]\{p\}_{t+\tau} + [T]\{\dot{p}\}_{t+\tau} + [H]\{\ddot{p}\}_{t+\tau} + \rho_f [S]^T\{\ddot{\delta}\}_{t+\tau} = \{0\}$$

where
$$(4.4.4)$$

$$\{R\}_{t+\tau} = \theta\{R\}_{t+\Delta t} + (1-\theta)\{R\}_t$$
$$(4.4.5)$$

According to the linear acceleration assumption:

$$\dot{\delta}_{t+\tau} = \dot{\delta}_t + \tau/2 \; (\ddot{\delta}_{t+\tau} + \ddot{\delta}_t), \qquad (4.4.6a)$$

$$\dot{p}_{t+\tau} = \dot{p}_t + \tau/2 \; (\ddot{p}_{t+\tau} + \ddot{p}_t), \qquad (4.4.6b)$$

$$\delta_{t+\tau} = \delta_t + \tau\dot{\delta}_t + \tau^2/6 \; (\ddot{\delta}_{t+\tau} + 2\ddot{\delta}_t), \qquad (4.4.7a)$$

and

$$p_{t+\tau} = p_t + \tau\dot{p}_t + \tau^2/6 \; (\ddot{p}_{t+\tau} + 2\ddot{p}_t) \qquad (4.4.7b)$$

Substituting Eqs. 4.4.6 and 4.4.7 in Eqs. 4.4.3 and 4.4.4 will yield the following equation:

$$[A]\{\ddot{\delta}\}_{t+\tau} + \tau^2/6 \; [S]\{\ddot{p}\}_{t+\tau} = \{f_1\}_t \qquad (4.4.8)$$

$$\rho_f [S]^T\{\ddot{\delta}\}_{t+\tau} + [B]\{\ddot{p}\}_{t+\tau} = \{f_2\}_t \qquad (4.4.9)$$

where

$$[A7p] = [K] \tau^2/6 + [C] \tau/2 + [M], \quad (4.4.10)$$

$$[B] = [H] \tau^2/6 + [T] \tau/2 + [G], \quad (4.4.11)$$

$$\{f_1\}_t = - [K]\{g_1\}_t - [C]\{g_2\}_t - [S]\{g_3\}_t + \{R\}_t, \quad (4.4.12)$$

and

$$\{f_2\}_t = - [G]\{g_3\}_t - [T]\{g_4\}_t, \quad (4.4.13)$$

in which

$$\{g_1\}_t = \{\delta\}_t + \tau\{\dot{\delta}\}_t + \tau^2/3\{\ddot{\delta}\}_t, \quad (4.4.14)$$

$$\{g_2\}_t = \{\dot{\delta}\}_t + \tau/2\{\ddot{\delta}\}_t, \quad (4.4.15)$$

$$\{g_3\}_t = \{p\}_t + \tau\{\dot{p}\}_t + \tau^2/3\{\ddot{p}\}_t, \quad (4.4.16)$$

and

$$\{g_4\}_t = \{\dot{p}\}_t + \tau/2\{\ddot{p}\}_t, \quad (4.4.17)$$

Multiplying Eqn. 4.4.9 by $[B]^{-1}$ yields

$$\{\ddot{p}\}_{t+\tau} = [B]^{-1}\{f_2\}_t - \rho_f[B]^{-1}[S]^T\{\ddot{\delta}\}_{t+\tau} \quad (4.4.18)$$

Substituting Eqn. 4.4.18 in Eqn. 4.4.8 results in the following equation

$$[X]\{\ddot{\delta}\}_{t+\tau} = \{f_3\}_t \quad (4.4.19)$$

where

$$[X] = [A] - \rho_f \tau^2/6 \ [S] \ [B]^{-1} \ [S]^T, \qquad (4.4.20)$$

and

$$\{f_3\}_t = \{f_1\}_t - \tau^2/6 \ [S] \ [B]^{-1} \ \{f_2\}_t. \qquad (4.4.21)$$

Eqn. 4.4.19 can be solved to determine $\{\delta\}_{t+\tau}$

Eqn. 4.4.9 can be rewritten as

$$[B] \ \{p\}_{t+\tau} = \{f_4\}_t \qquad (4.4.22)$$

where

$$\{f_4\}_t = \{f_2\}_t - \rho_f \ [S]^T \ \{\ddot{\delta}\}_{t+\tau} \qquad (4.4.23)$$

Again, Eqn. 4.4.22 can be solved after using the values of $\{\ddot{\delta}\}_{t+\tau}$ in Eqn. 4.4.23 and $\{p\}$ can be determined.

Then the displacement and pressure and their derivatives at time $(t+\Delta t)$ can be evaluated by using the relations:

$$\{\ddot{\delta}\}_{t+\Delta t} = (1-1/\theta) \ \{\ddot{\delta}\}_t + 1/\theta \ \{\ddot{\delta}\}_{t+\tau} \qquad (4.4.24)$$

$$\{\dot{\delta}\}_{t+\Delta t} = \{\dot{\delta}\}_t + \Delta t/2 \ (\{\ddot{\delta}\}_t + \{\ddot{\delta}\}_{t+\Delta t}), \qquad (4.4.25)$$

$$\{\delta\}_{t+\Delta t} = \{\delta\}_t + \Delta t \ \{\dot{\delta}\}_t + \Delta t^2/6 \ \{\ddot{\delta}\}_{t+\Delta t} + \Delta t^2/3 \ \{\ddot{\delta}\}_t, \qquad (4.4.26)$$

and

$$\{p\}_{t+\Delta t} = (1-1/\theta) \ \{p\}_t + 1/\theta \ \{p\}_{t+\tau}. \qquad (4.4.27)$$

$$\{p\}_{t+\Delta t} = \{p\}_t + \Delta t/2 \; (\{\ddot{p}\}_t + \{\ddot{p}\}_{t+\Delta t}), \qquad (4.4.28)$$

$$\{p\}_{t+\Delta t} = \{p\}_t + \Delta t \; \{\dot{p}\}_t + \Delta t^2/6 \; \{\ddot{p}\}_{t+\Delta t} + \Delta t^2/3 \; \{\ddot{p}\}_t \qquad (4.4.29)$$

The advantage of the proposed technique is that it reduces the coupled unsymmetric matrix Eqn. 4.3.74 into two uncoupled symmetric equations 4.4.20 and 4.4.22.

Since the fluid and structure matrices are symmetric by themselves, Eqs. 4.4.10 and 4.4.11 yield symmetric matrices [A] and [B]. Again, matrix [X] takes a symmetric form due to the unique relationship between the coupling matrices [S] and [S]^T.

By proper node numbering, i.e., starting the node numbers from the left hand side of the interface boundary, the matrix [X] can be made banded, symmetric. Hence, Eqs. 4.4.20 and 4.4.22 can be solved using the well-established symmetric matrix equation solver subroutines.

This procedure has been tested to be unconditionally stable for any integration step size as well as for high values of radiation and structural damping and surface wave boundary conditions. Further economy is achieved by using

the NONSAP algorithm (Bathe, Wilson, and Iding, 1974) of storing only non-zero elements above the skyline of the large banded matrices.

4.5 Approximate Analyses of Fluid-Structure Systems

The simplest form of evaluating the dynamic response of floating platforms, as illustrated by Reddy et al. (1978), is as follows. The effect of buoyancy of the fluid medium supporting the structure is included using one-dimensional axial stiffness (spring) boundary elements at the bottom of the platform structure. The added mass and damping coefficients are assumed to be independent of frequency/time. Radiation damping is neglected and the frequency independent added mass is evaluated to be equivalent to the displaced fluid volume and added to the structural mass matrix.

4.5.1 Incompressible Fluid With Rigid Body

If the fluid is assumed homogeneous, inviscid, incompressible and irrotational then Eqn. 4.3.40 reduces to

$$\nabla^2 p = 0 \qquad (4.5.1)$$

An equivalent formulation results from choosing the velocity potential, ϕ, instead of the dynamic fluid pressure, p. As mentioned before, the fluid velocity components u and v in the x and y directions, respectively,

are related to the velocity potential as shown below:

$$u = \partial\phi/\partial x, \quad v = \partial\phi/\partial y \tag{4.5.2}$$

Substituting Eqn. 4.5.2 in the continuity equation yields

$$\nabla^2\phi = 0 \tag{4.5.3}$$

with the boundary condition at the sea bottom as

$$\partial\phi/\partial y = 0, \tag{4.5.4}$$

the free surface wave condition as

$$\partial\phi/\partial y = -(1/g)\ \partial^2\phi/\partial t^2, \tag{4.5.5}$$

the fluid-structure interface condition as

$$\partial\phi/\partial n = v_n \tag{4.5.6}$$

and the radiation boundary condition as

$$\partial\phi/\partial x = -(1/c)\ \partial\phi/\partial t \tag{4.5.7}$$

where n is a local coordinate normal to the interface and v_n is the component of the ship interface velocity along the normal.

Again, the fluid domain is discretised using the fluid finite element. The complex velocity potential at any node in the fluid region is assumed as

$$\{\phi\} = [N] \{\phi_o\} \ e^{i\omega t} \qquad (4.5.8)$$

where $[N]$ is a matrix of shape functions and $\{\phi_o\}$ is a column vector of complex potential amplitudes. The velocity of the structure is assumed to be harmonic as

$$v_n = v_o e^{i\omega t} \qquad (4.5.9)$$

where v_o is the velocity amplitude, $i = \sqrt{-1}$ and ω is the circular frequency of oscillation.

Using Galerkin's weighted residual procedure the Laplace equation 4.5.3 and the boundary conditions 4.5.4 to 4.5.7 can be transformed into the following equation.(Newton, 1975):

$$(-\omega^2[H] + i\omega[T] + [G]) \ \{\phi_o\} = \{P_1\} \ v_o \qquad (4.5.10)$$

in which

$$\{P_1\} = \int_{\Gamma_i} N^T \ n d\Gamma \qquad (4.5.11)$$

is the fluid-structure interface vector and matrices $[H]$, $[T]$, and $[G]$ are as defined in Eqn. 4.3.68.

4.5.1.1 Heave.

If the unit normal vector, $\tilde{n}$, is decomposed into horizontal and vertical components, then the fluid-structure interface vector for heaving motion (vertical component) is:

$$\{P_{1h}\}^{\sim} = \int_{\Gamma_i} N^T \cos\theta \, d\Gamma \tag{4.5.12}$$

where θ is the angle between the normal (towards the body) and the vertical axis.

Using the relation

$$p = -\rho_f (\partial\phi/\partial t) \tag{4.5.13}$$

and excluding the buoyant force the amplitude of the vertical force due to the heaving motion can be evaluated using

$$\{F_{1h}\} = \int_{\Gamma_i} p \cos\theta \, d\Gamma = -i\omega\rho_f \{P_{1h}\}^T \phi_o \tag{4.5.14}$$

The imaginary part of $\{F_{1h}\}$ is in phase with the structure acceleration and the associated added mass:

$$m_a = Im (-F_{1h})/\omega v_o \tag{4.5.15}$$

where Im denotes the imaginary part, and ωv_o is the amplitude of the structure heave acceleration.

The added mass coefficient, C_{mh}, is obtained by normalizing the added mass with respect to the displaced mass of the structure as follows:

$$C_{mh} = m_a/\rho_f A = Re (\{P_{1h}\}^T \phi_o)/A v_o \tag{4.5.16}$$

where A is the cross-sectional area of the submerged portion of the structure and Re denotes the real part.

The real part of $\{F_{1h}\}$ is in phase with the velocity of the structure, following the above procedure gives

$$C_{dh} = -Im \ \{\{P_{1h}\}^T \ \phi_o\}/Av_o \tag{4.5.17}$$

4.5.1.2 Sway

The fluid-structure interface vector for sway motion (horizontal) is:

$$\{P_{1s}\} = - \int_{\Gamma_i} \{N\}^T \ Sin \ \theta \ d\Gamma \tag{4.5.19}$$

The associated amplitude of the horizontal force is:

$$\{F_{1s}\} = \int_{\Gamma_i} p \ sin \ \theta d\Gamma = i\omega\rho_f \ \{P_{1s}\}^T \ \phi_o \tag{4.5.15}$$

Following the same procedure outlined in Section 4.5.1.1, the added mass and damping coefficients can be obtained from

$$C_{ms} = - Re \ \{\{P_{1s}\}^T \ \phi_o\}/Au_o \tag{4.5.20}$$

$$C_{ds} = Im \ \{\{P_{1s}\}^T \ \phi_o\}/Au_o \tag{4.5.21}$$

where u_o is the amplitude of the sway (horizontal) velocity component.

It can be easily noted that for a given structure the added mass and damping coefficients are frequency dependent.

4.5.2 Incompressible Fluid with no Free Surface Wave

If the fluid is assumed to be incompressible and the surface wave is neglected, then the matrices $[H]$ and $[T]$ become zero and the fluid matrix equation 4.3.73 reduces to:

$$[G] \{p\} = - \rho_f [S]^T \{\ddot{\delta}\}.$$ (4.5.22)

$\{p\}$ can be solved from the above equation as

$$\{p\} = - \rho_f [G]^{-1} [S]^T \{\ddot{\delta}\}$$ (4.5.23)

Substituting the above equation in the structural matrix equation 4.3.29 yields

$$([M] + [\overline{M}]) \{\ddot{\delta}\} + [C] \{\dot{\delta}\} + [K] \{\delta\} = \{F\}$$ (4.5.24)

where

$$[\overline{M}] = \rho_f [S] [G]^{-1} [S]^T$$ (4.5.25)

Eqn. 4.5.25 gives the 'equivalent added mass matrix' (frequency independent). Eqn. 4.5.24 represents a standard dynamic problem with the mass matrix augmented by the hydrodynamic added mass matrix.

4.6 Numerical Examples

4.6.1 Hydrodynamic Analysis of Rigid Floating Structures

The hydrodynamic added mass and damping coefficients for floating platforms, evaluated using the approximate analysis (rigid body assumption described in Section 4.5.2), are first computed.

4.6.1.1 Ship-Hull Form

In order to verify the validity and accuracy of the results, the example of a ship hull shaped cylinder floating on water is chosen. The finite element idealization of the cylinder is shown in Fig. 4.2 and the results are given in Table 4.2 for the pure heave motion. The results, compared with a similar analysis by Newton (1975) show very good agreement.

4.6.1.2 Rectangular Cylinder

The next example solved is a rigid rectangular cylinder of 10' (3.05m) draft, 20' (6.1m) wide floating in a water depth of 240' (73.2m). The added mass and damping coefficients, evaluated for frequencies more than 5 rad/sec showed little change. The evaluated values were C_m =1.59 and C_d = 0.004 for heave motion and C_m = 0.51 and C_d = 0.0006 for sway motion. The same example, neglecting the surface wave and radiation damping, yielded C_m = 3.72 and C_d = 0.0 for heave, and C_m = 0.86 and C_d = 0.0 for sway motion respectively. This illustrates the importance of including the surface wave and radiation damping.

4.6.1.3 Floating Nuclear Plant

The second example is the analysis of a floating nuclear plant platform. The platform is 400' (122m) wide, 40' (12.2m) deep with a 32' (9.76m) draft and floating in a water depth of 72' (21.96m). After various trials of finite element discretisation the selected version of modelling (on the basis of computer
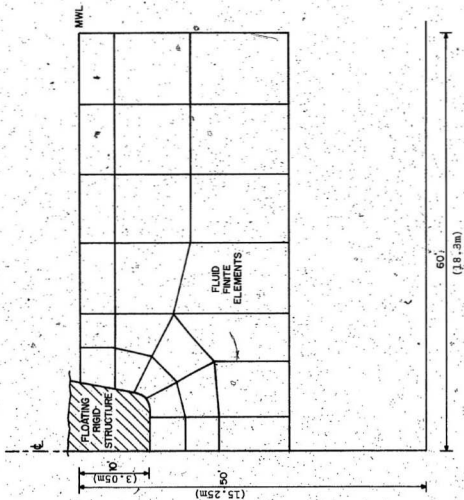
FIGURE 4.2. Finite Element Discretisation of the Fluid Region with a Rigid Floating Ship Hull

TABLE 4.2

Added Mass and Damping Coefficients of a Ship Hull Form

Full Hull Form draft = 10 ft.[†], semi-beam = 10 ft.[†]

	ω (rad/sec)	T = 2π/ω	C_m	C_d
	1.0	6.28	0.59	0.88
	1.1	5.71	0.60	0.75
	1.2	5.24	0.62	0.64
	1.3		0.63	0.54
	1.4		0.65	0.46
Heave	1.5	4.20	0.67	0.38
	1.6		0.70	0.31
	1.7		0.73	0.25
	1.8		0.76	0.20
	1.9		0.79	0.16
	2.0	3.14	0.83	0.12
Sway	1.0	0.23	0.11	

[†] 3.05 m

time and accuracy) of the fluid is shown in Fig. 4.3. The
model has 64 elements with 235 nodes with the freely
floating platform. The heave added mass and damping
calculated for frequencies ranging from 0.1 to 1.1 rad/sec
are shown in Table 4.3. The results compared with
experimental results of Nelson and Dean (1975) are shown in
Fig. 4.4. Though the results do not agree too well, the
trend of the variation is similar and the range of values
are of the same order. A possible reason may be that the
platform in this example simulates the freely floating
platform in transit condition (no moorings and surrounding
breakwater) whereas the experiments were conducted for a
moored platform within a breakwater.

The hydrodynamic pressure distribution calculated at the
fluid-structure interface for different frequencies is shown
in Fig. 4.5. It can be noticed that the maximum pressure
occurs around 1 rad/sec, very close to the natural
frequency of the structure.

4.6.2 Frequency Response of FNP Platform to Seismic Forces
(uncoupled)

In this example the fluid and structure parts are
isolated (rigid body assumption). The floating platform is
modelled with plane strain elements, the buoyancy of the
fluid is incorporated with appropriate axial stiffness
(spring) elements at the bottom nodes of the structure. The
time history of the Taft earthquake acceleration shown in
Fig. 3.8 is converted into the frequency domain using
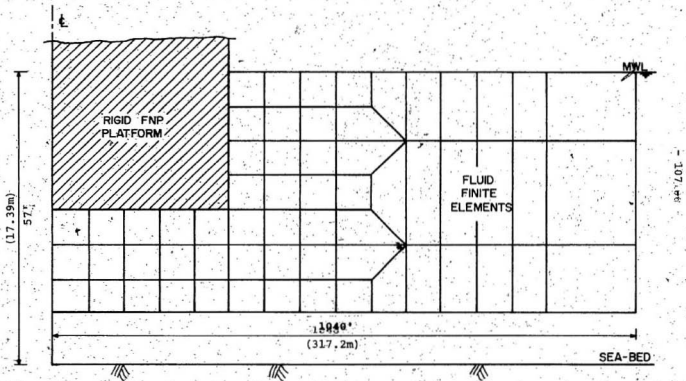
FIGURE 4.3. Finite Element Discretisation of the Fluid Region with a Rigid
Floating FNP Platform

TABLE 4.3

Heave Added Mass and Damping Coefficients of a Rigid FNP
Platform

ω (rad/sec)	Added Mass (M_{ah}/M)	Added Damping, D	$D' = D2\pi/\omega$
0.1	9.284	21.170	
0.2	8.911	9.769	306.920
0.3	12.201	4.254	89.106
0.4	17.463	14.588	229.140
0.5	8.031	1.741	21.880
0.6	13.232	2.460	25.764
0.7	9.986	0.460	4.133
0.8	5.930	3.102	24.370
0.9	10.829	0.061	0.425
1.0	10.849	0.012	0.074
1.1	10.542	0.002	0.011

Theoretical (h = 57') (17.39m)
Experimental (h = 47') (14.34m)
(Nelson and Dean, 1975)
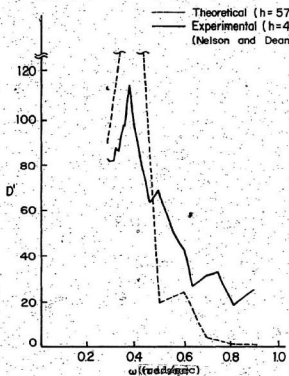
HEAVE ADDED DAMPING COEFFICIENT
WITH 1 FNP PLATFORM

$\frac{M_{ah}}{M_p}$
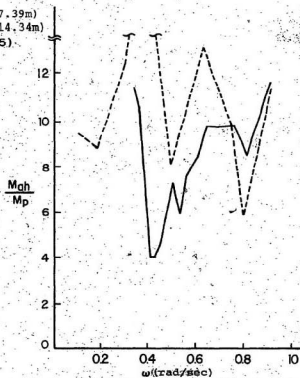
HEAVE ADDED MASS COEFFICIENT
WITH 1 FNP PLATFORM

FIGURE 4.4. Comparison of Theoretical and Experimental Heave Added Mass and
Damping Coefficients of FNP Platform
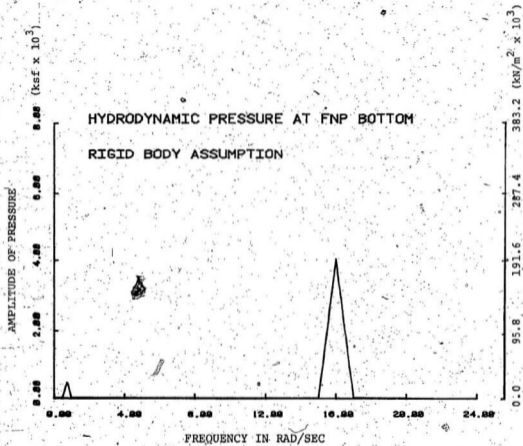
FIGURE 4.5. Frequency vs Hydrodynamic Pressure for the Rigid FNP Platform

Cooley-Tookey Fast Fourier Algorithm. This complex frequency
history of acceleration is input as the external load acting
at the mooring which in turn is transferred to the mooring
connection to the platform. In addition to this, the
frequency dependent hydrodynamic pressure evaluated in example
4.6.1.3 (shown in Fig. 4.5) is imposed as an external load
acting at the interface nodes. The evaluated heave response
at the center of the FNP platform for this loading is shown
in Fig. 4.6.

The probabilistic properties of the response of the FNP,
such as, the averaged output power spectrum, mean square
response, standard deviation etc. have been reported in
another paper (Thangam Babu, Arockiasamy, and Reddy, 1979).

4.6.3 Coupled Fluid-Structure Response of Floating Structures to Seismic Forces

4.6.3.1 Floating Nuclear Plant

The FNP platform, shown in Fig. 3.10 is modelled into
an equivalent isotropic plate of thickness 40' (12.2m) made up
of a pseudo-material so that the fundamental frequency of the
platform will be around 1 Hz. A perturbation study on the
frequency analysis of thin plates using SAP-IV yielded the
following material properties for a frequency compatible model.

Young's Modulus $E_x = E_y = 1.05 \times 10^6$ kips/ft^2 $(0.5 \times 10^8$ kN/m$^2)$

Poisson's Ratio $\nu_x = \nu_y = 0.25$

Density $\rho = 0.00125$ kip-sec^2/ft^4 $(0.643$ kN-sec^2/m$^4)$

Thickness h = 40' (12.2m)
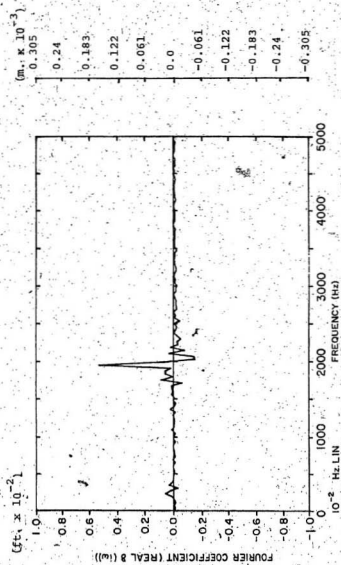
FIGURE 4.6. Frequency Response at the Centre of FNP Platform

The finite element modelling of the fluid-structure system is shown in Fig. 4.7. The left bottom node of the structure is hinged and the right bottom node is supported on vertical rollers so that the horizontal displacement is constrained; this simulates the cross-section of the platform moored at three corners with the fourth one free (Fig. 2.1). The fluid region is bounded by the fluid-structure interface nodes, the surface wave and the radiation boundaries, and the sea bottom. The radiation boundaries are located far enough so that any further increase does not change the result more than 1%. The amplified earthquake acceleration shown in Fig. 3.13 is the input and the evaluated heave and surge responses for the top right corner point of the FNP are shown in Figs. 4.8 and 4.9. The relatively smaller surge response is due to the boundary conditions constraining the horizontal movement. The maximum heave is -0.01654[1] at 6.4 sec and surge is -0.0121[2] at 7.6 sec. The time history of the maximum hydrodynamic pressure evaluated at the fluid-structure interface is shown in Fig. 4.10.

The same example was run with the amplified vertical earthquake acceleration as an uncoupled problem (without including the surrounding fluid medium in the finite element modelling) but representing the supporting fluid medium as an elastic foundation of stiffness proportional to the bulk modulus of water. The calculated maximum heave response is -0.01648[1] at 6.4 secs. and the surge is 0.0119[4] at 7.6 secs.

[1] -0.504cm, [2] -0.37cm, [3] -0.502cm, [4] 0.36cm
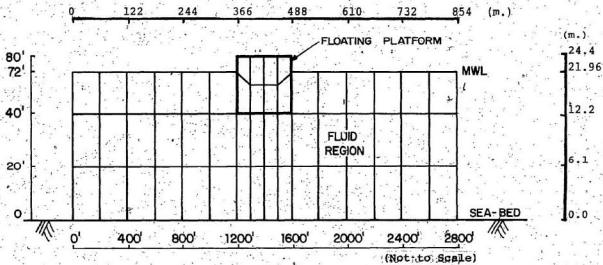
FIGURE 4.7. Finite Element Discretisation of Coupled Fluid-Structure System of FNP Platform
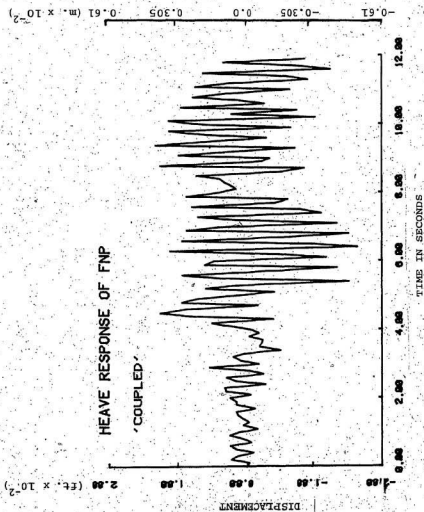
FIGURE 4.8. Time History Response of FNP Platform - Maximum Heave Motion
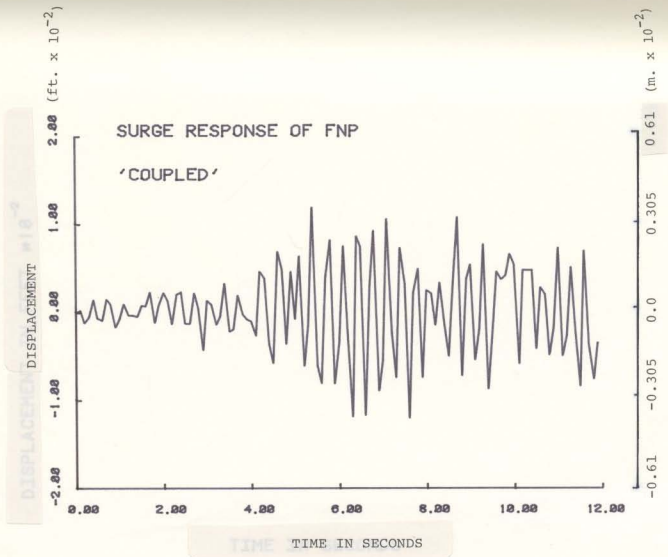
FIGURE 4.9. Time History Response of FNP Platform - Maximum Sway Motion
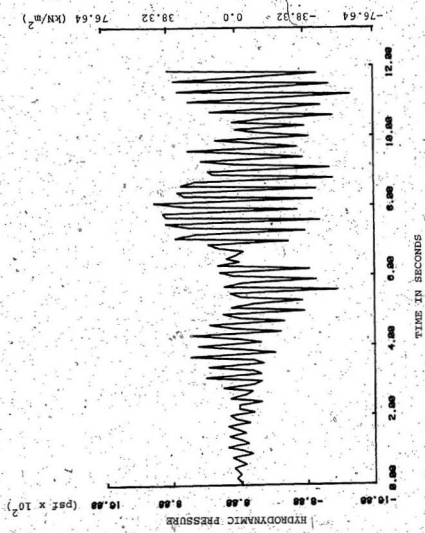
FIGURE 4.10. Time History of Hydrodynamic Pressure at the Bottom Centre of FNP Platform

Thus, the fluid can readily be simulated as an elastic foundation and the results have a marginal difference from those with coupled analysis.

The above example run with the Taft vertical acceleration component (unamplified) yielded a maximum heave of -0.0149' (-0.454cm) at 13.3 secs. and a maximum of 0.00184' (0.056cm) at 13.3 sec. Thus, there is a significant increase in the response for the amplified earthquake acceleration.

4.6.3.2 LPG Storage Plant

The second example selected for the coupled fluid-structure interaction analysis is the LPG platform shown in Fig. 3.5. Again, a frequency compatible model with a pseudo-material was obtained by performing a frequency analysis of LPG platform and the selected material properties are:

Young's Modulus $E_x = E_y = 4.2 \times 10^6$ kips/ft^2 (2.01 $\times 10^8$ kN/m^2)

Poisson's Ratio $v_x = v_y = 0.3$,

Density $\rho = 0.00126$ kip-sec^2/ft^4 (0.648 kN-sec^2/m^4), and

Thickness h = 56' (17.08m).

The finite element modelling of the fluid-structure system is shown in Fig. 4.11. The single leg mooring support is simulated by restraining both the horizontal and vertical displacements of the mooring connection to the platform (first node above the water surface on the left side of the structure). The amplified Taft earthquake shown in Fig. 3.9 is input at the bottom of the platform. Since the platform
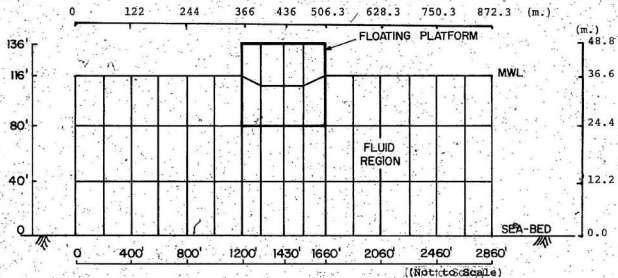
FIGURE 4.11. Finite Element Discretisation of Coupled Fluid-Structure System of LPG Platform

is supported by a single leg mooring, the horizontal component of the earthquake can be transferred to the platform through the mooring. To account for this the horizontal acceleration component (equal to the Taft acceleration) is input at the point connecting the structure and the mooring. The evaluated responses for the top right corner of the platform are shown in Figs. 4.12 and 4.13. The maximum heave calculated is 0.187'[1] at 13.1 secs. and maximum surge is 0.0192'[2] at 8.8 sec.

The time history of the maximum hydrodynamic pressure (fluid-structure interface node at the centre of the LPG bottom) is shown in Fig. 4.14.

4.7 Discussion

The development and application of isoparametric structural and fluid plane strain elements for the coupled fluid-structure analysis of floating structures has been presented. Different levels of approximations of hydrodynamic effects on the response of the structure have been illustrated.

In the finite element modelling, the number of elements chosen for the coupled problem are based on the economy and the accuracy needed. The infinite extent of the fluid region is restricted to a boundary beyond which the added mass and damping and hence the response do not change more than 1%. If the water depth is very large, then the depth

[1] 0.057m, [2] 0.0053m
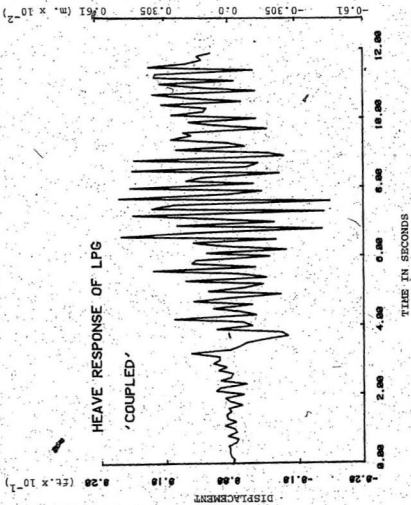
FIGURE 4.11 Time History Response of LPG Platform - Maximum Heave Motion
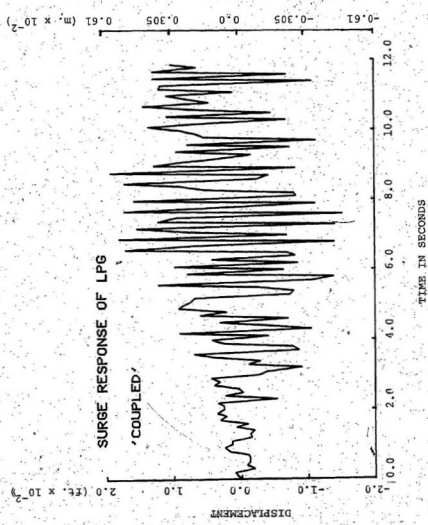
FIGURE 4.13. Time History Response of LPG Platform - Maximum Sway Motion
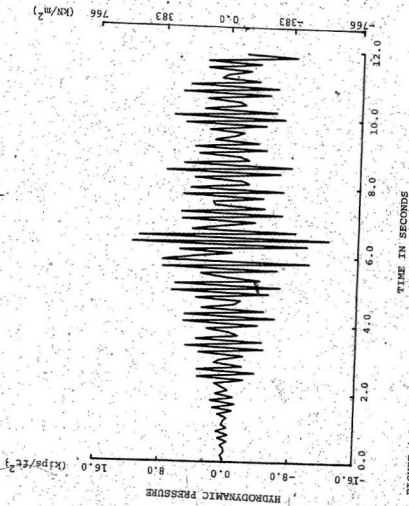
FIGURE 4.14: Time History of Hydrodynamic Pressure at the Bottom Centre of FNP Platform

equal to one half of the surface wave length expected in the region will be enough to simulate the infinite depth. The element sizes can be larger as the radiation boundary is approached, but a suggested upper boundary is almost 3/8 of the surface wave length. It has been observed that about a distance of three times the semi-width of the platform is far enough to impose the radiation boundary condition yielding satisfactory results (Chenault, 1975).

In the numerical example 4.6.3.2 the input horizontal component is the same as the horizontal component of the Taft earthquake. In actuality, this is not the case. The vertical component is amplified through the water medium whereas the horizontal component is the acceleration transmitted by the single leg mooring caisson to the structure. This really forms a part of the analysis of mooring caisson subjected to the seismic forces which is outside the scope of this research.

One of the basic advantages expected for the FNP concept is the minimization of the earthquake effect due to the cushioning effect of the fluid. But, the analysis presented in Chapter 3 proves that the fluid medium amplifies the vertical acceleration to about 30 times, which clearly nullifies that advantage.

Though the FNP is supported by mooring caissons at three points the mooring-strut is so designed to absorb all the horizontal accelerations transmitted to the platform. Hence, the FNP was analyzed for vertical amplified acceleration acting at the bottom of the platform.

Isolating the fluid from the structure, performing the hydrodynamic analysis of the fluid separately, and incorporating this hydrodynamic effect to the structure as additional external loads at the interface yielded responses about one third of those obtained from coupled analysis. The advantage of coupled analysis is the simultaneous incorporation of time/frequency dependent hydrodynamic inertial and damping effects.

CHAPTER 5

DYNAMIC "THICK PLATE ON ELASTIC FOUNDATION" ANALYSIS OF FLOATING PLATFORMS

5.1 Introduction

Three dimensional finite element analysis of the coupled fluid-structure system is expensive due to the large number of finite elements to be used to discretise the infinite fluid medium to a reasonable extent. In order to reduce the computation cost the following hybrid method is used to determine the dynamic response of the floating structure.

The floating structure is isolated from the fluid and the interactive effects of the fluid are incorporated in the structure, modelled as a thick plate on elastic foundation, as external pressure forces, in addition to the environmental forces, acting at the fluid-structure interface.

The reduction of a sixteen-noded three dimensional isoparametric finite element into an eight noded thick plate element, shown in Fig. 5.1 (Hinton, Razzaque, Zienkiewicz and Davis, 1975), justifies the fact that the modelling of a floating platform using a thick plate element is equivalent to using a sixteen noded three-dimensional finite element. The buoyancy effect of the supporting fluid medium is incorporated as an elastic foundation, resulting in a new thick plate bending element resting on elastic foundation.
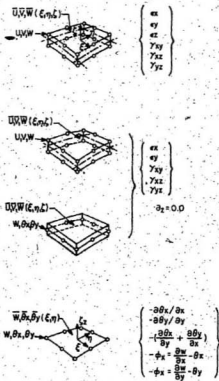
FIGURE 5.1. Evolution of Thick Plate Bending Element
(ref. Hinton, Razzaque, Zienkiewicz, and
Davis, 1975)

A displacement approach is adopted in developing the element matrices.

5.2 Review of Literature

The major improvement from thin plate theory to thick plate theory is the incorporation of the effects of shear deformation and rotary inertia. Donnell (1954) and Goldenveizer (1962) improved the thin plate theory by including the transverse shear effects. But, the most widely used thick plate bending theories are those of Reissner (1945) and Mindlin (1951). Analytical solutions for the static analysis of thick plates, with well defined boundaries and geometries, have been obtained by various authors. Similar solutions for dynamic analysis of thick plates are few in number. Analytical solutions for the free vibration of rectangular and circular plates have been presented by Mindlin and Deresiewicz (1954) and Mindlin, Shacknow and Deresiewicz (1956); the forced vibration analysis of thick rectangular plates has been carried out by Reissman and Lee (1968). Bending, vibration and buckling analyses of simply supported laminates and thick plates have been detailed by Srinivas and Rao (1968).

Application of finite element technique to the analysis of moderately thick plate was illustrated by Smith (1968) with only the transverse displacements as the unknowns.

Based on Mindlin's theory, Greiman and Lynn (1970) developed a rectangular finite element model considering the transverse displacement and two orthogonal rotations as the unknowns. Clough and Felippa (1968) introduced shear deformations in their refined quadrilateral finite element model in which the unknowns representing boundary conditions that could not be satisfied properly were eliminated in the formulation of stiffness matrix. Reissner's theory was used as the guideline for a rectangular plate bending model by Pryor, Barker and Frederick (1970) wherein the shear deformations were approximated by independent linear functions. An isoparametric quadrilateral thick plate bending element was developed by Rock and Hinton (1974) for the free vibration and transient response analysis of thin and thick plates. This element was developed using Mindlin's thick plate theory, similar to the one of Hinton and Razzaque (1973). Lynn and Dhillon (1971) developed a triangular thick plate bending element with nine degrees of freedom per node. A high precision triangular thin plate bending element developed by Cowper et al. (1968) was modified by Rao, Venkataramana and Raju (1974) into a thick plate bending element, by including shear deformations and rotary inertia with twelve degrees of freedom per mode. Mawenya and Davies (1974) analysed thick plate bending by incorporating the shear deformation in the finite strip method developed by Cheung (1968). A finite layer method was developed by Cheung and Chakrabarti (1972) for the frequency analysis of thick, layered rectangular plates.

Static, dynamic and stability analyses of curved thin and thick plates were carried out by Benson and Hinton (1976) using a thick finite strip method. Hinton (1976) extended the thick finite strip analysis to the forced vibration of laminated plates.

Analytical solutions have been developed for the bending of axially symmetric rectangular thick plates resting on Winkler's foundation by Naghdi and Rowley (1953) and Frederick (1957) using Levy and Navier type solutions. Svec (1976) used a triangular thick plate bending element resting on an elastic foundation for the static analysis of slab-foundation system. In this chapter the development of a high precision triangular thick plate bending element resting on an elastic foundation, an extension to the Rao et al. (1974) element, is detailed and its application to the dynamic response analysis of floating platforms is illustrated.

5.3 Theoretical Formulation

5.3.1 Reissner's Thick Plate Theory

Thick plate theory eliminates the Kirchhoff assumption in the classical thin plate theory in which the normal to the middle surface is assumed to remain straight and normal during deformation. Various attempts to correct the basic equation have been made by different authors (Love, 1927; Reissner, 1945; Mindlin, 1951).

The basic assumptions in Reissner's thick plate theory are as follows:

   i) the deflections are small;

  ii) the normals to the middle surface before deformation remain straight (but not normal) during the deformation; and

 iii) stresses in the direction normal to the middle plane of the plate are zero.

The second assumption implies that no warping of the section occurs due to shear deformation, i.e., the shear rotations, θ_x and θ_y, are to be considered as average rotations and subsequently corrected to account for the non-uniform shear deformation.

The resultant average rotations in x and y directions, θ_x and θ_y (Fig. 5.2), can be defined in terms of the transverse displacement w, and average shear deformations ϕ_1, and ϕ_2 as follows:

$$\begin{Bmatrix} \theta_x \\ \theta_y \end{Bmatrix} = \begin{Bmatrix} \partial w/\partial x + \phi_1 \\ \partial w/\partial y + \phi_2 \end{Bmatrix}$$

$$(5.3.1)$$

The displacements u, v and w in the x, y, and z directions, respectively, can be written as follows:

$$\begin{Bmatrix} u \\ v \\ w \end{Bmatrix} = \begin{Bmatrix} -z\theta_x \\ -z\theta_y \\ w \end{Bmatrix}$$

$$(5.3.2)$$
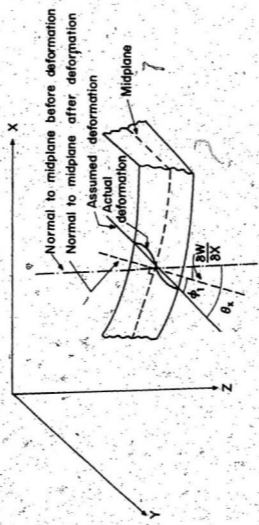
FIGURE 5.2: Deformation State for a Section y-constant

With these definitions, the generalized bending moment and shear force resultants of an orthotropic thick plate can be related to the generalized displacements w, ϕ_1 and ϕ_2, as given by Hinton et al. (1975)

$$\begin{Bmatrix} M_x \\ M_y \\ M_{xy} \\ Q_x \\ Q_y \end{Bmatrix} = \begin{bmatrix} D_x & D_1 & 0 & 0 & 0 \\ D_1 & D_y & 0 & 0 & 0 \\ 0 & 0 & D_{xy} & 0 & 0 \\ 0 & 0 & 0 & \beta S_x & 0 \\ 0 & 0 & 0 & 0 & \beta S_y \end{bmatrix} \begin{Bmatrix} \kappa_x \\ \kappa_y \\ \kappa_{xy} \\ \gamma_x \\ \gamma_y \end{Bmatrix} \quad (5.3.3)$$

or

$$(M) = [D]\{\kappa\} \quad (5.3.4)$$

where

$$\begin{Bmatrix} \kappa_x \\ \kappa_y \\ \kappa_{xy} \\ \gamma_x \\ \gamma_y \end{Bmatrix} = - \begin{Bmatrix} \partial^2 w/\partial x^2 + \partial\phi_1/\partial x \\ \partial^2 w/\partial y^2 + \partial\phi_2/\partial y \\ 2\partial^2 w/\partial x\partial y + \partial\phi_1/\partial y + \partial\phi_2/\partial x \\ \phi_1 \\ \phi_2 \end{Bmatrix} \quad (5.3.5)$$

The elastic rigidities in Eqn. 5.3.3 are defined as

$$D_x = E_x h^3/12(1-\nu_x\nu_y), \quad D_y = E_y h^3/12(1-\nu_x\nu_y), \quad D_1 = \nu_x D_y,$$

$$D_{xy} = G_{xy}h^3/12, \quad S_x = E_x h/2[1+\sqrt{(\nu_x\nu_y)}],$$

$$S_y = E_y h/2[1+\sqrt{(\nu_x\nu_y)}]$$

and

$$G_{xy} = \sqrt{(E_xE_y)}/2[1+\sqrt{(\nu_x\nu_y)}] \quad (5.3.6)$$

where E_x, E_y are the elastic moduli, ν_x, ν_y are the Poisson's ratios in the x and y directions respectively, and h is the thickness of the plate. For an isotropic thick plate the above constants simplify to

$$D_x = D_y = D = Eh^3/12(1-\nu^2), \quad D_1 = \nu D, \quad D_{xy} = [(1-\nu)/2] D,$$

$$\beta S_x = \beta S_y = 5(1-\nu)D/h^2, \quad \text{and} \quad \beta = 5/6 \quad (5.3.7)$$

5.3.2   Element Properties

Consider an arbitrarily oriented triangle with vertices 1, 2 and 3 as shown in Fig. 5.3 with its local co-ordinates $(\xi; \eta)$, and of dimensions a, b and c. Let (x, y) be the global co-ordinate system which describes the vertices of the element.

The trial displacement functions for the generalized displacement co-ordinates ϕ_1, ϕ_2, and w, corresponding to the two shear rotations and the transverse displacement are assumed as the following polynomials:

$$\phi_1 = \alpha_1 + \alpha_2\xi + \alpha_3\eta + \alpha_4\xi^2 + \alpha_5\xi\eta + \alpha_6\eta^2$$
$$+ \alpha_7\xi^3 + \alpha_8\xi^2\eta + \alpha_9\xi\eta^2 + \alpha_{10}\eta^3 \quad (5.3.8)$$

$$\phi_2 = \alpha_{11} + \alpha_{12}\xi + \alpha_{13}\eta + \alpha_{14}\xi^2 + \alpha_{15}\xi\eta + \alpha_{16}\eta^2$$
$$+ \alpha_{17}\xi^3 + \alpha_{18}\xi^2\eta + \alpha_{19}\xi\eta^2 + \alpha_{20}\eta^3 \quad (5.3.9)$$

and

$$w = \alpha_{21} + \alpha_{22}\xi + \alpha_{23}\eta + \alpha_{24}\xi^2 + \alpha_{25}\xi\eta + \alpha_{26}\eta^2$$
$$+ \alpha_{27}\xi^3 + \alpha_{28}\xi^2\eta + \alpha_{29}\xi\eta^2 + \alpha_{30}\eta^3 + \alpha_{31}\xi^4$$
$$+ \alpha_{32}\xi^3\eta + \alpha_{33}\xi^2\eta^2 + \alpha_{34}\xi\eta^3 + \alpha_{35}\eta^4 + \alpha_{36}\xi^5$$
$$+ \alpha_{37}\xi^3\eta^2 + \alpha_{38}\xi^2\eta^3 + \alpha_{39}\xi\eta^4 + \alpha_{40}\eta^5 \quad (5.3.10)$$
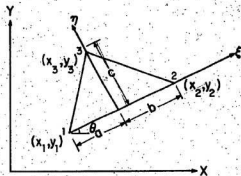
FIGURE 5.3. Element Co-ordinate Systems
(global and local)

The above expression can be rewritten as:

$$\phi_1 = \sum_{i=1}^{10} \alpha_i \zeta^{m_i} \eta^{n_i}$$

$$\phi_2 = \sum_{i=11}^{20} \alpha_i \zeta^{p_i} \eta^{q_i} \qquad (5.3.11)$$

and

$$w = \sum_{i=21}^{40} \alpha_i \zeta^{r_i} \eta^{s_i}$$

The omission of the term $\zeta^4 \eta$ in Eqn. 5.3.10 is to satisfy the condition that the normal slope along the edge η = 0 to be a cubic function, thus satisfying automatically the normal slope compatibility along this edge. Conformity, defined as slope continuity at element interfaces, is satisfied by this element since the shear deformations, expressed as cubic polynomials, are also compatible.

The convergence of this element has been evaluated to be of the order of n^{-6} (Cowper et al., 1968) where n is the number of elements per side of a plate.

The compatibility conditions for the normal slope variation along the edges (2-3) and (3-1) have been computed by Cowper et al. (1968) as:

$$5\bar{b}^4\bar{c}\alpha_{36} + (3\bar{b}^2\bar{c}^3 - 2\bar{b}^4\bar{c})\alpha_{37} + (2\bar{b}\bar{c}^4 - 3\bar{b}^3\bar{c}^2)\alpha_{38}$$
$$+ (\bar{c}^5 - 4\bar{b}^2\bar{c}^3)\alpha_{39}$$
$$- 5\bar{b}\bar{c}^4\alpha_{40} = 0 \qquad (5.3.12a)$$

and

$$5\bar{a}^4\bar{c}\alpha_{36} + (3\bar{a}^2\bar{c}^3 - 2\bar{a}^4\bar{c})\alpha_{37} + (2\bar{a}\bar{c}^4 - 3\bar{a}^3\bar{c}^2)\alpha_{38}$$

$$+ (\bar{c}^5 - 4\bar{a}^2\bar{c}^3)\alpha_{39}$$

$$+ 5\bar{a}\bar{c}^4\alpha_{40} = 0 \qquad\qquad (5.3.12b)$$

This reduces the number of equations required to evaluate the unknown coefficients from 40 to 38. These can be derived from the generalized displacement coordinates for each element taken to be the two shear rotations and their first derivative at each of the vertices, shear rotations at the centroid of the element, the transverse displacement, and the first and second derivatives with respect to ξ and η at each of the vertices. The displacement coordinates totalling thirty-eight are consistent with the thirty-eight unknown parameters. These generalized displacement co-ordinates can be assembled in a column vector as:

$$\{\bar{q}\} = [\delta_1 \ \delta_2 \ \delta_3 \ \phi_{1c} \ \phi_{2c}]^T \qquad\qquad (5.3.13)$$

where

$$[\delta_i] = [\phi_{1i} \ \phi_{1,\xi i} \ \phi_{1,\eta i} \ \phi_{2i} \ \phi_{2,\xi i} \ \phi_{2,\eta i} \ w_i \ w_{,\xi i} \ w_{,\eta i}$$

$$w_{,\xi\xi i} \ w_{,\xi\eta i} \ w_{,\eta\eta i}]$$

$$(5.3.14)$$

for $i = 1, 2$ and 3, representing the vertices; ϕ_{1c} and ϕ_{2c} are the shear rotations at the centroid, $\phi_{1,\xi i} = \partial\phi_1/\partial\xi_i$ and so on. Eqs. 5.3.11, 5.3.12 and 5.3.13 can be combined to

relate the generalized displacement co-ordinates to the unknown coefficients in a matrix form as:

$$\left\{ \begin{array}{c} \bar{w} \\ 0 \\ 0 \end{array} \right\}^i = [T]\{C\} \tag{5.3.15}$$

where

$$\{C\}^T = [a_1 \ a_2 \ a_3 \ \cdots a_{40}] \tag{5.3.16}$$

(The elements of $[T]$ are given in Table 5.1).

Eqn. 5.3.15 can be rewritten as:

$$\{C\} = [T]^{-1} \left\{ \begin{array}{c} \bar{w} \\ 0 \\ 0 \end{array} \right\}^i \tag{5.3.17}$$

i.e., $\{C\} = [B]\{\bar{w}\}$ (5.3.18)

where the matrix $[B]$ consists of the elements of $[T]^{-1}$.

5.3.2.1 Stiffness Matrix

For a thick orthotropic plate resting on an elastic foundation, the expression for the strain energy in bending can be written as:

$$u_1 = 1/2 \iint \{D_x(w^2_{,\xi\xi} + \phi^2_{1,\xi} + 2\phi_{1,\xi}w_{,\xi\xi})$$
$$+ D_1(2w_{,\xi\xi}w_{,\eta\eta} + 2\phi_{2,\eta}w_{,\xi\xi} + 2w_{,\eta\eta}\phi_{1,\xi} + 2\phi_{2,\eta}\phi_{1,\xi})$$
$$+ D_y(w^2_{,\eta\eta} + \phi^2_{2,\eta} + 2w_{,\eta\eta}\phi_{2,\eta})$$
$$+ D_{xy}(4w^2_{,\xi\eta} + \phi^2_{1,\eta} + \phi^2_{2,\xi} + 4w_{,\xi\eta}\phi_{1,\eta} + 2\phi_{1,\eta}\phi_{2,\xi} + 4w_{,\xi\eta}\phi_{2,\xi})$$
$$+ \beta S_x\phi^2_1 + \beta S_y\phi^2_2 + ew^2\}d\xi d\eta \tag{5.3.19}$$

TABLE 5.1
Transformation Matrix T (ref. Cowper et al., 1968)

where e is the spring constant of the elastic foundation.

Using Eqs. 5.3.3 to 5.3.5, the above expression can be written in matrix form as:

$$U_1 = 1/2 \iint \left\{ \{\kappa\}^T [D] \{\kappa\} + ew^2 \right\} \, d\xi d\eta \qquad (5.3.20)$$

Substituting Eqn. 5.3.12 into Eqn. 5.2.19 and carrying out the necessary integrations, the above energy integral can be written in terms of $\{a_i\}$ as:

$$U_1 = 1/2 \{C\}^T [k] \{C\} \qquad (5.3.21)$$

where $[k]$ is the stiffness matrix, the elements of which can be obtained from the following equation, once the values of a, b, c, m_i, n_i, p_i, q_i, r_i and s_i are furnished:

$$
\begin{aligned}
k_{ij} = & \; D_x [r_i r_j (r_i-1)(r_j-1) F(r_i+r_j-4, \; s_i+s_j) \\
& + m_i m_j F(m_i+m_j-2, \; n_i+n_j) + m_i r_j (r_j-1) F(m_i+r_j-3, n_i+s_j) \\
& + m_j r_i (r_i-1) \; F(m_j+r_i-3, \; n_j+s_i)] \\
& + D_1 [s_i (s_i-1) r_j (r_j-1) \; F(r_i+r_j-2, \; s_i+s_j-2) \\
& + s_j (s_j-1) r_i (r_i-1) \; F(r_j+r_i-2, \; s_j+s_i-2) \\
& + q_i r_j (r_j-1) \; F(p_i+r_j-2, \; q_i+s_j-1) + q_j r_i (r_i-1) \; x \\
& \quad F(p_j+r_i-2, \; q_j+s_i-1) + m_i s_j (s_j-1) F(m_i+r_j-1, n_i+s_j-2) \\
& + m_j s_i (s_i-1) \; F(m_j+r_i-1, \; n_j+s_i-2) \\
& + m_i q_j F(m_i+p_j-1, \; n_i+q_j-1) \\
& + m_j q_i F(m_j+p_i-1, \; n_j+q_i-1)] \\
& + D_y [s_i s_j (s_i-1)(s_j-1) \; F(r_i+r_j, \; s_i+4) \\
& + q_i q_j F(p_i+p_j, \; q_i+q_j-2) + q_i s_j (s_j-1) F(p_i+r_j, q_i+s_j-3) \\
& + q_j s_i (s_i-1) \; F(p_j+r_i, \; q_j+s_i-3)] \\
& + D_{xy} [4 r_i r_j s_i s_j F(r_i+r_j-2, \; s_i+s_j-2) \\
& + n_i n_j F(m_i+m_j, \; n_i+n_j-2) + p_i p_j F(p_i+p_j-2, \; q_i+q_j)
\end{aligned}
$$

$$+ 2n_i r_j s_j F(m_i+r_j-1, \ n_i+s_j-2)$$

$$+ 2n_j r_i s_i F(m_j+r_i-1, \ n_j+s_i-2)$$

$$+ n_i p_j F(m_i+p_j-1, \ n_i+q_j-1)$$

$$+ n_j \ p_i \ F \ (m_j+p_i-1, \ n_j+q_i-1)$$

$$+ 2p_j r_j s_j F(p_j+r_i-2, \ q_i+s_j-1)$$

$$+ 2p_j r_i s_i F(p_j+r_i-2, \ q_j+s_i-1)] + \beta S_x F(m_i+m_j, \ n_i+n_j)$$

$$+ \beta S_y F(p_i+p_j, \ q_i+q_j) + eF(r_i+r_j, \ s_i+s_j)$$

$$(5.3.22)$$

where

$$F(m, \ n) = \iint \zeta^m \eta^n d\zeta d\eta = \frac{\bar{c}^{n+1}[\bar{a}^{m+1} - (-\bar{b})^{m+1}]m!n!}{(m+n+2)!} \quad (5.3.23)$$

The stiffness matrix can be transformed to the global co-ordinates system using the relation:

$$[\bar{R}] = [R]^T[B]^T[k][B][R] \qquad (5.3.24)$$

where [R] is a (38 x 38) rotation matrix given in Table 5.2.

5.3.2.2 Consistent Mass Matrix

The kinetic energy of an elemental thick orthotropic plate element, taking into account the rotary inertia, can be written in the local co-ordinate system as (Donnell, Drucker and Goodin, 1946):

$$U_2 = \rho w^2/2 \ \iint \ (w^2 + h^2/12 \ \theta_\zeta^2 + h^2/12 \ \theta_\eta^2) \ d\zeta d\eta \qquad (5.3.25)$$

where ρ is the mass density per unit area.

TABLE 5.2

Rotation Matrix R (Reproduced from Cowper et al., 1966)

$$R_1 = \begin{bmatrix}
1 & 0 & 0 & 0 & 0 & 0 \\
0 & \cos\theta & \sin\theta & 0 & 0 & 0 \\
0 & -\sin\theta & \cos\theta & 0 & 0 & 0 \\
0 & 0 & 0 & \cos^2\theta & 2\sin\theta\cos\theta & \sin^2\theta \\
0 & 0 & 0 & -\sin\theta\cos\theta & \cos^2\theta-\sin^2\theta & \sin\theta\cos\theta \\
0 & 0 & 0 & \sin^2\theta & -2\sin\theta\cos\theta & \cos^2\theta
\end{bmatrix}$$

$$R = \begin{bmatrix}
R_1 & 0 & 0 \\
0 & R_1 & 0 \\
0 & 0 & R_1
\end{bmatrix}$$

Substituting Eqn. 5.3.1 in the above expression yields

$$U_2 = \rho \omega^2 / 2 \iint \{w^2 + h^2/12[(\partial w/\partial \eta)^2 + \phi_1^2 + \phi_2^2 + 2\partial w/\partial \xi \phi_1$$

$$+ 2\partial w/\partial \eta \phi_2]\} \, d\xi d\eta \qquad (5.3.26)$$

Substituting Eqn. 5.3.11 into Eqn. 5.2.26 and carrying out the proper integrations and transformations, the mass matrix in terms of the generalized displacements can be written as:

$$[\bar{M}] = [R]^T[B]^T[m][B][R] \qquad (5.3.27)$$

where the elements of $[\bar{M}]$ are given by the expression:

$$m_{ij} = \rho\{F(r_i+r_j, \ s_i+s_j) + h^2/12 \ [r_ir_jF(r_i+r_j-2, \ s_i+s_j)$$
$$+ s_is_jF(r_i+r_j, \ s_i+s_j-2)$$
$$+ F(m_i+m_j, \ n_i+n_j) + F(p_i+p_j, \ q_i+q_j)$$
$$+ r_iF(r_i+m_j-1, \ s_i+n_j) + r_jF(r_j+m_i-1, \ s_j+n_i)$$
$$+ s_iF(r_i+p_j, \ s_i+q_j-1) + s_jF(r_j+p_i, \ s_j+q_i-1)]\}$$

$$(5.3.28)$$

5.3.3 Condensation of Element Matrices

Since the centroidal deflections are unaffected when the elements are connected, it is convenient to condense out the centroidal displacements ϕ_1 and ϕ_2.

The dynamic equilibrium equation of a vibrating plate can be written in partitioned matrix form as

$$\begin{bmatrix} \bar{K}_{11} & \bar{K}_{12} \\ \bar{K}_{21} & \bar{K}_{22} \end{bmatrix} \begin{Bmatrix} W \\ W_c \end{Bmatrix} - \omega^2 \begin{bmatrix} \bar{M}_{11} & \bar{M}_{12} \\ \bar{M}_{21} & \bar{M}_{22} \end{bmatrix} \begin{Bmatrix} W \\ W_c \end{Bmatrix} = 0 \qquad (5.3.29)$$

where

$\{W_c\}$ is the centroidal displacement vector,

and

$\{W\}$ is the vector of the remaining 36 displacement components.

The above equation can be condensed by minimizing the strain energy (Przemieniecki, 1968) as

$$[K]\{W\} - \omega^2 [M]\{W\} = 0 \qquad (5.3.30)$$

where

$$[K] = [\bar{K}_{11}] - [\bar{K}_{12}]^{-1}[\bar{K}_{21}] \qquad (5.3.31)$$

$$[M] = [A]^T[\bar{M}][A] \qquad (5.3.32)$$

and

$$[A] = \begin{bmatrix} [I] \\ -[\bar{K}_{22}]^{-1}[\bar{K}_{21}] \end{bmatrix} \qquad (5.3.33)$$

in which $[I]$ is a (36×36) unit matrix, and $[K]$ and $[M]$ are the final condensed (36×36) stiffness and mass matrices of a thick orthotropic plate bending element on an elastic foundation.

5.3.4   Boundary Conditions

Since the principle of minimum potential energy is used in the present formulation, it is enough to satisfy only the kinematic boundary conditions, namely, the deflection, slope and shear deformation. The boundary conditions used for different edge conditions are tabulated in Table 5.3.

TABLE 5.3

Boundary Conditions for Different Supports

Simply Supported Edge Parallel To		Clamped Edge Parallel To	
x axis	y axis	x axis	y axis
$w = 0$	$w = 0$	$w = 0$	$w = 0$
$\phi_1 = 0$	$\phi_2 = 0$	$w_{,y} = 0$	$w_{,x} = 0$
		$\phi_1 = 0$	$\phi_1 = 0$
		$\phi_2 = 0$	$\phi_2 = 0$

This method of dealing with kinematic boundary conditions of edges parallel to the global co-ordinate system needs no comment. But if the edge is oblique, for example, a straight simply supported edge making an angle γ with the x axis, then the conditions of the simple support imply

$$w = 0, \text{ and } \phi_t = 0 \qquad (5.3.34)$$

where t is the axis perpendicular to the skewed axis. The above conditions expressed in terms of the global coordinates are:

$$w = 0, \text{ and } \phi_t = \phi_1 \cos \gamma + \phi_2 \sin \gamma = 0 \qquad (5.3.35)$$

5.3.5 Dynamic Analysis

Frequency analyses of thin and thick plates resting on elastic foundation have been illustrated by the author (Thangam Babu, Reddy, and Sodhi, 1979).

The dynamic equilibrium matrix equation is

$$[K]\{\delta\} + [C]\{\dot{\delta}\} + [M]\{\ddot{\delta}\} = \{F\} \qquad (5.3.36)$$

where

$[K]$ and $[M]$ are the stiffness and mass matrices of the structure assembled in the conventional manner.

The damping matrix $[C]$ is again evaluated on the basis of Rayleigh damping. The force matrix $\{F\}$ comprises the interface hydrodynamic fluid forces $\{P\}$ in addition to the external forces $\{R\}$ such as earthquake forces. Hence the equation changes to

$$[K]\{\delta\} + [C]\{\dot{\delta}\} + [M]\{\ddot{\delta}\} = \{P\} + \{R\} \qquad (5.3.37)$$

In the frequency domain analysis, the above equation transforms into the following

$$([K] + i\omega[C] - \omega^2[M])\{\delta\} = \{\bar{P}(\omega)\} + \{\bar{R}(\omega)\} \qquad (5.3.38)$$

where $\{\bar{P}(\omega)\}$ and $\{\bar{R}(\omega)\}$ are the hydrodynamic pressure and external load vectors in the frequency domain.

The frequency-dependent hydrodynamic pressures evaluated in the previous chapter (assuming the rigid body assumption) are used in the above equation for $\{\bar{F}(\omega)\}$. The external load vector due to ground motion, $\ddot{u}_g(\omega)$, is computed as

$$\{R\} = -[M]\{\ddot{u}_g(\omega)\} \qquad (5.2.39)$$

where $\ddot{u}_g(\omega)$ are the complex amplitudes of the earthquake acceleration in the frequency domain obtained by performing a Fast Fourier Transformation on the time history of the Taft earthquake.

5.3.6 Conversion of Two-Dimensional Hydrodynamic Pressures to Three-Dimensional Values

Since the hydrodynamic pressure evaluated in the previous chapter is based on a two dimensional model, a three dimensional transformation is required to distribute the hydrodynamic pressure along the breadth of the platform.

A multiplication factor to convert the two dimensional results to three dimensional ones was given by Johnson et al. (1975) for different frequencies as shown in Fig. 5.4. This factor, varying from 0.45 to 0.51, is used to convert the two dimensional hydrodynamic pressures evaluated in the previous chapter to three dimensional ones and distributed over the breadth of the platform.
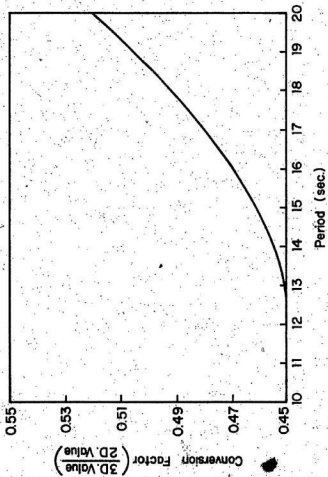
FIGURE 5.4. Conversion Factor (3-D Value/2-D Value) vs Period

5.4 'Equivalent' Thick Plate Modelling

The Schematic views of the FNP platform shown in Fig. 3.10 show that it is of a box girder type construction. In order to use the thick plate theory it has to be modelled into a monolithic thick orthotropic plate of an equivalent thickness, with modified rigidities to account for the voids. Based on theoretical considerations Pama, Imsom-Samboon and Lee (1975) developed expressions to evaluate flexural and torsional rigidities of such cross-sections sketched in Fig. 5.5.

Since the FNP platform has similar cavities in both the x and y directions and, also, is of almost equal dimensions on both sides it can be converted to an isotropic thick plate of equivalent thickness with modified rigidity. The rigidities of the voided slab shown in Fig. 5.5 are

$$D_x = D_y = \frac{Eh^3}{12(1-v^2)} \left[1 - \frac{3(d/h)^4 (h/t)}{16[1+(d/t)]} \right] \quad (5.3.40)$$

where

E is the Young's modulus of the material.

If the plate were a monolithic isotropic plate of equivalent thickness, h_e, the elastic rigidity would have been

$$D_{x_e} = Eh_e^3 / 12(1-v^2) \quad (5.3.41)$$
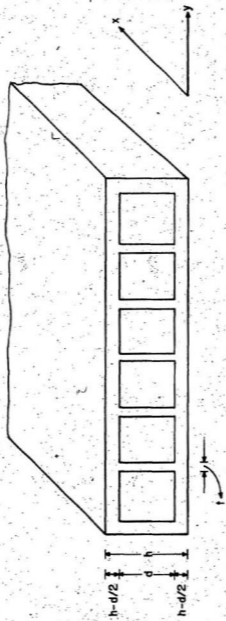
FIGURE 5.5. Cross-section of a Box Type Platform

Equating 5.2.40 and 5.2.41 the equivalent thickness of the plate can be evaluated as

$$h_e = h \left[1 - \frac{3\pi (d/h)^4 (h/t)}{16[1 + (d/t)]} \right]^{1/3} \tag{5.3.42}$$

5.5 Numerical Illustration

5.5.1 Convergence Study

In order to check the accuracy and the convergence properties of the element, a simply supported square thick plate is analyzed using two, four and six elements per side of a one-quarter plate (Fig. 5.6) and the results are presented in Table 5.4. The relative superiority of the element can be realized by noting the accuracy of the results for higher modes.

The free vibrations of thick isotropic simply supported plates with different thickness to side ratios have been evaluated using the N=6 finite element idealization, and the results tabulated are compared with those of other investigators in Table 5.5.

Further applications of the element for the free vibration analysis of various thick and thin plates are presented in the paper by Thangam Babu, Reddy and Sodhi (1979).
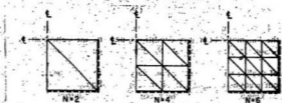
FIGURE 5.6. Finite Element Discretisations of a
Quarter Plate for Convergence Study

TABLE 5.4

Convergence Study of the Element for a Simply Supported Plate:
$a = b = 1$, $a/h = 1.0$. $E = 1.0$, $\rho = 1.0$, $\nu = 0.3$

			Eigenvalue $\lambda = \omega^2/\rho h/D$		
Mode (m, n)	N = 2	N = 4	N = 6	(Srinivas, et al., 1970) 3D Theory	Rock and Hinton, 1974*
(1,1)	368.06	366.31	(+0.38%) 365.81	364.43	(-0.1%) 363.88
(2,2)	5698.11	4894.68	(-0.75%) 4874.74	4912.48	(-1.1%) 4809.32
(1,3)	7943.31	7311.19	(-0.91%) 7239.05	7306.89	(+3.4%) 7509.36
(2,4)	63752.84	24096.48	(-1.27%) 23391.06	23694.35	(+7.1%) 27183.24

*Eight quadrilateral elements for half plate.

TABLE 5.5

Eigenvalues $\lambda = \omega/\sqrt{(\rho h^2/G)}$ for a Simply Supported Square
Plate: $a = b = 1.0$, $G = 1.0$, $\rho = 1.0$, $\nu = 0.3$

			Eigenvalue			
a/h	Number of Half Waves in x and y Directions (m,n)	Present Element	(Srinivas, et al., 1970) 3D Theory	Rock and Hinton, 1974	Mindlin Theory 1956	(Przemieniecki, 1968) Thin Plate Theory
10	(1,1)	0.0944	0.0935	0.0931	0.0930	0.0963
10	(2,1)	0.2222	0.2226	0.2237	0.2217	0.2408
10	(3,1)	0.4158	0.4174	0.4312	0.4144	0.4816
10	(3,2)	0.5217	0.5239	0.5379	0.5197	0.6261
10	(2,3)	0.6528	0.6889	0.7661	0.6821	0.8669
10	(4,2)	0.7489	0.7511	0.8045	0.7431	0.9632
20	(2,1)	0.0589	0.0589	0.0591	0.0588	0.0602
20	(2,2)	0.0929	0.0931	0.0946	0.0930	0.0963
5	(1,1)	0.3426	0.3421	0.3407	0.3402	0.3852
5	(2,1)	0.7454	0.7511	0.7493	0.7431	0.9631
5	(2,2)	1.0792	1.0889	1.0564	1.0735	1.5411

5.5.2 Floating Nuclear Plant

The free and forced vibration analysis of floating nuclear plant is performed by modelling the floating platform as a thick plate resting on elastic foundation.

5.5.2.1 Approximate Frequency Analysis

Since the platform is almost square, with similar stiffeners along the longitudinal and transverse directions, it is converted to an isotropic thick plate of equivalent thickness of 26.74'[1] using the relation 75.3.42. Since the platform is restrained by mooring caissons on two sides as shown in the plan view, Fig. 3.10, the plate is assumed to be supported at the three corners and free at one corner. The buoyancy of the supporting fluid is incorporated as the elastic foundation of stiffness proportional to the bulk modulus of the water.

In view of the frequency dependence of the added water mass, the approximations of setting it to equal to the mass of the displaced water is not valid. Therefore, different percentages of the total displaced water masses (0% to simulate the neglecting of the effect of the surrounding fluid medium and 100% to simulate the added mass equal to

[1] 8.156m

the displaced water mass) have been added to the platform
mass and the evaluated frequencies are presented in Table
5.6. The reported (Nelson and Dean, 1975) experimental
value of the fundamental frequency of about 1 Hz. checks
well with the value evaluated with an added mass of 50%.
Evidently, this means that the added mass coefficient of
the platform is approximately 0.5. The first six mode
shapes of the platform are shown in Fig. 5.7.

5.5.2.2 Seismic Response of the FNP Platform

For this analysis idealization of the FNP platform as
an equivalent thick plate is achieved by the frequency
compatible modelling technique. The fundamental frequency of
the platform was experimentally determined by Nelson and
Dean (1975) to be 1 Hz. A series of three-dimensional free
vibration analysis of the FNP platform have been performed
using SAP-IV by changing the input parameters such as plate
thickness and the material properties. The following two
frequency-compatible models were determined.

i) FNP modelled as a thick plate on elastic foundation
with the material properties of steel and modified
equivalent thickness:

Thickness = 33.85' (10.24m)

Young's Modulus $E_x = E_y = 4.176 \times 10^5$ kips/ft^2

$(1.99 \times 10^8$ kN/m$^2)$

Mass density $\rho = 0.001479$ kip-sec^2/ft^4

$(0.761$ kN-sec^2/m$^4)$

TABLE 5.6

Frequencies of the FNP Platform for Different Percentages

of Added Water Mass

a=400', b=400', h=26.74'[3], $E_x=E_y=4.32 \times 10^6$ kips/ft[2][4]

$v_x=v_y=0.3$, e=0.0624 kip/ft[5], $\rho=0.061618$ kip sec^2/ft^4[6]

(no added mass)

Frequency (Hz.)

Mode No.	Added Water Mass as % of Total Displaced Water Mass				
	0%	25%	50%	75%	100%
1	2.1065	1.7569	1.1573	0.8032	0.7793
2	3.7014	3.3056	2.9367	2.6689	2.3979
3	5.6652	4.9841	4.5307	4.1490	3.8758
4	7.3056	6.4735	5.8724	5.3667	4.9928
5	9.5772	8.4951	7.7285	7.1355	6.6447
6	14.5564	12.9657	11.7926	10.9169	10.2107

[3] 122m, [4] 8.156m, [4] 2.06 $\times 10^8$ kN/m^2, [5] 0.912kN/m

[6] 31.686 kN-sec^2/m^4
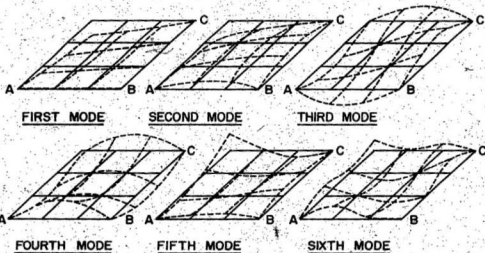
FIGURE 5.7. Mode Shapes of the FNP Platform Supported on Three Corners

- 158 -

ii) FNP modelled as a thick plate of original thickness
and made up of a pseudo material

Thickness = 40' (12.2m)

Young's Modulus = 1050000 kips/ft^2 (50.3 x 10^{6}kN/m^2)

Mass density = 0.00125 kip sec^2/ft^4(0.643 kN sec^2/m^4)

The finite element discretization of the FNP is shown in
Fig. 5.8. A time domain analysis is performed by inputting
the amplified earthquake acceleration evaluated at the
bottom of FNP, shown in Fig. 3.13, as the extremely applied
force. The hydrodynamic pressure evaluated at the bottom of
the FNP from the 2D coupled fluid-structure formulation,
shown in Fig. 4.10, is incorporated as the additional
loading at the interface nodes representing the hydrodynamic
interaction of the fluid and the structure. The maximum
heave displacement and acceleration response of the FNP are
shown in Figs. 5.9 and 5.10.

Frequency domain response analysis is carried out as
follows. The amplified earthquake accelerations are
transformed into frequency domain by a forward Fast Fourier
Transform, the amplitude of which is shown in Fig. 5.11.
The hydrodynamic pressures evaluated in the frequency domain
from the rigid body hydrodynamic analysis (Fig. 4.5) are
added to the above acceleration loads and the frequency
response of the platform is evaluated. The heave
displacement is shown in Fig. 5.12. It can be noticed that
the maximum heave occurs around 1 Hz as expected.
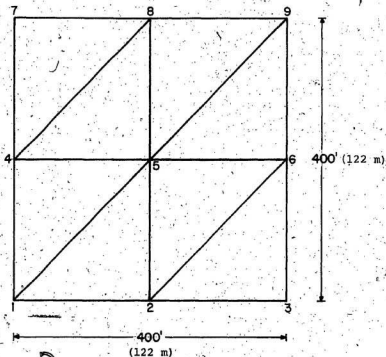
FIGURE 5.8. Finite Element Discretisation of FNP
Platform (Nodes 1, 7, and 9 are
corner supported)
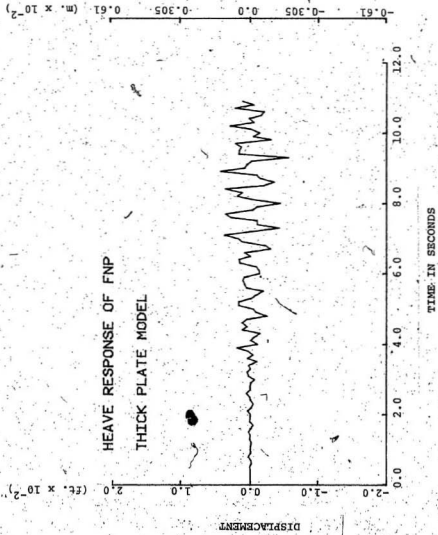
FIGURE 5.9. Time History Response of FNP Modelled as a Thick Plate with Three Corner Supports - Maximum Heave Displacement
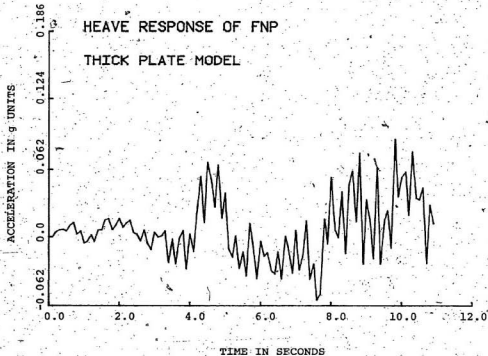
FIGURE 5.10. Time History Response of FNP Modelled as a Thick Plate with Three Corner Supports — Maximum Heave Acceleration
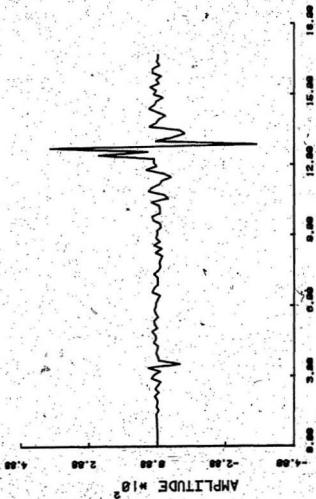
FIGURE 5.11. Amplitude of the Complex Frequency History of the Amplified Vertical Acceleration Acting at the Bottom of FNP
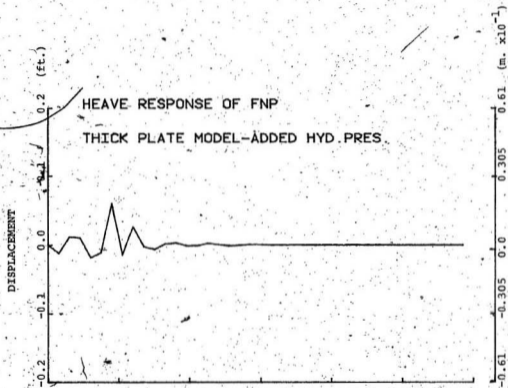
FIGURE 5.12. Frequency Response of FNP Platform Modelled as a Thick Plate
Supported at Three Corner Nodes - Maximum Heave Displacement

5.5.3 Seismic Response of LPG Platform

The modelling of LPG platform into an equivalent isotropic thick plate on elastic foundation is also based on the frequency compatibility technique as mentioned before. The thickness of the platform was kept unchanged and the material properties are iterated until the frequency of desired value is arrived. The material properties of the LPG platform with pseudo material are

Thickness = 56.42' (17.208m)

Young's Modulus, $E_x = E_y = 4.2 \times 10^6$ kips/ft^2 (2.01 $\times 10^8$ kN/m^2)

Mass density, $\rho = 0.00126$ kip sec^2/ft^4 (0.648 kN sec^2/m^4)

The platform is modelled as a cantilever thick plate as shown in Fig. 5.13. The amplified earthquake acceleration at the bottom of LPG, shown in Fig. 3.9, and the hydrodynamic pressure evaluated by the 2D coupled model, Fig. 4.14, is input as the external loading acting at the bottom of the plate. The evaluated heave responses are shown in Figs. 5.14 and 5.15.

5.6 Discussion

The development of a new conforming, high precision triangular thick plate bending element resting on elastic foundation is presented. Its accuracy and applicability for determining the response of floating platforms (in both time and frequency domain) are illustrated.
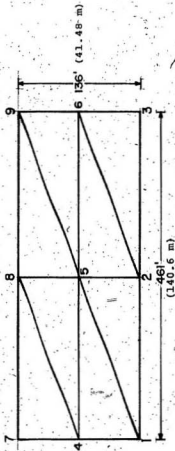
FIGURE 5.13: Finite Element Discretisation of LPG Platform (Nodes 1, 4 and 7 are supported)
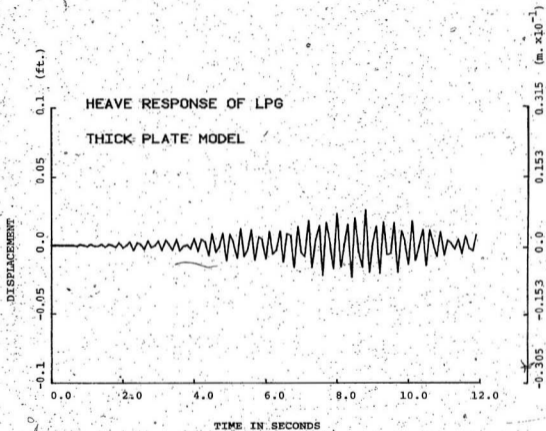
FIGURE 5.14. Time History Response of LPG Platform Modelled as a Cantilever Thick Plate - Maximum Heave Motion
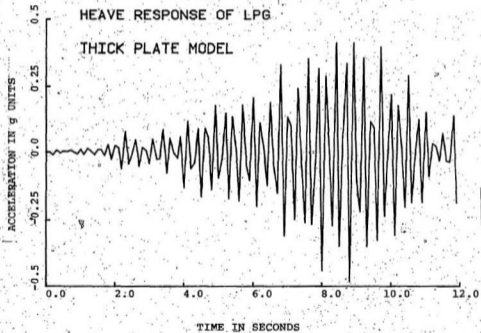
FIGURE 5.15. Time History Response of LPG Platform Modelled as a Cantilever Thick Plate – Maximum Heave Acceleration

It must be mentioned at this context that the use of hydrodynamic presssure evaluated using 2D model for this equivalent 3D model is based on the conversion factor, calculated by Garrison (1975) and presented in the paper by Johnson et al (1975).

The hydrodynamic loads applied at all the nodes correspond to the maximum hydrodynamic pressure evaluated for that instant of time or frequency. The earthquake acceleration consists of only the vertical component, acting simultaneously at all the nodes. It is assumed that water does not transmit the horizontal accelerations. However, for a complete analysis, these accelerations will have to be added at the nodes where the moorings are connected, since they can transmit both horizontal and vertical accelerations as a result of the mooring response to sea bed accelerations.

An improved finite element model with more number of elements per side should also be studied for confirming the accuracy of the results.

CHAPTER 6

COMPUTER SOFTWARE 'FLUSIN' FOR COUPLED
FLUID-STRUCTURE INTERACTION

6.1 Introduction

Many general purpose finite element programs have been
developed and well-tested for the dynamic analysis of
structures. The purposes and the efficiencies of these
programs in handling different classes of problems have been
described by Belytschko (1976) and Marcal (1972). Marcus
(1978) has reported the use of NASTRAN in solving submerged
cantilever plate vibration problems including fluid-
structure interaction. Bathe and Hahn (1979) updated ADINA
to include three-dimensional isoparametric fluid elements
with the displacements as unknowns, similar to structural
finite elements, and studied the transient response of
fluid-structure systems.

Rather than attempting to develop new software for the
coupled fluid-structure interaction, it is far more fruitful
and less time consuming to make use of a well-tested
structural dynamics program as a base to build upon and
incorporate fluid finite elements with pressures as the
unknowns and the thick plate element as an extension to the
element library. NONSAP (Bathe, Wilson and Iding, 1974) was
selected as the basis of the computer software development.
Though this program is written for both linear and nonlinear
structural dynamic analyses, only the linear analysis part

of it has been used in the coupled fluid/structure interaction analysis.

The element libraries available in NONSAP are:

a) three dimensional truss element,

b) two-dimensional plane strain and plane stress elements (the node numbering sequence is different from those developed in Chapter 4),

c) two-dimensional axisymmetric shell element,

d) three-dimensional solid element, and

e) thick-shell element.

None of the above elements have been used in the present analysis. The updated version, PLUSIN, an acronym for FLuid-Structure INteraction, includes the following new element libraries:

a) two-dimensional, eight-noded, quadrilateral, isoparametric plane-strain orthotropic structural element, developed in Section 4.2,

b) two-dimensional, eight-noded, quadrilateral, isoparametric fluid finite element with pressure as the unknown at each node, developed in Section 4.3,

c) one-dimensional, three-noded, isoparametric fluid surface wave element,

d) one-dimensional, three-noded, isoparametric fluid radiation damping element,

e) one-dimensional, three-noded, isoparametric fluid-structure interface element, and

f) a triangular thick orthotropic plate bending element resting on elastic foundation.

A compact storage scheme (Figure 6.1) is used; only elements below the skyline are stored and processed resulting in minimum storage requirements and computations.

A new routine to evaluate the earthquake loading has been added in the load evaluation scheme. The numerical time step-by-step integration routine has been modified to include the solution algorithm of unsymmetric coupled equations described in Section 4.4. In addition to the time domain analysis, a procedure for frequency domain analysis of the coupled problem is also included.

Since a dynamic storage scheme is used in the program, there is no limit to the high-speed storage and hence the size of the problem and the number of finite elements used. Again, to minimize the storage requirements the program uses the 'overlay' technique. In this way, only the requested element library and the connected routines as per the requested execution contol cards are processed and executed.

The organization of the program, its capabilities and an explanation of the input and output of the program are discussed below.
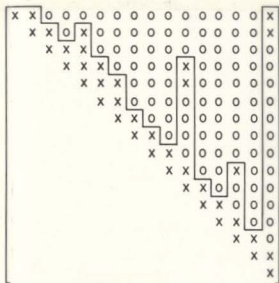
(a) Original Matrix
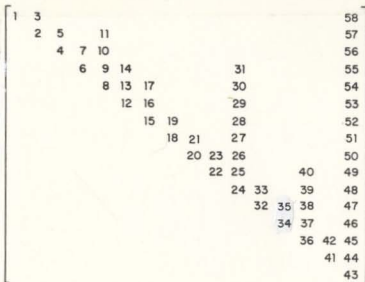
(b) Storage Sequence

FIGURE 6.1 Element Matrices Storage Scheme

6.2 Program Organization

The operational sequence of the main routine of FLUSIN is shown in Fig. 6.2. The solution phase is divided into three categories. When NSOLN=1 the program performs the dynamic analysis of structure without taking into consideration the fluid-structure interaction effects. This is independent of the element type chosen (two-dimensional/thick plate).

When NSOLN=2 the program solves the dynamic equations in frequency domain. Here again the fluid interaction is not directly included, but considered as external loads as a function of frequency. This is also independent of the element type used.

When NSOLN=3 the program includes the fluid element package and solves the coupled dynamic equation using the modified numerical method for coupled equation; for this case only the two-dimensional plane strain fluid and structure element can be used.

The dynamic storage allocations used for the solution phase of coupled fluid-structure interaction are given in Table 6.1.

```
                    Control Data
          Reads and Prints Control Information
```

```
                  Structural Data
Reads and generates if necessary, the nodal point data, structural properties.
Generates equation nos. for the active degrees of freedom.  Prints the nodal
information and equation numbers.
```

```
                    Load Data
Reads the external load applied to the structure, calculates and stores the
load vector at each time/frequency step of integration.
```

```
Assembles the structure stiffness, mass and damping matrices as well as the
effective stiffness of the matrix in compact storage form and stores them in
tapes.
```

```
Evaluates earthquake load vector, adds with the other external loads, updates
the load vector and stores in tape.
```

```
Reads or generates initial displacement, velocity, and acceleration of the
structure and prints.
```

```
Selects step by step
numerical integration
procedure and solves          = 1              = 2
the dynamic equation                NSOLN              Performs frequency analysis
without fluid-structure                                and prints the results
interaction and prints
the result                            = 3
```

```
Reads and generates the fluid nodal point data and fluid properties.
Generates the equation numbers for the active d.o.f.  Prints nodal infor-
mation and equation numbers.
```

```
Assembles fluid stiffness, mass, radiation damping, and surface wave
matrices in compact form and the total fluid-structure interface (non-
symmetric, non-square) matrix.
```

```
Reads and prints initial values of pressures and its derivatives.
```

```
Selects the numerical integration procedure, evaluates coupled load vector,
and solves the coupled dynamic equations.  Prints the displacements,
velocities and accelerations of the structure at required printing intervals
and prints, as well, the hydrodynamic pressures and their derivatives at these
printing intervals.
```

```
                    STOP
```

FIGURE 6.2. Flow Sequence of the Subroutine FLUSTR

The 'overlay' technique used to further save the storage is shown in Fig. 6.3. The figure shows the overlay structure of the program chosen corresponding to different phases of execution.

The nodal points are specified in terms of the x and y coordinates for the 2D elements and the thick plate element

TABLE 6.1

Locations Allocated to Store Different Variables in the Computer Program 'PLUSIN'

Variable	No. of Locations	Starts At	Ends Before
δ_t	NEQS*	N1	N2
$\dot{\delta}_t$	NEQS	N3	N4
$\ddot{\delta}_t$	NEQS	N5	N6
P_t	NEQ*	N7	N8
$\dot{P}_t$	NEQ	N9	N10
$\ddot{P}_t$	NEQ	N11	N12
MAXAS	NEQS	N0	N1
MAXA	NEQ	N121	N122
K	NWKS	N13	N14
M	NWKS	N15	N16
C	NWKS	N17	N18
A	NWKS	N19	N20
H	NWK	N21	N22
Q	NWK	N23	N24

Table 6.1 (Continued)

D	NWK	N25	N26
S_e	6X3	N27	N28
S_e^T	3X6	N29	N30
B	NWK	N31	N32
B	Lower half of (NEQxNEQ)	N33	N34
B^{-1}	Lower half of (NEQxNEQ)	N35	N36
S	(NEQSxNEQ)	N37	N38
SB^{-1}	(NEQSxNEQ)	N39	N40
$_wS^T$	(NEQxNEQS)	N41	N42
$SB^{-1}S^T$	Upper half of (NEQSxNEQS)	N43	N44
X	Lower half of (NEQSxNEQS)	N45	N46
t+ t	NEQS	N51	N52
$P_{t+ t}$	NEQ	N53	N54
$f_1(t)$	NEQS	N51	N52
$f_2(t)$	NEQ	N53	N54
$f_3(t)$	NEQS	N51	N52
$f_4(t)$	NEQ	N53	N54

*NEQS - number of equations for structure nodal unknowns

NEQ - number of equations for fluid nodal unknowns
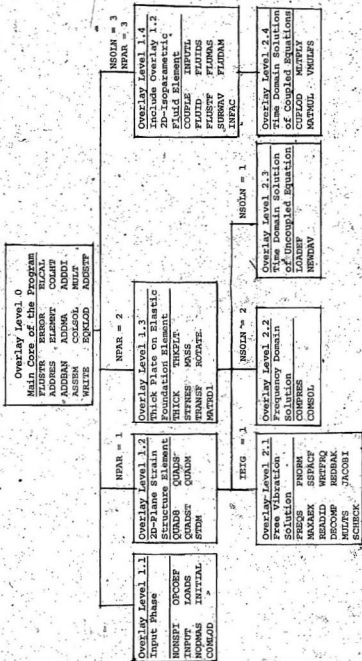
FIGURE 6.3: 'OVERLAY' Organization

Overlay Level 0
Main Core of the Program
FLUSTR ERROR BLCAL
ADDRES ELEMENT COMBST
ADDBAN ADDMA ADDDI
ASSEM COLGOL MULT
WRITE EQUGOD ADDSTF

NPAR = 1

Overlay Level 1.1
Input Phase
NONSPI OPCOEF
INPUT LOADS
NODMAS INITIAL
COMLOD

Overlay Level 1.2
2D-Plane Strain
2D-Plane Element
QUAD8 QUAD5
QUAD5T QUADM
STDM

NPAR = 2

Overlay Level 1.3
Thick Plate on Elastic
Foundation Element
THICK THICPL
STRNES MASS
TRANSF ROTATE
MATBD1

NSOLN = 1

Overlay Level 1.4
Include Overlay 1.2
'separate 2-d' 'c'
Fluid Element
COUPLE INPUTL
FLUID FLUIDS
FLUSTF FLDMAS
SHFRAV FLDDAM
INFAC

NSOLN = 3   NPAR = 3

Overlay Level 1.2.4
Time Domain Solution
of Coupled Equations
CUPLOD MLTPLY
MATMUD VNDUFS

IEIG = 1

Overlay Level 2.1
Free Vibration
Solution
FREQS PNORM
MAXAEX SSPACF
READID WRITFQ
DECOMP REDBAK
MULDS JACOB1
SCHECK

NSOLN = 2

Overlay Level 2.2
Frequency Domain
Solution
COMPRES
COMSOL

Overlay Level 2.3
Time Domain Solution
of Uncoupled Equation
LOADEF
NEWDAV

Overlay Level 1.2.3
Time Domain Solution
of Coupled Equation
MLTPLY
NEWDAV

(z coordinate is zero for this version of the program). The 2D plane structure element has 2 d.o.f. per node, the fluid element has one d.o.f. at each node, and the thick plate bending element has 12 d.o.f. per node.

The term time is used synonymously to frequency in the input and output phase. The external loads can be specified as time varying or frequency varying, or constant concentrated loads. Also a load multiplier can be defined to increase or decrease these loads or change direction.

6.2.1   Storage and Retrieval of Assembled Matrices

In order to save storage requirements all the structure and fluid characteristic matrices are established, assembled and stored in a low-speed storage system such as magnetic tapes. These matrices are later retrieved depending on the type of analysis requested. Table 6.2 lists the designated numbers of the tapes used and the matrices stored in these tapes. It should be noted that only those matrices which are needed later in the solution phase are stored in the tapes. Unless otherwise mentioned all the matrices are stored in compact storage form, in a one-dimensional array. All the elements, including zeros, below the skyline (Fig. 6.1) are stored. A minimum number of storage locations are used by storing and processing only the elements below the skyline.

TABLE 6.2

Storage and Retrieval Sequence of Different Matrices

in the Low Speed Storage Tapes

Tape No.	Data Stored and Retrieved
1	Element group information from the input, such as its coordinates, number of equations and related d.o.f., etc.
2	The triangularized effective stiffness matrix, to be used for the time domain step-by-step integration of uncoupled equations.
3	Total (earthquake plus any other) external load vectors acting on the structure at each time step (for time domain analysis), or stores complex load vectors (earthquake and hydrodynamic) acting on the structure at each frequency step (frequency domain analysis).
4	In sequence: a) stiffness matrix of the structure b) consistent mass matrix of the structure c) concentrated nodal damping vector (if specified)
8	For the uncoupled problem, stores: a) ID arrays, and b) initial displacements, velocities, and accelerations of the structure sequentially. For the coupled problem, stores: a) ID array for the structural part b) initial displacements, velocities, and accelerations of the structure sequentially c) ID array for the fluid part, and d) initial values of pressures, and their first and second derivatives of the fluid nodes.
10	Stiffness matrix of the structure for frequency analysis
11	Nodal stiffeners, masses, and dampers vector during the assemblage of the structural matrices, or the eigenvalues and eigenvectors during the frequency analysis.
12	The structural mass matrix for the frequency analysis.

Table 6.2 (continued)

15	For the coupled problem, stores sequentially: a) MAXAS b) MAXA c) fluid stiffness matrix, d) fluid mass matrix, e) surface wave matrix, f) radiation damping matrix, g) fluid-structure interface matrix (non-square matrix), and h) transpose of fluid-structure interface matrix (non-square matrix)

6.3 Functions of Subroutines

FLUSTR The main subroutine containing the calling sequences of all other subroutines depending on the code 'NSOLN'.

ADDBAN Adds the upper halves of the element matrices to form the compacted global matrices.

ADDCM   Adds specified concentrated nodal masses and dampers to the global mass matrix and global effective stiffness matrix.

ADDRES Calculates the addresses of the diagonal elements in the banded matrices from the known column heights.

ADDSTF Adds specified concentrated nodal stiffnesses due to elastic supports to the global stiffness matrix.

ASSEM   Assembles the matrices needed for the solution (free vibration and dynamic analyses).

COLHT   Estimates the column heights below the skyline of the upper half of the symmetric banded global matrices.

COMLOD   Estimates the complex load vector for each frequency step.

COMRES   Finds the complex frequency response of the system for each frequency step.

COMSOL   Solves static equilibrium equations stored in a compact storage form using column reduction scheme.

DECOMP   Decompose the stiffness matrix into LDL^T, from where L is the lower triangle of the matrix and D is the diagonal matrix.

ELCAL   Calls appropriate element subroutines for reading, storing and generating the necessary element data.

ELEMNT   Selects the element (plane strain or thick plate or fluid package) depending on the parameter 'NPAR'

EQKLOD   Reads ground accelerations, in x and y directions, in the time domain or real and imaginary parts of the complex amplitudes in the frequency domain. Evaluates the load vector due to these accelerations in time or frequency domain and adds with any other load vectors.

FUNCTION   Evaluates the values of the function given by Eqn. 5.2.23 for different values of m and n.

FREQS   Finds the requested number of lowest frequencies and associated mode shapes of the structure.

INITIAL   Sets the initial conditions of the displacements, velocities and accelerations of the structure.

INPUT   Reads, generates, and prints the nodal coordinates. Calculates equation numbers and stores them in ID array.

INVERS   Inverts a symmetric square matrix and replaces with the inverse of the matrix at its location.

JACOBI   Solves the generalized eigenvalue problem using the Jacobi iteration technique.

LOADEF   Calculates the effective load.

LOADS   Reads the load table and interpolates the load value for the required time or frequency steps.

MASS   Evaluates the element mass matrix of thick plate bending element resting on an elastic foundation.

MATRD1   Matrix reduction subroutine.

MLTPLY   Multiplies a matrix stored in a compact form with a vector.

MULT   Multiplies a matrix stored in a compact form with a vector and adds it to another vector stored in a compact form.

MULTS   Multiplies two matrices stored in a compact storage form and stores the result in a compact form.

NEWDAV   Evaluates new displacements, velocities, and accelerations for time (t+ t).

NODMAS   Reads concentrated nodal mass, stiffness and damping values, evaluates the nodal vectors and writes them on tape 11, to be used by ADDSTF, ADDCM.

NONSPI   Main input subroutine. Reads control information, calls subroutines to initialize solution variables, sets time step integration coefficients, reads nodal point data, calculates and stores load vector, etc.

OPCOEF   Calculates coefficients of time integration operators for either Wilson- method or Newmark method.

PNORM   Finds norm of a matrix.

QUADM   Calculates the elements of the mass matrix of an eight noded quadrilateral isoparametric element.

QUADS   Calls subroutines to evaluate stiffness and mass matrices of two dimensional eight noded quadrilateral isoparametric elements and assembles the structure stiffness and mass matrices.

QUADST   Calculates the structure element stiffness matrix using eight noded quadrilateral isoparametric element.

QUAD8   Sets up the required storage space and calls QUADS to generate the element matrices.

REDBAK   Reduces and back substitutes the iteration vectors in the sub-space iteration process.

ROTATE   Generates the rotation matrix required to transform the element matrices to the global system for the thick plate bending element model.

SCHECK   Evaluates shift for the Sturm sequence check.

SSPACE   Evaluates the smallest eigenvalues and associated eigenvectors in the generalized eigenvalue problem using the subspace iteration procedure.

STDM   Evaluates the strain-displacement relationship matrix.

STFNES   Calculates the elements of stiffness matrix of a thick plate bending element on elastic foundation.

THICK   Sets up the storage required and calls the subroutine sequences to use the thick plate on elastic foundation finite element package.

THKPLT   Reads, generates, and prints thick plate element node characteristics. Calls the subroutines to generate element matrices and assembles the global matrices.

TRANSF   Generates the transformation matrix to convert the element matrices from the generalized displacement coordinates to global displacement coordinates.

WRITE   Prints the displacements, velocities and accelerations of the structure.

WRTFRQ   Prints the results of the free vibration analysis, frequencies and associated mode shapes.

MATMUL   Multiplies two general matrices

COUPLE   Calls the subroutine sequences required to generate the fluid element stiffness, mass, and damping matrices, and assembles the global fluid domain matrices.

CUPLOD   Evaluates the effective coupled load matrix needed to solve the coupled fluid-structure interaction problem.

FLUDAM   Generates the elements of the fluid damping matrix.

FLUID   Sets the storage space required and calls FLUIDS, the fluid finite element program package.

FLUIDS   Calls the sequence of subroutines to read, generate, and print the fluid element characteristics, and assembles the global fluid domain matrices.

FLUMAS   Generates the elements of the fluid mass matrix.

INTFAC   Generates the elements of the fluid-structure interface matrix and its transpose.

SURWAV   Generates the elements of the surface wave matrix.

COLSOL   Solves simultaneous equations in storage using compact storage and column reduction scheme.

INPUTL   Reads the input data required to generate the fluid element matrices

FLUSTF   Generates the elements of the fluid stiffness matrix.

ADRES & ADRES1   Routines to locate proper storage addresses in the compact storage scheme, required for matrix operations.

6.4 Data Input for FLUSIN

6.4.1   Control Data

Card No. 1 (12A6):

Columns	Variable	Explanation
1-72	HED(12)	Title of the problem to be used in labelling and identifying the output.

Card No. 2 (5I5):

1-5	NUMNP	Total number of structural nodal points.
6-10	NEGL	Number of element groups = 1 for linear element group.
11-15	MODEX	Flag indicating the mode of solution; = 0, data checking only = 1, execution of the program.
16-20	NSTE	Number of time steps for the time domain solution.
21-25	IPRI	Solution printing interval; = 0, default set to "1", meaning, solution at each step to be printed out

Card No. 3 (2F10.0):

1-10	DT	Time step increment interval
11-20	TSTART	Time at which solution step starts

Card No. 4 (6I5):

1-5	ISTIFF	Flag indicating added stiffness, for example, spring supports; = 0, no added stiffness = 1, if lumped noded stiffness present

6-10	IMASS	Flag indicating static or dynamic analysis and also lumped or consistent mass matrix;
		= 0, static analysis,
		>0, dynamic analysis,
		= 1, lumped mass case,
		= 2, consistent mass case,
11-15	IDAMP	Flag indicating damping type;
		= 0, no damping effect,
		= 1, Rayleigh damping.
16-20	ISTIFN	Number of concentrated nodal stiffnesses.
21-25	IMASSN	Number of concentrated nodal masses.
26-30	IDAMPN	Number of concentrated nodal dampers.

Card No. 5 (I5):

1-5	IEIG	Flag indicating frequency solution mode;
		= 0, no free vibration analysis
		= 1, free vibration analysis to find the lowest specified number of frequencies and associated modes.

Card No. 6 (I5):

1-5   NSOLN   Flag indicating the type of solution;

= 1, structures on land, time domain analysis

= 2, external loading of hydro-dynamic pressures vs frequency, frequency domain analysis;

= 3, coupled fluid-structure interaction, time domain analysis.

Card No. 7 (I5):

1-5   IEQKN   Flag indicating the earthquake load acting;

= 0, no earthquake load

= 1, earthquake load acting

Card No. 8 (I5):

1-5   IFLGX   Flag indicating the x component of acceleration acting;

= 0, no x component of acceleration acting,

= 1, x component of acceleration is present.

Card No. 9 (I5):

1-5	IFLGY	Flag indicating the component of acceleration acting;

= 0, no y acceleration component acting,

= 1, - y component of acceleration is acting.

Card No. 10 (I5):

1-5	NDOF	Number of degrees of freedom of each structural node;

= 2, for plane stain element

= 12, for thick plate on elastic foundation element.

Card No. 11 (I10, 7F10.0):

1-10	IOPE	Method of numerical integration used;

= 0, default set to "1",

= 1, Wilson- method;*

= 2, Newmark- method

11-20	OPVAR(1)	The integration parameters;

= 0, default sets = 1.4 for Wilson- method and = 0.5 for Newmark method

= 1.4 for Wilson- method

= 0.5 for Newmark method

OPVAR(2) The second integration parameter for Newmark- method; = 0, default is specified as below**

*If NSOLN=1, regular Wilson- method,

If NSOLN=3, modified Wilson- method to solve the fluid-structure coupled equations.

** =0.25 (+0.5)**2

Card No. 12 (16I5):

1-5	NPB	Number of blocks of results to be printed out; = 0, default sets to printout of the results of all nodal points.
6-10	IDC	Flag for displacement printout code; = 0, no displacement ptintout, = 1, print displacements.
11-15	IVC	Flag for velocity printout code; = 0, no velocity printout, = 1, print velocity components.
16-20	IAC	Flag for acceleration printout; = 0, no acceleration printout = 1, print accelerations

If NPB = 0, omit the next card.

Card No. 13 (16I5):

1-5	IPNODE(1,1)	First node of printout block no. 1
6-10	IPNODE(2,1)	Last node of printout block no. 1
11-15	IPNODE(1,2)	First node of printout block no. 2, etc.

6.4.2 Nodal Point Data

Card No. 14 (I5, 3F10.0, 13I2):

1-5	N	node number; greater than 0 and less than NUMNP
6-15	X(N)	x - coordinate
16-25	Y(N)	y - coordinate
26-35	Z(N)	z - coordinate = 0, for this program
36-37	KN	Flag for automatic nodal data generation*; = 0, no generation
38-39	IDOF(1,N)	x - translation boundary condition code; = 0, free or unknown = 1, fixed or known

40-41	IDOR(2,N)	y - translation boundary condition code
42-43	IDOR(NDOF,N)	z - translation boundary condition code**

*For the thick plate element, there will be twelve boundary conditions for each node corresponding to the 12 degrees of freedom

**If KN_1 is the generation parameter for the card with node number N_1, then the next node generated is N_1+1*KN_1, and the next is N_1+2*KN_1, etc. until N_2-KN_1 is established.

6.4.3 External Load Data

Card No. 15 (16I5):

1-5	NLOAD	Number of cards to be read prescribing the external loads acting at the nodes
6-10	NLCUR	Number of load cases (time functions or frequency functions)*
11-15	NPTM	Maximum number of points describing load functions**

*At least two values per load function are required for interpolation

**No function should be represented by more than NPTM number of points.

Card No. 16 (2I5):

1-5	NTF	Load function number, should be greater than or equal to 1 and less than NLCUR
6-10	NPTS	Number of points in the function, should be greater than 2 and less than NPTM

Card No. 17a (8F10.0):

1-10	TIMV(1)	First time value, t_1
11-20	RV(1)	Load function value at time, t_1
21-30	TIMV(2)	Second time value, t_2
31-40	RV(2)	Load function value at time, t_2
.	.	
.	.	
.	.	
71-80	RV(4)	Load function value at time, t_4

Card No. 17b (8F10.0) if necessary**

RV (NPTS)

*The first value of time must be zero. The last value of
the time should be greater than the time at the end of the
solution. Otherwise an error message will be printed.
**Input as many cards as required to input NPTS values, with
four pairs of values in each card.

Card No. 18a (3I5, F10.0):

This card must be skipped if NLOAD is equal to zero.
Otherwise NLOAD number of cards must be input this section.

1-5	NOD	Node number to which the first load function is applied; must be greater than or equal to 1 and less than NUMNP.
6-10	IDIRN(1)	Direction in which the first load function is acting;
		= 1, x direction
		= 2, y direction
		= 3, z direction

11-15	NCUR(1)	Load curve number that describes the load function; ≥ 1 and $\leq$ NLCUR
16-25	FAC(1)	Multiplication factor to be used to scale the load function, = 0, default sets to unity

Card No. 18b (3I5, F10.0)* if necessary:

1-5	NOD

*Input NLOAD number of cards, one for each node on which the load function is acting.

6.4.4 Damping Information

Card No. 19 (2F10.0):

1-10	ADAMP	Rayleigh damping coefficient, *
11-20	BDAMP	Rayleigh damping coefficient, *

*These coefficients are used to calculate the structural damping matrix defined as:

$$[C] = [M] + [K]$$

where [M] is the mass and [K] is the stiffness matrix of the structure.

6.4.5 Concentrated Stiffness, Mass and Damping Data

Card No. 20 (I10, 6F10.0):

Concentrated nodal stiffness data, e.g., elastic supports. If ISTIFN.EQ.0, skip this card. If not, input ISTIFN number of cards.

1-10	N	Node number at which the concentrated stiffness is added.
11-20	XSTIFF(1)	Stiffness added in x direction.
21-30	XSTIFF(2)	Stiffness added in y direction.

Card No. 21 (I10, 6F10.0):

Concentrated nodal mass data, i.e., added mass. If IMASSN.EQ.0 skip this card. If not, input IMASSN number of cards.

1-10	N	Node number at which the concentrated mass is added.
11-20	XMASS(1)	Mass added in x direction
21-30	XMASS(2)	Mass added in y direction

Card No. 22 (I10, 6F10.0):

Concentrated nodal damper data, i.e., added damping. If IDAMPN.EQ.0 skip this card. If not, input IDAMPN number of cards.

1-10	N	Node number at which the concentrated damping is added
11-20	XDAMP(1)	damping added in x direction
21-30	XDAMP(2)	Damping added in y direction

6.4.6 Initial Conditions

Card No. 23 (I5):

1-5	ICON	Flag indicating the initial condition; = 0, zero initial condition for MODEX=2; NE.0, non zero initial condition.

Card No. 24:

If ICON.EQ.0 skip this card.

Format	Variable	Explanation
6E12.6	(DISP(I), I=NEQ)	Initial values of displacements
6E12.6	(VEL(I), I=1, NEQ)	Initial values of velocities

6E12.6　(ACC(I), I=1, NEQ)　Initial　values　of
　　　　　　　　　　　　　　　accelerations

*NEQ is the number of equations, equal to the number of
unknowns.

6.4.7　Element Properties

Card No. 25 (20I4):

Columns	Variables	Explanation
1-4	NPAR(1)	Parameter specifying the element type to be used,
		= 1, 2D plane strain element
		= 2, thick plate on elastic foundation element
		= 3, fluid element
5-8	NPAR(2)	Parameter specifying the total number of elements in that type
9-12	NPAR(3)	Number of material types in the specified element

If NPAR(1) = 1 input the following card

Card No. 26 (I5, 3F10.0):

1-5	N	Material number, greater than 1 and less than NPAR(3)
6-15	E(N)	Young's modulus of the material
16-25	PR(N)	Poisson's ratio of the material

| 26-35 | RO(N) | Mass density of the material |

If NPAR(1) = 2 input the following card

Card No. 26 (I5, 7F10.0):

1-5	N	Material number
6-15	ELX	Young's modulus in x direction
16-25	ELY	Young's modulus in y direction
26-35	POIX	Poisson's ratio in x direction
36-45	POIY	Poisson's ratio in y direction
46-55	RO	Mass density
56-65	THK	Thickness of the material

(For NPAR(1) = 3 corresponding input is explained later)

6.4.8 Element Data

If NPAR(1) = 1 input the following card

Card No. 27 (11I5):

1-5	MEL	Element number
6-10	I1	Node number 1*
11-15	I2	Node number 2
16-20	I3	Node number 3
21-25	I4	Node number 4
26-30	I5	Node number 5
31-35	I6	Node number 6
36-40	I7	Node number 7
40-45	I8	Node number 8
46-50	MTYP	Material type number

51-55	KG	Automatic node increment generation code**	

*The element node numbering should be in anti-clockwise order.

Caution: the interface nodes must be numbered first for the case NSOLN = 3

If NPAR(1) = 2 input the following card:

Card No. 27 (11I5):

1-5	MEL	Element number
6-10	I1	node number 1*
11-15	I2	node number 2
16-20	I3	node number 3
21-25	MTYP	material type number
26-30	KG	automatic node increment generation code**

*the node numbering must be in the anticlockwise order.

**If KG=0, default sets KG=1. Elements must be input in increasing element number order. If cards for elements [(M+1), (M+2), ...(M+J)] are omitted, these elements are generated by increasing the node number of successive elements with the value KG; KG being taken from the Mth element card.

6.4.9   Earthquake Record Data

If (IEQKN).NE.0 input the following cards

Card No. 27a (3I5):

1-5	NPTS	number of data points in the earthquake input. (The time interval is set to 0.01 secs.)

If (NSOLN).NE.2 give the following input

Card No. 27b (8F9.0):

1-9	DTE	Time interval of accelertion values

If (IFLGX.EQ.1) input the next set of cards

Card No. 27c (8F9.0):

1-9	XACCN(1)	x-acceleration value at time DTE secs.
10-18	XACCN(2)	x-acceleration value at 2*DTE secs.

XACCN(NPTS)

If (IFLGY.EQ.1) input the next set of cards

Card No. 27d (8F9.0):

1-9	YACCN(1)	y-acceleration value at time DTE secs.
10-18	YACCN(2)	y-acceleration value at time 2*DTE secs.

YACCN(NPTS)

If (NSOLN).EQ.2 give the following cards (freq. domain record of earthquake data)

Card No. 27e (10F8.0):

1-8	DFRFQ	frequency interval of the earthquake input

Card No. 27f (10F8.0):

1-8	XACCN(1)	real part of the earthquake acceleration at first frequency interval
9-16	YACCN(1)	imaginary part of the acceleration record at the first interval.

XACCN(2)

YACCN(NPTS)

Card No. 27g (I5):

1-5	NODHIS	Node at which the time history response output is requested.

6.4.10 Fluid Domain Data

If NSOLN.EQ.3 input the following cards regarding fluid elements:

Card No. 28 (3I5):

1-5	NNT	total number of fluid nodes.
6-10	NET	total number of fluid elements.

Card No. 29 (3I5):

1-5	NSWT	total number of surface wave nodes.
6-10	NRDT	total number of radiation damping nodes.
11-15	NSIT	total number of fluid-structure interface nodes.

6.4.11 Fluid Element Information

Card No. 30 (I5, 2F10.0, I5):

1-5	J	node number.
6-15	X1(J)	x-coordinate.
16-26	X2(J)	y-coordinate.
27-30	ID(1,J)	boundary condition code.
		= 0 for all nodes with unknown pressure.
		= 1 for nodes with known pressure.

Card No. 31 (16I5):

1-5	1 (sequence number)	first surface wave node.
6-10	NSW(1)	first surface wave node number
11-15	2	second surface wave node.
16-20	NSW(2)	second surface wave node number.

NSWT

NSW(NSWT)

Card No. 32 (16I5):

1-5	1 (sequence number)	first radiation damping node.

6-10	NRD(1)	first radiation node number.
11-15	2	second radiation damping node.
	NRD(2)	second radiation node number.

.

.

.

NRDT

NRD(NRDT)

Card No. 33 (16I5):

1-5	1 (sequence number)	first interface node.
6-10	NSI(1)	first interface node number.
11-15	2	seccond interface node.
16-20	NSI(2)	second interface node number.

.

.

.

NSIT

NSI(NSIT)

6.4.12   Fluid Properties

Card No. 34 (3F10.0):

1-10	RHO	water density.
11-20	G	acceleration due to gravity.

| 21-30 | XCL | x-coordinate at the centre line of the structure. |

6.4.13 Frequency Analysis Information

Card No. 35 (3I5)

1-5	NOMEGA	number of frequency increments.
6-10	OMEGA	starting frequency value.
11-15	DOMEGA	frequency increment.

6.4.14 Fluid Elements Data

Card No. 36 (3I4):

1-4	OPVAR(1)	element type.
		= 3 for fluid element.
5-8	OPVAR(2)	number of elements.
9-12	OPVAR(3)	number of different materials.

Card No. 37 (11I5):

1-5	MEL	element number.
6-10	I1	node number 1,
11-15	I2	node number 2,
16-20	I3	node number 3,
21-25	I4	node number 4,
26-30	I5	node number 5,
31-35	I6	node number 6,
36-40	I7	node number 7,
41-45	I8	node number 8.
46-50	MTYP	material type number.

51-55   KG   element generation code.

The nodes must be input in anti-clockwise order.

Repeat inputting number of cards equal to number of fluid elements.

Card No. 38 (5I5):

1-5   NUMESW   total number of surface wave
                           elements.

Card No. 39 (5I5):

1-5   NSWE   surface wave element number.

6-10   JK(1)   first node number 1*.

11-15   JK(2)   node number 2.

16-20   JK(3)   node number 3.

*The node numbering must be in the order of right to left.

Repeat inputting NUMESW cards equal to the total number of surface wave elements.

Card No. 40 (5I5):

1-5   NUMERD   total number of radiation
                           damping elements.

Card No. 41 (5I5):

1-5	NRDE	radiation damping element number.
6-10	JK(1)	node number 1,
11-15	JK(2)	node number 2,
16-20	JK(3)	node number 3.

The node numbering must be in the order from bottom to top.

Repeat inputting NUMERD cards equal to the total number of radiation damping element.

Card No. 42 (5I5):

1-5	NUMEIF	total number of interface elements.

Card No. 43 (5I5):

1-5	NIFE	interface element number.
6-10	JK(1)	node number 1,
11-15	JK(2)	node number 2,
16-20	JK(3)	node number 3.

The node numbering must be in the order from left to right for horizontal, and bottom to top for vertical line elements.

Repeat inputting NUMEIF cards equal to the number of interface elements.

6.5. Output from FLUSIN

The sequence of output printed by the program is as follows:

1) Title of the problem and the control information.

2) Structural element data (nodal point coordinates, boundary conditions, equation numbers associated with the unknown d.o.f.).

3) Details of externally applied loads.

4) Damping coefficients.

5) Initial conditions of the structure displacements velocities, and accelerations.

6) Element information in the following sequence:

    i) element group selected, number of elements,

    ii) material number and its elastic properties, and

    iii) element number, associated nodes and material.

7) Time vs earthquake acceleration data.

8) If the free vibration analysis is requested, the iteration steps, the frequencies and associated mode shapes of the structure.

9) For the uncoupled problem, the following responses of the structure for each printing interval in time domain analysis

a) heave (vertical) and surge (horizontal) displacements for the requested node and also the maximum heave and surge responses for that time and the associated node numbers (in case of thick plate model, only heave responses); and

b) the heave and surge velocities and accelerations for the printing interval (in the same fashion as explained above).

In frequency domain analysis prints the complex response of the structure (node number, real and imaginary parts of the displacement).

10) For the coupled problem solved by time domain analysis,

a) the fluid element node number, its coordinates and boundary condition,

b) the surface wave nodes in sequential order,

c) the radiation damping nodes in sequential order,

d) the fluid-structure interface nodes in sequential order,

e) the fluid density, the acceleration due to gravity, and the x-coordinate of the symmetry of the structure,

f) the unknown d.o.f. and the associated equation numbers,

g) the initial conditions of dynamic pressure and its derivations, and

h) fluid element characterisitcs

      i) element group and number of elements, and

     ii) element numbers, associated nodes, and material
        types.

11) For the coupled problem prints the following results of
    the response calculation at each printing interval:

    a) the heave and surge displacements at the specified
       node and maximum heave and surge responses at the
       printing time and the associated node numbers

    b) the velocities and accelerations at that printing
       time in the same fashion as mentioned above,

    c) the hydrodynamic pressures at the fluid-structure
       interface nodes,

    d) the hydrodynamic pressure derivatives at that time
       for all the fluid nodes, and

    e) the hydrodynamic pressures at that time for all the
       fluid nodes.

6.6 Discussion

    The software described is a general purpose program for
any coupled fluid-structure interaction system. Though the
program is written for floating structures it can easily be
adapted for bottom fixed, semi-submersible, or gravity type
structures. Also, the response of offshore structures to
loading, other than earthquake, can be evaluated by
inputting the time vs. load table (current or ice) or
frequency vs load (wave) table as the externally applied
load to the structure.

The program can be extended to handle three dimensional (structure and fluid) finite elements. Nonlinearities of the fluid medium, and thus the cavitation effect, can also be incorporated in the analysis. More sophisticated techniques such as the Boundary Integral Technique (DeRuntz and Geers, 1978; Zienkiewicz, 1975), the Boundary Element Method (Brebbia, 1978), and infinite elements (Zienkiewicz and Bettess, 1975) can be incorporated to model the infinite extent of the fluid medium. In the present program the width of the fluid region is set sufficiently large such that any increase in it should not affect the hydrodynamic pressure values more than 1%. Another improvement would be the incorporation of wave diffraction and refraction effects using finite and infinite elements (Bettess anad Zienkiewicz, 1977).

The present version can perform only time-domain analysis of the coupled fluid-structure interaction problem. Free vibration and frequency domain analysis of the coupled problem can be a valuable addition to the program. The program has been tested with FPS units but can be adapted to handle SI units with minor modifications.

CHAPTER 7

GENERAL DISCUSSION AND CONCLUSIONS

7.1 Contributions to the Field of Research

The contributions of the present study to coupled fluid-structure interaction analysis are as listed below.

One of the indicated reasons for selecting floating production-storage or power plant facilities is the earthquake cushioning effect of the fluid medium supporting the floating structure. The study of earthquake phenomena in the offshore environment detailed in Chapter 3 has proved that, in fact, the vertical acceleration component of the earthquake will be amplified to as much as 35 times to that at the seabed. The fluid medium does not transmit the horizontal earthquake acceleration component since it is a shear-free medium. But, most of the station-keeping floating platforms are moored to the sea-bottom either by single anchor leg mooring or mooring caissons, unless they are dynamically positioned. Hence the horizontal earthquake acceleration component will be transferred to the structure through the mooring system. Thus, the floating structure can be subjected to more severe seismic accelerations compared to those on land. This justifies the significance and the need for further elaborate analysis of floating structures, including the nonlinear hydrodynamic interactions effect of the surrounding fluid.

Though the coupled fluid-structure interaction problems have been discussed by various authors in the past, no attempts were made to illustrate the applicability of the procedure to any sample structure. The numerical examples in Chapter 4 are first of their kind wherein complete hydrodynamic interaction effects, namely, surface wave effects, interface hydrodynamic pressure effects, radiation boundary conditions, and the flexibility of the structure are incorporated. The response of a floating structure subjected to amplified earthquake accelerations is found to be about 10 percent higher than those for a comparable structure on land.

One of the main reasons for the few applications of the procedure is the difficulty in solving the resulting unsymmetric coupled equations of motion. Various approximations were made by previous investigators to modify the final equations symmetric. Sharan (1978) developed a modified Newmark-β method to solve the unsymmetric coupled equations and tested it with numerical examples without surface wave effects and radiation damping. In Chapter 4 a new numerical integration scheme, based on the Wilson-θ method, has been developed to solve the coupled unsymmetric equations of motion. The scheme has been tested with the numerical examples and proved to be stable for comparatively high damping levels.

An innovative approximate modelling technique to study the coupled fluid-structure system is to isolate the fluid from the structure, evaluate the hydrodynamic effects of the fluid on the floating rigid body, incorporate these effects as an addition to the earthquake force on the structure, and evaluate the response of the structure. To illustrate this procedure the floating platform is assumed as a thick plate resting on elastic foundation. A new high precision triangular thick plate bending element resting on elastic foundation has been developed in Chapter 5 to model the floating platform. The hydrodynamic pressures evaluated with a rigid body assumption (Chapter 4) are incorporated as the external load at the fluid-structure interface in addition to the external earthquake accelerations, and the response evaluated. The results show a significant improvement over those obtained ignoring the hydrodynamic interaction. The disadvantage of this procedure is the incapability of evaluating the importance of radiation damping or surface wave effects.

Two different techniques of idealizing the complex cross-sectional properties of the floating platforms have been adopted for the numerical examples.

i) Modelling the platform as a thick plate made up of the same orthotropic material but of an equivalent thickness, reduced from the original, so that the

fundamental frequency of the equivalent structure will be very close or equal to the original one, or

ii) Modelling the platform as a thick plate one with the same thickness as the original platform with a pseudo material of reduced elastic and orthotropic material properties so that the fundamental frequency of the model and the original structure are compatible.

By performing the frequency analysis of the modelled structure, with perturbations of the unknowns, the values corresponding to the best compatible frequency are chosen as the data.

A general purpose computer program PLUSIN has been developed to study the coupled fluid-structure systems. The program can be used for time and frequency domain analyses of coupled and uncoupled fluid-structure systems.

The program organization is similar to NONSAP. It includes the flexibility of incorporating any finite-element module, dynamic storage allocation scheme, storing only non-zero elements of the upper half of the large symmetric system matrices, efficient free-vibration and forced response algorithms, etc.

7.2 Limitations of the Study

The assumptions and limitations of the present study are:

i) the interaction between the structure and the fluid are assumed to be linear,

ii) the infinite extent of the fluid medium is restricted to a finite region, beyond which the change in the accuracy of the result is less than 1%;

iii) the wave refraction and diffraction effects are neglected;

iv) only earthquake accelerations are permitted, as the external forces, in the computer algorithm;

v) the effects of the superstructure on the floating platform are neglected.

7.3 Conclusions

A comprehensive study of the fluid-structure interaction effects on the dynamic response of floating structures subjected to earthquake accelerations has been presented.

The study of the seaquake phenomenon presented in Chapter 3 shows that water does not seem to afford the cushioning effect as popularly believed, in fact it amplifies the accelerations. It has been estimated that the accelerations transmitted to the bottom of FNP platform floating at a water depth of 40' is amplified to about 22 times to those at the seabed, and the corresponding

amplification factor for a LPG platform in a water depth of 80' is estimated to be 31. For shallow and moderately deep conditions, it appears amplification increases with the water depth. These large accelerations could induce large negative hydrodynamic pressures and could eventually lead to the cavitation phenomenon, a non-linear effect of the fluid medium which is beyond the scope of this thesis. Further improvement in the estimation of amplification factors may be achieved by modelling the fluid medium using more lumped masses and springs.

In Chapter 4 the Euler-Lagrangian approach of the development of the coupled fluid-structure interaction equation is detailed in its entirety and the implications of various approximations, such as the rigid body assumption and neglect of compressibility, have been explained. From the approximate analysis assuming the FNP platform as a rigid rectangular body floating in a water depth of 40%, the hydrodynamic pressure at the fluid-structure interface were evaluated for different frequencies. It was noted that the maximum pressure results for a frequency of about 1 Hz. Another interesting observation is the high heave added mass and damping coefficient values for the FNP platform.

The application of the new numerical integration procedure developed to solve the unsymmetric coupled matrix equation has been demonstrated successfully in

evaluating the coupling effect of the fluid on the dynamic response of the FNP and LPG platforms. The marginal difference between the response of the structure with and without the fluid-structure interaction effect (but including the elastic foundation) does not seem to warrant the computational cost, about three to four fold. It leads to a conflicting situation between the computational cost and the sophistication in the modelling. More parametric studies are to be carried out for other types of structures located in deeper waters before making more definite comment. However, it is clear that the acceleration amplification effects in water are much higher than those on land.

The two-phase solution of the coupled problem, namely, isolating the fluid from the structure, performing the hydrodynamic analysis of the fluid (with a rigid floating body) separately, and then incorporating this effect to the structure as additional external loading at the fluid-structure interface, yielded responses of about one third of those with the complete fluid-structure interaction. A further advantage of the coupled analysis is the simultaneous incorporation of the time/frequency dependent hydrodynamic inertial and damping properties, including the flexibility of the structure.

The evolution of a thick plate bending element from the sixteen noded three dimensional isoparametric finite element (Fig. 5.1) permits modelling of the platform using a thick plate element accounting for the three dimensionality, with a considerable reduction in computation cost. Hence the new high precision triangular thick plate bending element resting on elastic foundation, developed in Chapter 5, can be an effective technique of modelling the floating platforms. As further improvement, the hydrodynamic pressures evaluated by the approximate techniques were converted to three dimensional values, and incorporated as external loads acting on the platform in addition to the earthquake accelerations.

A frequency domain analysis has also been illustrated using the 'thick plate on elastic foundation' model. The amplified earthquake accelerations were transferred into the frequency domain by using a forward Fast Fourier Transform for this purpose. Again, it has been noticed that maximum heave response occurs around 1 Hz, as expected.

The computer software developed for this research is a versatile one. It can handle

i) two-dimensional free vibration analysis of structures;

    ii) two-dimensional dynamic response analysis of structures subjected to earthquake acceleration (in both time and frequency domain);

   iii) two-dimensional dynamic response of floating structures without and with fluid-structure interaction effects

and

   iv) free vibration analysis and forced response analysis of thick plates on elastic foundation (in both the time and the frequency domain) subjected to earthquake accelerations.
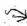
    The software includes the NONSAP algorithm of dynamic storage allocation technique, virtually eliminating the limitation on the size of the structure (number of degrees of freedom) that can be analyzed. It also incorporates the scheme of storing only the elements below the skyline of the upper half of the symmetric matrices. Since the new numerical integration procedure developed in Chapter 4 converts the unsymmetric coupled matrix equation into two symmetric equations, a considerable saving in storage space is achieved by this procedure.

    The program can also handle any other types of external time/frequency dependent loads very easily. External nodal stiffeners (elastic supports) or nodal masses and dampers on the structure can easily be taken into account.

The coupled fluid-structure interaction analysis for other types of offshore structures can easily be performed by perscribing the proper boundary conditions.

7.4 Scope for Further Research

Useful foreseeable extensions of the present study are the following:

i) Inclusion of cavitation effect for the estimation of amplified earthquake accelerations in the offshore environment by considering the nonlinear effects of the fluid medium.

ii) Three-dimensional finite element coupled fluid-structure interaction analysis, in spite of the expense involved.

iii) Extension of the coupled fluid-structure formulation to study semi-submersibles and tether-moored platforms.

iv) Incorporation of the non-linear effects of the structure as well as the fluid in the coupled fluid-structure formulation.

v) Investigation of the response of the coupled fluid-structure system subjected to other environmental forces such as wave, tsunami, ice, wind, etc.

vi) Incorporation of improved finite element modelling of the infinite radiation boundary (by including boundary integral or infinite elements).

vii) Study of wave radiation and diffraction effects in
view of the largeness of the structure.

viii) Probabilistic and spectral analysis of the coupled
fluid-structure system.

ix) Elaborate parametric studies of the relative
importance of various hydrodynamic effects taking
into account the nonlinearity.

REFERENCES

Ahmad, S., B.M. Irons and O.C. Zienkiewicz, 1970. Analysis of Thick and Thin Shell Structures by Curved Elements, Int. J. Num. Meth. Eng, 2.

Anderson, A.R., 1975. Prestressed Concrete Floating Structures (State-of-the-Art), presented at the 1975 Spring Meeting, The Society of Naval Architects and Marine Engineers, Vancouver, B.C., Paper II C.

Bai, K.J. and R.U. Yeung, 1974. Numerical Solutions to Free Surface Flow Problems, Tenth Symp. on Naval Hydrodynamics, M.I.T., Cambridge, Mass.

Bai, K.J., 1975. A Localized Finite Element Method for Steady Two-Dimensional Free Surface Flow Problems, Proc. First National Conf. on Numerical Ship Hydrodynamics.

Bai, K.J., 1977a. A Localized Finite Element Method for Steady Three-Dimensional Free Surface Flow Problems, Proc. Second National Conf. on Numerical Ship Hydrodynamics, Univ. of Calif. Berkeley.

Bai, K.J., 1977b. Zero-frequency Hydrodynamic Coefficients of Vertical Axisymmeric Bodies at a Free Surface, J. Hydronautics, Vol. 11, No. 2.

Bai, K.J., 1977c. The Added Mass of Two-dimensional Cylinders Heaving in Waters of Finite Depth, J. Fluid Mech., Vol. 81, Part I.

Bai, K.J., 1977d. Dual Extremum Principle of the Added Mass of Two-dimensional Cylinders in Restricted Waters (submitted for publication to J. Ship Res.).

Bai, K.J., 1977e. Added Mass of a Rectangular Cylinder in a Rectangular Channel, J. Hydronautics, Vol. II, No. 1.

Bai, K.J., 1978. Sway Added Mass of Cylinders in a Canal Using Duel Extremum Principles, J. Ship. Res., 21, No. 4.

Bathe, K.J., E.L. Wilson, and R.H. Iding, 1974. NONSAP - A Structural Analysis Program for Static and Dynamic Response of Non-linear Systems, Structural Engineering Laboratory, Univ. of California, Berkeley.

Bathe, K.J. and E.L. Wilson, 1976. Numerical Methods in Finite Elements, Prentice Hall, Inc., New Jersey.

Bathe, K.J. and W.F. Hahn, 1979. On Transient Analysis of Fluid-Structure Systems, Int. J. Computers and Structures, Vol. 19.

Bedel, G.W. and C.M. Lee, 1971. Numerical Calculations of Added Mass and Damping Coefficients of Cylinders Oscillating in or Below a Free Surface, NRSDC Report No. 3591.

Belytschko, T., 1976: A Survey of Numerical Methods and Computer Programs for Dynamic Structural Analysis, Nuclear Engineering and Design, Vol. 37.

Benson, P.R. and E. Hinton, 1976. A Thick Finite Strip Solution for Static Free Vibration and Stability Problems, Int. J. Num. Meth. Engng, 10.

Berkhoff, J.C.W., 1972. Computation of Combined Refraction - Diffraction, Proc. ASCE 13th Coastal Engng. Conf., Vol. 2.

Bettess, P. and O.C. Zienkiewicz, 1977. Diffraction and Refraction of Surface Waves Using Finite and Infinite Elements, Int. J. for Numerical Methods in Engineering, Vol. 11.

Black, J.L. and C.C. Mei, 1975. Scattering and Radiation of Water Waves, M.I.T. Report No. 121, Dept. of Civil Engineering, 248 pages.

Blaker, B., 1975. Vibration of Submerged Structures as Computed by the Finite Element Method, Proc. Conf. on World Congress on Finite Element Techniques, London, U.K. Paper No. 18.

Brebbia, C.A., 1978. The Boundary Element Method for Engineers, Pentech Press, London.

Carley, T.G. and H.L. Langhaar, 1968. Transverse Shearing Stress in Rectangular Plates, J. Engng Mech. Div., ASCE, 94.

Chakrabarti, P. and A.K. Chopra, 1973. A Computer Program for Earthquake Analysis of Gravity Dams Including Hydrodynamic Interaction, Earthquake Engineering Research Centre, Report No. EERC73-7, Univ. of Calif., Berkeley.

Chen, H.S. and C.C. Mei, 1975. Calculation of Two-Dimensional Ship Waves by a Hybrid Element Method Based on Variational Principles, Proc. First Conf. on Numerical Ship Hydrodynamics, sponsored by D.W. Taylor Naval Ship Research and Development Centre, Bethesda, Maryland.

Cheung, Y.K., 1968. The Finite Strip Method in the Analysis of Elastic Plates with Two Opposite Sides Simply Supported, Proc. Inst. Civil Engrs, 40, 1-7.

Cheung, Y.K. and S. Chakrabarti, 1972. Free Vibration of Thick, Layered Rectangular Plates by a Finite Layer Method, J. Sound and Vibration, 21.

Clough, R.W., 1971. Analysis of Structural Vibration and Dynamic Response, Recent Advances in Matrix Methods in Structural Analysis and Design, University of Alabama Press.

Clough, R.W. and C.A. Felippa, 1968. A Refined Quadrilateral Element for Analysis of Plate Bending, Proc. 2nd Conf. Matrix Meth. Struct. Mech., Wright-Patterson A.F.B., Ohio.

Cowper, G.R., E. Kosko, G.M. Lindberg and M.D Olson, 1968. A High Precision Triangular Plate Bending Element, Report LR-514, N.R.C. Canada.

Cowper, G.R., G.M. Lindberg and M.D. Olson, 1970. A Shallow Shell Finite Element of Triangular Shape, Int. J. Solids and Struct., 6.

Den Hartog, J.P., 1956. Mechanical Vibrations, Fourth Edition, McGraw Hill Book Company.

DeRuntz, J.A. and T.L. Geers, 1978. Added Mass Computation by the Boundary Integral Method, Int. J. for Numerical Methods in Engineering, Vol. 12.

Donea, J., Fasoli-Stella and S. Giuliani, 1977. Lagrangian and Eulerian Finite Element Techniques for Transient Fluid-structure Interaction Problems, Proc. 4th Int. Conf. SMiRT, San Francisco, Paper No. B 1/2.

Donnell, L.H., 1954. A Theory for Thick Plates, Proc. 2nd U.S. Nat. Cong. Appl. Mech. ASME.

Donnell, D.L., D.C. Drucker and J.N. Goodier, 1946. Discussion of 'On the Theory of Bending of Elastic Plates', by E. Reissner, J. Appl. Mech., Vol. 13.

Dotson, C. and R.S. Orr, 1973. Design Aspects of a Platform for a Floating Nuclear Plant, Proc. O.T.C., Paper No. OTC 1885, Texas.

Dubois, J.J. and A.L. De Rouvray, 1978. An Improved Fluid Superelement for the Coupled Solid Fluid Surface Wave Dynamic Interaction Problems, Earthquake Engineering and Structural Dynamics, Vol. 6.

Duggar, G.L., H.L. Olsen, W.B. Shippen, E.J. Francis, and W.H. Avery, 1975. Floating Ocean Thermal Power Plants and Potential Products, J. Hydronautics, Vol. 9, No. 4.

Dungar, R., 1974. The Effects of Foundation Radiation Damping on the Response of Gravity Platforms, Chap. 10, Numerical Methods in Offshore Engineering, John Wiley and Sons, Edited by O.C. Zienkiewicz, R.W. Lewis, and K.G. Stagg.

Frank, W., 1967. Oscillations of Cylinders in or Below the Free Surface of Deep Fluids, Report No. 2875, NSRDC.

Frederick, D., 1957. Thick Rectangular Plates on Elastic Foundation, Trans., ASCE, 122, Paper No. 2898.

Fujino, M., 1973. Application of Hypercircle Methods for Estimating the Transverse Added Mass of Two-Dimensional Bodies in Restricted Waters, J. Soc. Nav. Arch. Japan, Vol. 134.

Fujino, M. and M. Sugita, 1974. On the Added Mass of a Two-Dimensional Rectangular Cylinder Vibrating in Parallel to the Free Surface and in Perpendicular Direction in Restricted Waters, J. Soc. Nav. Arch., Japan, Vol 136.

Fujino, M., 1975. On the Added Mass of a Rectangular Cylinder Moving in a Rectangular Channel, Int. Ship Build. Prog., Vol. 22, No. 248.

Fujino, M., 1976. The Effect of the Restricted Waters on the Added Mass of a Rectangular Cylinder, The Eleventh ONR Symp. on Naval Hydrodynamics, London.

Garrison, C.J., 1978. Hydrodynamic Loading of Large Off-shore Structures: Three-dimensional Source Distribution Methods, Chapter 3, Numerical Methods in Offshore Engineering, Edited by O.C. Zienkiewicz, R.W. Lewis, and K.g. Stagg, John Wiley & Sons.

Geers, T.L., 1975. Transient Response Analysis of Submerged Structures, Proc. Conf. on Finite Element Analysis of Transient Non-Linear Structural Behaviour, Edited by T. Belytschko, T. Oslas, and P.V. Marcal, AMD, Vol 14, ASME, New York.

Geers, T.L., 1978. Doubly Asymptotic Approximations for Transient Motions of Submerged Structures, J. Acoustical Society of America, Vol. 64, No. 5.

Geers, T.L. and C.A. Felippa, 1977. Doubly Asymptotic Approximations for Transient Motions of Submerged Structures, Proc. Conf. CANCAM-77, Vancouver, B.C.

Gerwick, B.C., Jr., 1973. Design and Construction of Pre-
stressed Concrete Vessels, presented at the April 24 -
May 2 Offshore Technology Conference, held at Houston,
Texas (preprint 1886).

Gerwick, B., 1975. The ARCO-LPG Terminal Vessel, Proc.
Conf. on Concrete Ships and Floating Structures,
Berkeley.

Goldenveizer, A.L., 1962. Derivation of an Approximate
Theory of Bending of a Plate by the Method of Asymptotic
Integration of the Equations, J. Appl. Math. and Mech.
26.

Green, A.E., 1949. On Reissner's Theory of Bending of
Elastic Plates, Quart. Appl. Math, Vol. 7.

Greimann, L.F. and P.P. Lynn, 1970. Finite Element Analysis
of Plate Bending with Transverse Shear Deformation,
Nucl. Engng. and Des. 14.

Gupta, S.S., 1964. Grand Banks Earthquake of 1929 and the
Instantaneous Cable Failures, Nature, Vol. 204, No.
4959.

Harlow, E.H., F.R. Harris and M. Kehnemuyi, 1974. Mooring
System for Atlantic Generating Station, Paper No. OTC
2065, Vol. II, Proc. Offshore Tech. Conf., Houston,
Texas.

Heinen, R., 1976. German Design of Floating Concrete
Structures, ASCE National Water Resources and Ocean
Engineering Convention held at San Diego, California
(preprint 2660).

Hellen, T.K., 1972. Effective Quadrature Rules for
Quadratic Solid Isoparametric Finite Elements, Int. J.
Num. Methods in Engineering, Vol. 4.

Hess, J.L. and D.C. Wilcox, 1969. Progress in the Solution
of the Problem of a Three-Dimensional Body Oscillating
in the Presence of a Free Surface, McDonnell Douglas
Report No. DAC 67647.

Hinton, E., 1976. A Note on a Thick Finite Strip Method for
the Free Vibration of Laminated Plates, Earthquake Eng.
Struct. Dyn. 4.

Hinton, E. and A. Razzaque, 1973. Finite Element Analysis
of Plates Allowing for Transverse Shear Deformation
Effects, Internal Report C/R/192/73, Civil Eng. Dept.
Univ. College, Swansea.

Hinton, E., A. Razzaque, O.C. Zienkiewicz and J.D. Davis, 1975. A Simple Finite Element Solution for Plates of Homogeneous Sandwich and Cellular Construction, Proc. Inst. Civ. Engrs., Part 2.

Ho, R.T. and A. Harten, 1975. Green's Function Technique for Solution of Floating Body Problem, Proc. Civil Engineering in the Oceans, III, Univ. of Delaware, Newark, Delaware.

Ho, R.T. and H. Bomze, 1975. Basin Oscillations in an Offshore Harbour, Paper No. OTC2331, Proc. Offshore Tech. Conf., Houston, Texas, Vol. II.

Holand, I., 1969. Finite Elements for the Computation of Hydrodynamic Mass, ISD-ISSC Symp. on Finite Element Techniques at the Institut fur Statik and Dynamik der Luft und Raumfahrt-Konstruktionen, Univ. of Stuttgart.

Hooft, J.P., 1970. Hydrodynamic Aspects of Semi-submersible Platforms, Ph.D. Thesis, Tech. University, Delft, The Netherlands.

Hubolt, J.C., 1959. A Recurrence Matrix Solution for the Dynamic Response of Elastic Aircraft, J. of Aeronautical Science, Vol. 17.

Hunt, J.T., M.R. Knittel and D. Barach, 1974. Finite Element Approach to Acoustic Radiation from Elastic Structures. Journal of the Acoustical Society of America, Vol. 55.

Hutton, A.G., 1974. A Survey of Theory and Applications of the Finite Element Method in the Analysis of Viscous Incompressible Newtonian Flow, Central Electricity Generating Board, Report No. RD/B/N3049, Berkely Nuclear Laboratories, England.

Irons, B.M., 1971. Quadrature Rules for Brick Based Finite Elements, Int. J. for Numerical Methods in Engineering, Vol. 3.

Ishibashi, T., 1977. Design and Construction of a Platform-Mounted Pulp Plant for Brazil, Paper No. 8A, Proc. Conf. on Oceans 77.

John, F., 1950. On the Motion of Floating Bodies - II Simple Harmonic Motions, Comm. of Pure Appl. Math., Vol. 3.

Johnson, H.W., A.K. Vaish, F.P. Porter and R. McGeorge, 1975. Three Dimensional Dynamic Response Modelling for Floating Nuclear Power Plants using Finite Element Methods, Proc. Conf. ELCALAP '75, Berlin, W. Germany, Paper No. U4/5.

Kaul, M.K., 1977. Response Analysis of Floating Structures, ASCE Proc. J. Engineering Mechanics Division, Vol. 103, No. EM 6.

Katona, M.G. and H.J. Migliore, 1977. Solid Fluid Interaction with Finite Element Method, T.M. No. M-44-77-6, Civil Engineering Lab., Port Hueneme, California.

Kennedy, R.P., et al 1969. TDYNE, A Computer Program to Perform Model and Time Dependent Dynamic Analysis of Spring-Mass Systems with Crushable and Jumping Bases Subjected to Ground Motion, Holmes and Narver, Inc., Las Vegas, Nevada.

Kim, C.H., 1969. Calculation of Hydrodynamic Forces for Cylinders Oscillating in Shallow Water, J. Ship Res., 13.

Kim, W.D., 1965. Oscillations of a Rigid Body in a Free Surface, J. Fluid Mech., Vol. 21.

Kim, W.D., 1969. On a Free Floating Ship in Waves, J. Ship. Res., Vol. 13.

Koeller, R.C. and F. Essenberg, 1962. Shear Deformation in Rectangular Plates, Proc. Fourth U.S. Nat. Cong. Appl. Mech., ASME 1.

Kopal, Z., 1961. Numerical Analysis, 2nd Edition, Chapman and Hall.

Lee, C.M., 1968. The Second Order Theory of Heaving Cylinders in a Free Surface, J. Ship Res., Vol.

Lee, C.M., 1976. Motion Characteristics of Floating Bodies, J. Ship Res., Vol. 20, No. 4.

Lehnoff, T.F. and R.E. Miller, 1969. Influence of Transverse Shear on the Small Displacement Theory of Circular Plates, AIAA J. 7.

Leissa, A.W., 1969. Vibration of Plates, NASA-SP-160, Scientific and Technical Information Division, NASA, Washington, D.C.

Liaw, C.Y. and A.K. Chopra, 1973. Earthquake Response of Axisymmetric Tower Structures Surrounded by Water, Earthquake Engineering Research Center, Report No. EERC 73-25, Univ. of Calif. Berkeley.

Love, A.E.H., 1927. The Mathematical Theory of Elasticity, 2nd Edition, Cambridge University Press.

Lynn, P.P. and B.S. Dhillon, 1971. Triangular Thick Plate Bending Elements, Proc. 1st Int. Conf. Struct. Mech. Reactor Tech., Berlin, 6, Paper M61-365.

Marcal, P.V., 1972. Survey of General Purpose Programs, Proc. 2nd U.S.-Japan Symposium on Recent Advances in Computational Methods of Structural Analysis and Design, Berkely, California.

Marcus, M.S., 1978. A Finite Element Method Applied to the Vibration of Submerged Plates, J. Ship Res., Vol. 22, No. 2.

Matsumoto, K., 1972. Vibration of an Elastic Body Immersed in a Fluid, Advances in Computational Methods in Structural Mechanics and Design, edited by J.T. Oden et al., Huntsville, Alabama.

Matsuura, Y. and H. Kawakami, 1970. Calculation of Added Virtual Mass and Added Virtual Mass Moment of Inertia of Ship Hull Vibration by the Finite Element Method, J. Soc. Nav. Arch. Japan, No. 127.

Mawenya, A.S. and J.D. Davies, 1974. Finite Strip Analysis of Plate Bending Including Transverse Shear Effects, Building Sci. 9.

Mei, C.C. and H.S. Chen, 1976. A Hybrid Element Method for Steady Linearized Free Surface Flows, Int. J. Num. Methods in Engineering, Vol. 10.

Mindlin, R.D., 1951. Influence of Rotary Inertia and Shear on Flexural Motions of Isotropic, Elastic Plates, J. Appl. Mech., 18.

Mindlin, R.D. and H. Deresiewicz, 1954. Thickness, Shear and Flexural Vibrations of a Circular Disc, J. Appl. Phys. 25.

Mindlin, R.D., A. Shacknow and H. Deresiewicz, 1956. Flexural Vibrations of Rectangular Plates, J. Appl. Mech. 23.

Monacella, V.J., 1966. The Disturbance Due to a Slender Ship Oscillating in Waves in a Fluid of Finite Depth, J. Ship Res., Vol. 10, No. 4.

Muga, B.J., 1967. Experimental and Theoretical Study of Motion of a Barge as Moored in Ocean Waves, Hydraulic Engineering Series No. 13, Univ. of Illinois, Urbana, Illinois.

Naghdi, P.M. and J.C. Rowley, 1953. On the Bending of
Axially Symmetric Plates on Elastic Foundation, Proc.
1st Mid-Western Conf. Solid Mech., Univ. of Illinois,
Urbana, Illinois.

Nahsavandi, A.N., G.J. Bohm and R.R. Pedrido, 1975.
Structurally Compatible Fluid Finite Element for Solid-
Fluid Interaction, Nuclear Engineering and Design, Vol.
35.

Nath, J.H., 1974. General Considerations for the Design of
the Moorings for Offshore Nuclear Power Generating
Stations, Dept. of Mech. Engng. and School of Oceano-
graphy, Oregon State Univ. Corvallis, Oregon,
NTIS-RLO-2227-T17-2.

Natvig, B.J. and J.W. Pendered, 1977. Nonlinear Motion
Response of Floating Structures to Wave Excitation, OTC
Paper No. 2796, Offshore Tech. Conf., Houston, Texas,
Vol. 1.

Nelson, C.W. and R.G. Dean, 1975. Hydrodynamic Coefficients
for Offshore Nuclear Power Plants, paper presented at
the ASCE National Structural Engineering Convention, New
Orleans, Louisiana.

Newmark, N.M., 1959. A Method of Computation for Structural
Dynamics, ASCE, J. of Eng. Mech. Div., Vol. 85.

Newton, R.E., 1975. Finite Element Analysis of Two-
Dimensional Added Mass and Damping, Proc. Conf. on
Finite Elements in Fluids, Vol. 1, Edited by R.H.
Gallagher et al.

Nigam, N.C. and R.C. Jennings, 1968. Digital Calculation of
Response Spectra from Strong Motion Earthquake Records,
EERA Laboratory, California Institute of Technology,
Pasadena, Ca.

Park, K.C., C.A. Felippa, and J.A. DeRuntz, 1976.
Stabilization of Staggered Solution Procedures for
Fluid-Structure Interaction, Proc. Conf. on
Computational Methods for Fluid-structure Interaction
Problems, T. Belytschko and T.L. Geers, Editors,
AMD-Vol. 26, Atlanta, Georgia.

Penzien, J. and W.S. Tseng, 1977. Three-dimensional Dynamic
Analysis of Fixed Offshore Platforms, paper presented at
the Int. Symp. on Numerical Methods in Offshore
Engineering, Wales, Swansea, England.

Person, A., 1977. Barge-Mounted Offshore LNG Liquefaction
Plants, Paper No. 8D, Proc. Conf. on Oceans 77.

- 234 -

Poma, R.P., S. Insom-Somboon and S.L. Lee, 1975. Elastic
    Rigidities of Circularly Voided Slabs, Building Science,
    Vol. 10.

Pryor, C.W., R.M. Barker, and D. Frederick, 1970. Finite
    Element Bending Analysis of Reissner Plates, J. Engng.
    Mech. Div. ASCE.

Przemieniecki, J.S., 1968. Theory of Matrix Structural
    Analysis, McGraw-Hill, New York.

Rao, G.V., J. Venkataramana and I.S. Raju, 1974. A High
    Precision Triangular Plate Bending Element for the
    Analysis of Thick Plates, Nucl. Engng. and Des.

Reissner, E., 1945. On the Effect of Transverse Shear
    Deformation on the Bending of Elastic Plates, J. Appl.
    Mech. 12.

Reissman, H. and Y.C. Lee, 1968. Forced Vibrations of
    Rectangular Plates, Paper presented at the 4th Biennial
    South-Eastern conf. Theoretical Appl. Mech., Tulane
    University, New Orleans.

Remery, G.F.M. and A.J. Hermans, 1977. The Slow Drift
    Oscillations of a Moored Object in Random Seas, Paper
    No. OTC 1500, Offshore Tech. Conf., Houston, Texas, Vol.
    11.

Richter, C.F., 1958. Elementary Seismology, W.H. Freeman
    Company, San Francisco.

Rock, T.A. and E. Hinton, 1974. Free Vibration and
    Transient Response of Thick and Thin Plates Using the
    Finite Element Method, Earthqu. Eng. Struct. Dyn. 3.

Roren, E.M.Q., 1969. Impact of Finite Element Techniques on
    Practical Design of Ship Structure, ISD-ISSC Symp. on
    Finite Element Techniques at the Institut fur Statik und
    Dynamik der Luft und Raumfahrt-Konstruktionen, Univ.
    Stuttgart.

Rudolph, E., 1887. Uber Submarine Erdeben Und Eruptionen
    [Gerlends], Beitrage Zur Geophysik, Vol. 1.

Rye, H., S. Rynning, and H. Moshagen, 1975. On the Slow
    Drift Oscillations of a Moored Structure, Paper No. OTC
    2336, Offshore Tech. Conf., Houston, Texas, Vol. 111.

Saini, S.S., O.C. Zienkiewicz and P. Bettess, 1976a.
    Modelling of Hydrodynamic Effects on Dams Using Finite
    Elements, Dept. of Civil Engineering, Univ. College of
    Wales, Swansea Research Report C/R 1269/76.

Saini, S.S., O.C. Zienkiewicz and P. Bettess, 1976b.
Coupled Hydrodynamic Response of Concrete Gravity Dams
Using Finite and Infinite Elements, Dept. of Civil
Engineering, Univ. College of Wales, Swansea, Research
Report No. C/R/271/76.

Salerno, V.L. and M.A. Goldberg, 1960. Effect of Shear
Deformations on the Bending of Rectangular Plates, J.
Appl. Mech. 27.

Sayer, P. and F. Ursell, 1976. On the Virtual Mass, at Long
Wave Lengths of a Half-immersed Circular Cylinder
Heaving on Water of Finite Depths, Eleventh Symp. on
Naval Hydrodynamics, Office of Naval Research, Univ.
College, London.

Schuman, U., 1979. On the Stability of Fluid-Structure
Computations, Proc. Conf. on Structural Mechanics in
Reactor Technology, Berlin, W. Germany.

Shantaram, D., D.R.J. Owen and O.C. Zienkiewicz, 1976.
Dynamic Transient Behaviour of Two and Three Dimensional
Structures, Including Plasticity, Large Deformation and
Fluid Interaction, Earthquake Engineering and Structural
Dynamics, Vol. 4.

Sharan, S.K. and G.M.L. Gladwell, 1977. A Method of
Analysing Dam-Reservoir-Foundation Interaction Problems,
Proc. Conf. CANCAM '77, Vancouver, B.C.

Sharan, S.K., 1978. Earthquake Response of Dam Reservoir
Foundation Systems, Ph.D. Dissertation, Dept. of Civil
Engineering, Univ. of Waterloo, Ontario.

Shinozuka, M., S.S. Fang, K. Kitutake and G. Matsui, 1978.
Response of Open Bottom Floating Platforms to Wind, ASCE
Proc. J. Hydraulics Div., Vol. 104, No. HY5.

Smith, I.M., 1968. A Finite Element Analysis for Moderately
Thick Rectangular Plates in Bending, Int. J. Mech. Sci.,
10.

Smith, P.D., A.K. Vaish and F.L. Porter, 1977. Site-
structure Interaction for a Floating Nuclear Power Plant
Under Seismic Loading, Proc. 6th World Conf. on Earth-
quake Engineering, Vol. 4.

Srinivas, S. and A.K. Rao, 1970. Bending, Vibration and
Buckling of Simply Supported Thick Orthotropic
Rectangular Plates and Laminates, Int. J. Solids and
Struct. 6.

Svec, O.J., 1976. Thick Plates on Elastic Foundations by
Finite Elements, ASCE, J. Engng. Mech. Div. 102, EM3.

Timoshenko, S.P., 1937. Vibration Problems in Engineering, 2nd. Edn., Constable, London.

Ursell, F., 1974. Note on Virtual Mass and Damping Coefficients in Water of Finite Depth, Univ. of Manchester, Dept. of Maths. Report.

Van Huena, R., 1972. Seaquakes, The Great Alaskan Earthquake of 1964, Vol. 6, Oceanography and Coastal Engineering, National Academy of Science.

Van Oortmerssen, G., 1976. The Motion of a Moored Ship in Waves, Ocean Eng., Vol. 3, No. 4.

Visser, W. and van der Wilt, M., 1975. A Numerical Approach to the Study of Irregular Ship Motions, Proc. Conf. on Finite Elements in Fluids, Vol. 1, edited by R.H. Gallagher et al.

Vughts, J.H., 1968. The Hydrodynamic Coefficients for Swaying, Heaving and Rolling Cylinders in a Free Surface, Report no. 194, Lab. for Ship Building, Univ. of Delft, Delft, The Netherlands.

Vughts, J.H. and D.J. Hayes, 1979. Dynamic Analysis of Fixed Offshore Structures: A Review of Some Basic Aspects of the Problem, J. Engineering Structures, Vol. 1.

Wang, S., 1966. The Hydrodynamic Forces and Pressure Distribution for an Oscillating Sphere in a Fluid of Finite Depth, Ph.D. Dissertation, Dept. of Naval Architecture and Marine Engineering, M.I.T.

Wang, C.Y., Y.W. Chang and S.H. Flistedis, 1977. An Eulerian Algorithm for Analyzing Fluid-Structure Interaction in the Fast Reactor Containment, Proc. 4th. Int. Conf. SMiRT, San Francisco, Paper No. E1/3.

Wehausen, J.V., 1971. The Motion of Floating Bodies, Ann. Rev. Fluid Mech., Vol. 3.

Wertheimer, T.B. and P.V. Marcal, 1977. Fluid-solid Interaction by Finite Element Techniques, Proc. 4th Int. Conf. SMiRT, San Francisco, Paper No. B1/4.

Williamson, R.A., R.P. Kennedy, R.E. Bachman and A.W. Chow, 1975. Response to a Proposed Nuclear Powered Ship to Water-Transmitted Earthquake Vibrations, Technical Report, Nuclear and Systems Science Group, Holmes and Narver, Inc.

Wilson, E.L., 1968. A Computer Program for the Dynamic Stress Analysis of Underground Structures, Report UC SESM68-1, Dept. of Civil Engineering, University of California, Berkeley.

Wilson, E.L., 1975. Joint and Fluid Elements in Geomechanics, Int. Symp. on Numerical Methods in Soil Mechanics and Rock Mechanics, Karlsruhe, Germany.

Wilson, E.L., 1977a. CAL - Computer Analysis Language for the Static and Dynamic Analysis of Structural Systems, Report UC SESM-77-2, Dept. of Civil Engineering, University of California, Berkeley.

Wilson, E.L., 1977b. Finite Elements for Foundations, Joints and Fluids. Chapter 10, Finite Elements in Geomechanics, Edited by Gudehus, G., Wiley, Chichester.

Yang, I.M., 1972. Motions of a Moored Ship in Six Degrees of Freedom, 9th Symp. on Naval Hydrodynamics, Paris, France.

Yu, Y.S. and F. Ursell, 1961. Surface Waves Generated by an Oscillating Circular Cylinder on Water of Finite Depth: Theory and Experiment, J. Fluid Mech., Vol. 11.

Zarda, P.R., 1976. A Finite Element Analytical Method for Modelling a Structure in an Infinite Fluid. NASTRAN User's Experiences, NASA-TMX-3428, National Aeronautics and Space Administration.

Zienkiewicz, O.C., 1975. The Finite Element and Boundary Solution Procedures as General Approximation Methods for Field Problems, Proc. World Cong. Finite Element Methods in Struct. Mech., Bournemouth, England.

Zienkiewicz, O.C., 1977. The Finite Element Method, Third Edition, McGraw-Hill Pub. Co. Ltd., New York.

Zienkiewicz, O.C., B. Irons, and B. Nath, 1966. Natural Frequencies of Complex, Free or Submerged Structures by the Finite Element Method, Vibrations in Civil Engineering, Edited by B.O. Skipp, Butterworths, London.

Zienkiewicz, O.C. and R.E. Newton, 1969. Coupled Vibrations of a Structure Submerged in a Compressible Fluid, ISD-ISSC Symp. on Finite Element Techniques at the Institut fur Statik und Dynamik der Luft und Raumfahrt-Konstruktionen, Univ. of Stuttgart.

Zienkiewicz, O.C. and Taylor, C., 1971. Weighted Residual Procedures in Finite Element with Particular Reference to Some Transient and Coupled Problems, Lectures on Finite Element Methods in Continuum Mechanics, Edited by J.T. Oden and E.R.A. Oliveira, Lisbon, Portugal.

Zienkiewicz, O.C. and P. Bettess, 1975. Infinite Elements in the Study of Fluid-Structure Interaction Problems, Second Int. Symp. on Computing Methods in Applied Science and Engineering, Versailles, France.

Zienkiewicz, O.C. and P. Bettess, 1978a. Dynamic Fluid Structure Interaction Numerical Modelling of the Coupled Problem. Chapter 5, Numerical Methods in Offshore Engineering, Edited by O.C. Zienkiewicz, R.W. Lewis and K.G. Stagg, J. Wiley & Sons.

Zienkiewicz, O.C. and P. Bettess, 1978b. Fluid-Structure Dynamic Interaction and Wave Forces. An Introduction to Numerical Treatment, International Journal for Numerical Methods in Engineering, Vol. 13, No. 1.

APPENDIX

COMPUTER PROGRAM VERIFICATION

In order to verify the validity of the computer program
a well-known example of a floating rigid circular cylinder
is selected. The added mass and damping coefficients
evaluated using the program are compared in Fig. A-1
with those of Newton (1975) and the results are found to
check very well.

As a second example a dam-reservoir interaction study
is compared. A constant acceleration a_0 is applied to the
base of the dam and the hydrodynamic pressure at various
depths along the interface is evaluated; incorporating
the flexibility of the structure, surface wave, and
radiation damping effects. The result is compared with
that of Sharan (1978) in Fig. A-2 wherein the structure
is assumed to be rigid and the surface wave and radiation
damping effects were neglected. The maximum pressures
compare very well, but the variation across the depth
evaluated by the author is more realistic to what is expected,
namely, the hydrodynamic pressure at the fixed bottom should
be near zero.
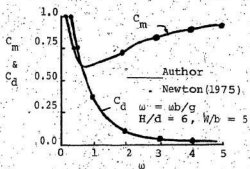
(a) Freq. vs Hydrodynamic coefficients
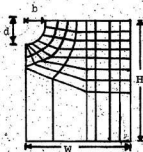
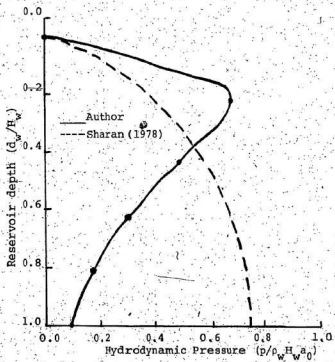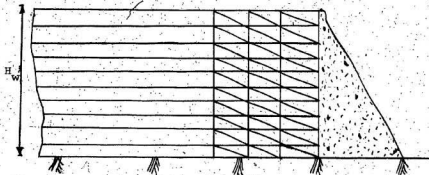(b) Finite Element Modelling of Floating Circular Hull

Figure A-1

Figure A-2